High-Resolution Deformation Modelling for a National Geodetic Datum

High-Resolution Deformation Modelling for a National Geodetic Datum

Nicolas Ian Donnelly

A thesis in fulfilment of the requirements for the degree of

Doctor of Philosophy

School of Civil and Environmental Engineering

Faculty of Engineering

University of New South Wales

March 2020

Thesis/Dissertation Sheet

Surname/Family Name	:	**Donnelly**
Given Name/s	:	**Nicolas Ian**
Abbreviation for degree as give in the University calendar	:	**PhD**
Faculty	:	**Engineering**
School	:	**Civil and Environmental Engineering**
Thesis Title	:	**High-Resolution Deformation Modelling for a National Geodetic Datum**

Abstract

Demand for high-accuracy spatial data has never been higher. Whether for traditional uses, such as precise location of property boundaries, or more innovative applications, such as augmented reality apps showing the location of buried infrastructure, high accuracy is expected and essential. On a dynamic planet, where plate tectonics and other phenomena cause constant movement of all objects on the Earth's surface, this is also a considerable challenge, particularly at local scales where deformation can vary rapidly over short distances. The cost of geodetic survey data collection at high resolutions can be prohibitive. But if this local deformation is not accounted for in a national datum, that datum cannot be said to fully meet the positioning and data management needs of the local community. Consequently, this inhibits analysis and decision-making on regional and national scales, since there may be numerous areas of local deformation in a country.

This research investigates two low-cost alternative data sources, not previously used for direct modelling of ground movement within a national datum: digital cadastral data for horizontal modelling and synthetic aperture radar data for vertical modelling. The success of these alternatives is demonstrated through their application to three deformation scenarios where high-resolution models are essential: earthquake-induced shallow ground movement, deep-seated earthquake movement in urban areas and ongoing subsidence due to geothermal activity.

A prototype model is incorporated into the geodetic datum and used to answer important questions relating to the impact of deformation on infrastructure and property boundaries. In addition, an automated approach to regularly updating a high-resolution model is developed, using cadastral data collected over a period of several years after an earthquake. This study also introduces a novel approach to updating height control within the national datum in the aftermath of an earthquake, recognising that it may be some time before full resurveys can occur. Overall, this research clearly demonstrates that high-resolution modelling significantly enhances the usefulness of the national geodetic datum, without requiring expensive additional data collection.

INCLUSION OF PUBLICATIONS STATEMENT

UNSW is supportive of candidates publishing their research results during their candidature as detailed in the UNSW Thesis Examination Procedure.

Publications can be used in their thesis in lieu of a Chapter if:

- The student contributed greater than 50% of the content in the publication and is the "primary author", ie. the student was responsible primarily for the planning, execution and preparation of the work for publication
- The student has approval to include the publication in their thesis in lieu of a Chapter from their supervisor and Postgraduate Coordinator.
- The publication is not subject to any obligations or contractual agreements with a third party that would constrain its inclusion in the thesis

Please indicate whether this thesis contains published material or not.

☐ *This thesis contains no publications, either published or submitted for publication*

☒ *Some of the work described in this thesis has been published and it has been documented in the relevant Chapters with acknowledgement*

☐ *This thesis has publications (either published or submitted for publication) incorporated into it in lieu of a chapter and the details are presented below*

CANDIDATE'S DECLARATION

I declare that:

- I have complied with the UNSW Thesis Examination Procedure
- where I have used a publication in lieu of a Chapter, the listed publication(s) below meet(s) the requirements to be included in the thesis.

Name	**Signature**	**Date (dd/mm/yy)**
Nicolas Donnelly		

COPYRIGHT STATEMENT

Signed

Date

AUTHENTICITY STATEMENT

‘I certify that the Library deposit digital copy is a direct equivalent of the final officially approved version of my thesis.’

Signed

Date

ORIGINALITY STATEMENT

‘I hereby declare that this submission is my own work and to the best of my knowledge it contains no materials previously published or written by another person, or substantial proportions of material which have been accepted for the award of any other degree or diploma at UNSW or any other educational institution, except where due acknowledgement is made in the thesis. Any contribution made to the research by others, with whom I have worked at UNSW or elsewhere, is explicitly acknowledged in the thesis. I also declare that the intellectual content of this thesis is the product of my own work, except to the extent that assistance from others in the project's design and conception or in style, presentation and linguistic expression is acknowledged.’

Signed

Date

Acknowledgements

I wish firstly to thank the institutions that have made this research possible. The University of New South Wales, Land Information New Zealand and the Cooperative Research Centre for Spatial Information.

My supervisor, Chris Rizos, ensured that the research commenced on a sound foundation and provided much-appreciated focus as it progressed. Craig Roberts took over as supervisor part way through my thesis and guided its successful completion, providing a vital sounding board and wise advice.

Many friends and colleagues at Land Information New Zealand have supported this research. My particular thanks to Graeme Blick and Jan Pierce for their unwavering support over the past seven years. To Chris Crook, who has been the driving force behind New Zealand's implementation of deformation models, to which this research seeks to contribute. And to Anna de Raadt, for her relentless positivity and encouragement to really tell the story of my research.

Abstract

Demand for high-accuracy spatial data has never been higher. Whether for traditional uses, such as precise location of property boundaries, or more innovative applications, such as augmented reality apps showing the location of buried infrastructure, high accuracy is expected and essential. On a dynamic planet, where plate tectonics and other phenomena cause constant movement of all objects on the Earth's surface, this is also a considerable challenge, particularly at local scales where deformation can vary rapidly over short distances. The cost of geodetic survey data collection at high resolutions can be prohibitive. But if this local deformation is not accounted for in a national datum, that datum cannot be said to fully meet the positioning and data management needs of the local community. Consequently, this inhibits analysis and decision-making on regional and national scales, since there may be numerous areas of local deformation in a country.

This research investigates two low-cost alternative data sources, not previously used for direct modelling of ground movement within a national datum: digital cadastral data for horizontal modelling and synthetic aperture radar data for vertical modelling. The success of these alternatives is demonstrated through their application to three deformation scenarios where high-resolution models are essential: earthquake-induced shallow ground movement, deep-seated earthquake movement in urban areas and ongoing subsidence due to geothermal activity.

A prototype model is incorporated into the geodetic datum and used to answer important questions relating to the impact of deformation on infrastructure and property boundaries. In addition, an automated approach to regularly updating a high-resolution

model is developed, using cadastral data collected over a period of several years after an earthquake. This study also introduces a novel approach to updating height control within the national datum in the aftermath of an earthquake, recognising that it may be some time before full resurveys can occur. Overall, this research clearly demonstrates that high-resolution modelling significantly enhances the usefulness of the national geodetic datum, without requiring expensive additional data collection.

Contents

List of Figures

List of Tables

1. Introduction

The world has experienced a spatial data and positioning explosion over the past two decades. Everyday activities have become inherently reliant on determining positions in real time, and relating these positions to existing spatial data to gain some insight or make a decision. From in-car navigation, to geo-tagging of photos, to catching a train, users just expect that spatial data and positioning are fit-for-purpose, accurate and reliable. Increasingly, accuracy requirements for innovative applications are at the decimetre level. Farmers want to use geo-fencing to keep their stock away from sensitive waterways, whilst still maximising the use of their land. Drivers want to know which lane they are in, so they can be better guided on manoeuvres by their navigation system. Landowners want to be able to visualise the location of property boundaries and buried services so that they can best utilise their property without damaging critical infrastructure. Innovations such as these, requiring accuracy at the decimetre level or better, can only succeed at a national level if national datums have the accuracy and currency to support them. It is of little value to have decimetre-accurate absolute positioning in a personal device if it cannot be accurately matched with other spatial data.

There are many challenges to supporting decimetre-level positioning and data management at a national level. One of the most significant is dealing with the complex deformation environment that exists in many areas where this accuracy is required. Since the late 1990s, a number of countries have recognised this fundamental challenge and developed deformation models that are incorporated into their national datums to account for ongoing tectonic movement (Blick & Donnelly, 2016; Grant, 1995). A number have also added models to account for significant earthquakes (Miyahara et al.,

2016; Crook et al., 2016; Pearson et al., 2010). This has been an essential and successful step in the evolution of national datums, but it is not sufficient to meet current and future needs. National or regional-scale deformation models cannot account for the complex reality of localised deformation (Blick et al., 2009). Yet users will expect their decimetre level positioning to work everywhere, including areas of localised deformation, just as they expect to be able to tell the time everywhere.

This research investigates several innovative approaches to developing localised deformation models and incorporating these into a national datum. It seeks to overcome potential barriers to widespread calculation and adoption of localised models. These potential barriers include the high cost of data collection, the requirement for specialist geophysical or geotechnical knowledge to process it, complexity or lack of availability of software to do the processing and lack of understanding of how to practically incorporate the models into the datum. Three diverse but reasonably common scenarios form the basis of the research: liquefaction-induced movement after an earthquake, large-scale coseismic earthquake deformation and continuous deformation in a geothermal zone. While the research scenarios are focussed on New Zealand, the concepts and techniques developed can be widely applied. For example, the characteristics of geothermal deformation in the central North Island are similar to deformation related to resource extraction elsewhere in the world. This research demonstrates that high-resolution models for a local area can be developed cheaply, simply and effectively and incorporated into a national geodetic datum.

1.1. Context

National datums or reference frames need to constantly evolve to meet the needs of the user community. They exist to account for local conditions and user requirements, for

the jurisdiction(s) within their stated extent. In a world where decimetre-level positioning in personal devices is likely soon to be mainstream, one might question whether there is still a role for a national datum. Surely in a globally-connected world, where positioning is carried out using global systems (for example, GPS, the Global Positioning System), national datums are fast becoming an anachronism. But despite embracing global positioning technologies, the vast majority of positioning and data analysis/visualisation/management applications are local or national in nature. Here there is a fundamental tension: users want positioning and coordinates to be accurate. They also want positioning and coordinates to be stable[1] over time, despite those locations being on the surface of a dynamic planet. Global datums or reference frames can readily achieve the first objective (accuracy) but from a user perspective, they do not achieve the second objective (stability). Coordinates in a global frame change by several centimetres every year, even in the absence of earthquakes or other deformation events.

This is where a national datum, with an associated national deformation model, provides the vital link between global positioning technologies and the needs of the user. The national deformation model is key to the success of the datum. But a national deformation model needs to have more than just nationwide coverage. It needs to be accurate at scales from a few hundred metres to thousands of kilometres, accounting for deformation at each end of that spectrum. This is what users expect. The value proposition of a national datum is just as dependent on its ability to account for deformation in the local neighbourhood, as it is on the ability to account for deformation across the country. Indeed, many spatial positioning and data management activities are

[1] In this context, ‘stable’ means that where objects do not appear to move in the day-to-day experience of users (ie they are fixed to the ground), the coordinates should not change

fundamentally local in nature. It is more important to be accurate relative to nearby objects than to far away objects.

Previously, deformation modelling for national datums has been seen to be the domain of jurisdictions with part or all of their area on or near a plate boundary. So the case for a deformation model was obvious in the case of New Zealand. Less so in the case of Australia, where national-scale movement over time can be accurately modelled with a simple plate motion model (ICSM, 2018; Stanaway et al., 2014a).

But even countries with high overall levels of stability need to model localised deformation. Why should spatial professionals and the general public receive a degraded national datum in Perth, just because there is subsidence due to water abstraction? Certainly it may not be practicable to maintain millimetre levels of accuracy everywhere and at all times. But there are few applications requiring this level accuracy. The vast majority can accept accuracies at the centimetre level. For many mapping applications, decimetre accuracies are adequate. What is required is a national datum that can operate with different accuracies at different scales, depending on what the user requires and what is practically achievable.

Some may consider that accuracies at the centimetre or decimetre level are fundamentally not of the geodetic domain. Rather, these accuracies pertain to the domain of surveying and mapping. This view sees the role of the national datum as being to support the highest levels of accuracy, leaving spatial data collection and management in areas of localised deformation to the surveyor, who can connect to stable marks outside the deforming area.

This perspective ignores the fact that in decades past, prior to the advent of Global Navigation Satellite System (GNSS) technology, national datums based on precise

astronomical measurements were the norm. These datums frequently had uncertainties at the decimetre level, even over relatively short distances due to the nature of error propagation from traditional geodetic surveying technologies. Furthermore, in the absence of any practical capability to model deformation, these datums would degrade with time. Yet until the widespread availability of GNSS to the spatial community, these datums generally met the user needs, despite these limitations. So while high levels of accuracy in a modern national geodetic datum are desirable, there is historical precedent for there being value where aspects can only practically be defined at the decimetre level.

The perspective that national datums must focus only on accuracies at the millimetre and low centimetre level also ignores the practical requirements of users. There is no doubt that surveyors are well-capable of collecting accurate data in areas of localised deformation by connecting to stable marks with coordinates in terms of the national datum. The problem is one of collation and publishing of such data in a form suitable for consumption by geospatial software. Furthermore, maintaining the accuracy of the data over time becomes near-impossible. Regular surveys are expensive and can generally only be justified in areas of particular interest to a party who is willing to pay for them. If one of the roles of the national datum is to enable accurate management of data collected at multiple epochs, then nowhere is this role more necessary than in the case of local deformation which is typically characterised by large variations over small areas.

The measurement and modelling of localised deformation requires data to be collected at high spatial and/or temporal resolutions. The term “high-resolution” is used here in the context of a national datum. In the spatial domain, it refers to having a capability to

identify areas of deformation as small as 25 hectares (500m by 500m). These areas of deformation should then be observed and/or modelled at a resolution (raster pixel-size) of 50m. Compare this with applications such as aerial imagery acquisition, where high-resolution would typically refer to resolutions of 10cm or better.

In the temporal domain, "high-resolution" in the national datum context refers to having a capability to repeat measurements in areas of continuous deformation over intervals not exceeding several weeks. It is acknowledged that this definition is somewhat inconsistent with the presence of Continuously Operating Reference Station(s) CORS in modern national datums, which often make measurements every second. It is the expense of installing and operating CORS that makes them unsuitable for high-resolution deformation modelling over localised areas.

High-resolution, localised deformation models are not required everywhere. There are many rural and wilderness areas where the value of creating a model is negligible. This is because there tends to be substantially less high-accuracy spatial data to manage in rural areas. Conversely, urban areas typically have many layers of high-accuracy spatial data. In addition, with regards to vertical modelling, there is far more gravity reliant infrastructure, such as sewerage systems, in urban areas. The density of development also means that hazards such as flooding often have a greater impact in urban areas.

1.2. Research Problem

The forgoing discussion has demonstrated why accounting for localised deformation is critical if a modern national datum is to meet the needs of its users, even in apparently stable countries. The problem is not one of technology, but of the scales over which it is practical and efficient to operate those technologies. There is no doubt that GNSS can

accurately measure deformation to any resolution that the user desires. All that is required is a sufficiently dense network of passive control marks and sufficiently regular repetition of the GNSS surveys, and within a short period of time an accurate, high-resolution model of the deformation could be calculated.

But this approach would be expensive to the point of being fiscally irresponsible. Consider, for example, the liquefaction-related deformation associated with the Christchurch earthquakes. High-resolution modelling using geodetic GNSS surveying would require inter-station spacing of no more than 100m, preferably less. This network would have needed to be in place *before* the earthquake to enable post-earthquake measurements to be made. Considering that Christchurch was not in an area of high seismic risk, there was no reason to particularly target the city with such a dense network prior to the earthquake. Thus, such a network would need to be installed and surveyed across all urban areas of the country. A prohibitively expensive exercise.

Thus alternatives must be investigated that can provide high density, but without the costs of traditional GNSS surveying. These data sources must provide observations, or enabling modelling, at spatial resolutions of approximately 50m, and temporal resolutions of a few weeks for ongoing deformation. They also need to be suitable for multiple deformation scenarios, either in isolation or together.

There are three main research questions to be answered for each data source. Firstly, how should the data be processed to extract the maximum coverage and accuracy from it? Secondly, how can the data be incorporated into a national geodetic datum that is fundamentally built on observations? That is, what is the nature of the "observations" that can be extracted from the data source and how can these be seamlessly combined into the national datum alongside other types of observations? Thirdly, how can these

new observation types be used to produce accurate models of localised deformation, in a form suitable for use in mainstream commercial spatial software.

1.3. Chapter Outline

This thesis consists of four main chapters.

Chapter 2 focusses on deformation modelling within a national geodetic datum or reference frame. It explores some of the key terminology used, particularly that which can be contentious. It then outlines the key characteristics of global, regional and national datums, with a particular focus on the national geometric[2] and vertical datums for New Zealand, including assessment of the current approaches to monitoring deformation at local scales. The chapter then focusses more closely on deformation modelling as it pertains to national datums, reviewing some of the approaches taken by countries with varying deformation environments, before describing the framework for datum deformation modelling used in New Zealand. The chapter next turns to consideration of potential alternatives to GNSS surveys for high-resolution deformation modelling. Firstly, Interferometric Synthetic Aperture Radar (InSAR) is described, including the persistent scatterer technique which is particularly well-suited to urban areas. This remote sensing technique is particularly strong in the vertical component. Secondly, cadastral data is described, including its typical characteristics and limitations. Cadastral data is almost exclusively horizontal in nature, providing a useful complement to SAR.

Chapter 3 comprehensively details a new approach to high-resolution modelling, using cadastral data from surveys carried out during and after the 2010-16 Canterbury

[2] The terms “geometric datum” and “geodetic datum” are often used interchangeably. They refer to a 3D datum where coordinates consist of latitude, longitude and ellipsoidal height.

Earthquake Sequence. This was a sequence of five major earthquakes that took place near Christchurch, Canterbury between 2010 and 2016. Further details of these earthquakes are provided in section 3.4.1. After describing the characteristics of the earthquakes, the impact on the dynamic cadastre is discussed, which explains why high-resolution horizontal modelling is essential in this scenario. For the first time, a model based directly on surface observations at geodetic marks is developed and incorporated into the framework of the national datum to model residual tectonic movement not accounted for in the previously published dislocation models. Having accounted for deep-seated movement as far as possible, attention turns to the remaining deformation, resulting from shallow ground movement, such as that caused by liquefaction-induced lateral spreading. The process for bringing disparate cadastral data into a common reference frame is described, providing a consistent set of post-earthquake coordinates across the city. The computation of the shallow ground movement model is then described. To demonstrate its utility, it is shown how the model can be used to answer critical questions relating to properties in the post-earthquake environment. For example, dilatation analysis is used to identify areas of contraction at an unprecedented level of detail. Finally, there is a description of how the entire process has been automated, such that it can be easily rerun as new cadastral data becomes available. This ability to quickly re-generate the model is essential if it is to be relied on to make quick and effective decisions.

Chapter 4 uses the M7.8 2016 Kaikoura Earthquake (see section 4.2), New Zealand's largest for many decades, as a case study to demonstrate the use of InSAR to re-establish height control in an emergency response situation. There are two aspects to the emergency response modelling. The first is the use of InSAR to identify and quantify deformation over approximately a quarter of the country using images collected within a

day of the earthquake. It is shown how the wrapped interferogram can be used to make quick decisions about which areas most urgently need GNSS height control, so that they can be prioritised accordingly. However, the utility of InSAR goes well beyond being a tool to triage the geodetic response in a large scale event. A method is developed for calculating post-earthquake height differences from InSAR, using the town of Kaikoura as an example. These height differences can then be combined with post-earthquake GNSS data collected as part of the emergency response using the standard observation equations model of least squares. In this way InSAR and GNSS are optimally combined to calculate post-earthquake heights on marks throughout the town – including those at which no GNSS data has been collected. The only requirement is that they have a reliable pre-earthquake height.

In Chapter 5, continuous deformation in the town of Taupo is investigated using PS-InSAR. Using this technique, subsidence at thousands of points across the town is quantified. For comparison, there are fewer than 20 GNSS control marks in the same area. These observations of persistent scatterers provide a source of direct observations of displacement in a given time period. For the first time, a subsidence model based purely on PS-InSAR is developed in a form suitable for inclusion in a national datum.

Chapter 6 summarises the research findings and suggests some areas of related future research.

2. Deformation Modelling in a National Geodetic Datum: New Zealand

2.1. Introduction

National geodetic datums or reference frames have traditionally been static. That is, they assume that points can be fixed on the surface of the Earth and that these points will remain motionless over long timescales and over the extent for which the datum is defined. Indeed, this is the origin of the term *datum* which implies a fixed reference to which other quantities relate. It has long been understood that this is not strictly true, due to the impacts of tectonic plate motion, whether from earthquakes or long-term motion. However, the static assumption was a useful one, particularly in the pre-GNSS and pre-GIS era when surveying and mapping was primarily a local activity. Even if these so-called fixed points were moving, only the most accurate geodetic surveying techniques could measure such movements, which were of little practical importance.

With the emergence of civilian GNSS and GIS in the 1980s, and increasing adoption of these technologies in the 1990s, it became apparent that static datums were inadequate to meet user demands for accuracy in a dynamic geophysical environment. While many spatial applications remained local in nature, they relied on GNSS, a technology that provides positions in terms of global reference frames, not local datums. This became a driver for several nations to define new national geodetic datums that incorporated deformation models to incorporate the impacts of long-term differential land movements over large areas.

This chapter describes the geometric and vertical datums used in New Zealand, focusing on how deformation is incorporated into a national geodetic datum. It then explores the characteristics of alternative datasets that might be used to improve the resolution of deformation models to better account for localised phenomena.

2.2. Datums and Reference Frames

The national geodetic datum is a core part of a nation's fundamental spatial infrastructure. It exists to enable the accurate and seamless integration of diverse spatial datasets. In a sense, this is the same role that datums have fulfilled for hundreds of years; it is just that contemporary digital mapping applications often demand accuracy at the level of a few centimetres, rather than the few metres that was often acceptable in a paper-based world. But in other ways, the role of the datum has changed irrevocably. No longer is making accurate measurements on a datum the sole domain of the surveyor. Managers of spatial data systems rely on the datum to enable them to manage their spatial data in a consistent framework, without needing to have an understanding of how that is achieved.

GNSS-enabled technologies have driven this step-change in spatial accuracy requirements. For example, asset management staff with little or no surveying education are able to position infrastructure to within a few centimetres using techniques such as Network Real-Time Kinematic GNSS (NRTK). The aircraft used to capture aerial imagery can similarly be positioned to within a decimetre or better using GNSS. The resultant ortho-rectified imagery may have sub-decimetre resolution, with an absolute uncertainty of 0.1-0.3m.

This spatial data explosion in the 1990s identified weaknesses in existing datums. For example, New Zealand Geodetic Datum 1949 (NZGD1949) had distortions and errors of up to 5m in it (Grant, 1995). Previously, only the most precise geodetic surveys were able to identify these discrepancies. It was clear that a new datum, appropriately accounting for deformation, would be required for New Zealand.

One of the major drivers for any new datum is that it should be consistent with the reference frame used by GNSS. As a global system, GNSS uses a global reference frame, thus any new datum must align itself to the global frame. This relates to the absolute accuracy of the datum. A second major driver is the continued need for local accuracy. In general, accurate relationships among nearby objects are more important than accurate relationships to distant objects. For example, people care more about the relationship of their property to their neighbour's, than they do about the relationship to a property on the other side of the city or country. In the GIS world, high levels of local spatial accuracy are required to accurately manage the relationships among adjacent spatial features, without inappropriate gaps or overlaps.

This ongoing need for local accuracy over small to moderate areas is one of the primary reason why national geodetic datums are still an essential component of a nation's spatial infrastructure (Donnelly et al., 2014).

2.2.1. Terminology

There is a range of terminology used to describe modern geodetic datum concepts. Terms from geodesy, surveying and GIS may exist to describe concepts that are the same, or nearly the same. The purpose of this section is to discuss key terminology that may be found in the literature, and explain the terminology chosen for this thesis.

The term *terrestrial reference frame* describes a geospatial reference system that is a realisation of a Terrestrial Reference System (Petit & Luzum, 2010). The term *datum* describes how the reference frame is fixed to the body on which spatial references are required. This would normally be the Earth, but could also be an aircraft or some other body. For example, the *datum* for a realisation of the International Terrestrial Reference Frame (ITRF) is the definition of the origin, axes and scale (Drewes, 2009). Technically, a *datum* should always refer to the fixing of some parameters, whether it be the geocentre in the case of modern referencing systems, or points on the surface of the Earth, as was traditionally done.

But a focus on the above technicalities is not always particularly useful. The reason being that national datums may evolve from a datum to reference frame to meet user needs, without this being formally reflected in documentation. Using New Zealand's national datum, New Zealand Geodetic Datum 2000 (NZGD2000), as an example, language used in technical documentation in the late 1990s indicates that it was a datum, rather than a reference frame, being defined in terms of fixed stations. For example, Pearse (2000) states:

> *"The primary stations and coordinates that define (realise) the New Zealand Geodetic Datum 2000 (NZGD2000) are those in the Zero and First Order networks as listed…"*

By 2007, when the official standard was published (LINZ, 2007), there was no mention of the datum being defined by particular stations. Furthermore, a footnote was added to clarify that there was no requirement for coordinates for a station to remain constant. Coordinate changes, even on fundamental marks, indicate that this "national datum" is now operating as a "national reference frame".

One may look to other international authorities for terminology guidance. The International Organization for Standardization (ISO) has recently published a significant revision to ISO 19111, *Geographic information – Referencing by coordinates* (ISO, 2019). This standard is used by information architects and others who design and develop software that is used to manage spatial data. As such, the content of this standard carries a considerable amount of weight. The previous version of the standard, published in 2007, used the term *datum* rather than *reference frame*. This version treats *reference frame* and *datum* synonymously, explicitly allowing them to be used interchangeably. This compromise reflects a pragmatic approach by ISO to terminology, recognising that to the user, there is no practical difference between a datum and a reference frame.

This user perspective is important. A national geodetic datum is only useful if people use it. While this can sometimes be mandated, often there is no regulation requiring the use of official datums. *Datum* has long-standing use by both surveyors and other geospatial professionals. It provides connectivity between the past and present in a way that *reference frame* does not. It is for this reason that the term *datum* is still preferred to *reference frame* by many datum managers, including New Zealand (LINZ, 2007) and Australia (ICSM, 2018), thus that is the term used in this research.

Another area of contention is the terminology used to describe datums where coordinates change with time. *Dynamic datum* means that the coordinates of a ground-fixed feature are changing over time within that datum (Stanaway et al., 2014a). The confusion and contention arise for two reasons. Firstly, the datum itself is not dynamic at all. It is typically Earth-centred Earth-fixed (ECEF), that is, the datum is fixed. It is the ground-fixed features which are moving with the tectonic plates which results in the

time-varying coordinates. Secondly, the term *dynamic* could imply that some geodynamic force is driving the coordinate movement. This is not usually the case, particularly where the feature is moving at a constant velocity (ie no acceleration). *Kinematic* is the more technically correct term as it implies nothing about the reasons a particular feature exhibits movement in terms of the datum. From a technical geodetic perspective, the term *kinematic reference frame* would be most correct.

However, once again the user community needs to be considered. Terms such as *dynamic datum* have been used for several decades and are well-embedded in the lexicon (for example, (Grant, 1995)). *Dynamic* is also the terminology used in recent international standards (ISO, 2019), which means it will be used in software and other user-facing products and services. For this reason, *dynamic* is used in this thesis to describe coordinates that change with time.

The term *semi-dynamic datum* is not well-defined, although it is widely used to describe national datums that include a deformation model to enable coordinates at a reference epoch to be calculated (LINZ, 2007). There is an implication in the term that the datum manager may update coordinates from time to time, perhaps due to local deformation or the availability of an improved secular[3] deformation model (Donnelly et al., 2014). But in this case, there is little to distinguish it from a series of static frames updated every few years as the need arises.

Overall, this thesis aims to use terminology that is likely to be most familiar to users of datums.

[3] Long term changes that occur imperceptibly

2.2.2. Global Reference Frames

Global positioning technologies operate in terms of global reference frames. Thus the use of global reference frames is deeply embedded in the technologies people use on a daily basis. The de-facto standard for the global reference frame is a realisation of the ITRF, the current version being ITRF2014 (Altamimi et al., 2016). This global frame is realised using the integration of data from four techniques of space geodesy. Firstly, Very Long Baseline Interferometry (VLBI) observes radio signals emitted by distant quasars which can be treated as fixed objects. Measuring the time delay between the same signal reaching two radiotelescopes on the Earth's surface enables the distance between those stations to be very precisely determined. Thus VLBI primarily provides the scale for the ITRF. Secondly, Satellite Laser Ranging (SLR), makes precise laser measurements to retro-reflectors on satellites, enabling their orbits to be precisely tracked as they progress across the horizon. Since satellite orbits are primarily determined by the Earth's gravitational field, this enables the geocentre to be precisely determined. Thirdly, Doppler Orbitography and Radiopositioning Integrated by Satellite (DORIS) uses ground stations to emit a signal that can be detected by certain satellites as they pass overhead. By measuring the Doppler shift, the location of the beacons can be determined. The primary contribution of DORIS is as an independent technique to strengthen the parameters determined by VLBI and SLR. Finally, GNSS data supports integration of the other three techniques, since a GNSS CORS is almost always co-located at VLBI and SLR sites. It is GNSS that makes the global reference frame accessible. The density of GNSS CORS far exceeds that of the other techniques, although is not generally at a level that enables users to directly connect to the ITRF. From a national datum perspective, inclusion of GNSS CORS that are part of the ITRF

in processing regimes means that the national datum can be accurately aligned to the global frame.

ITRF coordinates are published at a defined epoch, and station velocities or the ITRF plate motion model can be used to determine coordinates at any other epoch (Altamimi et al., 2017). The ITRF is a dynamic datum, with coordinates that vary with time due to tectonic motion. Consequently, while it is directly or indirectly used for all GNSS-based positioning, it is not commonly used for spatial data management, where static coordinates are preferred.

2.2.3. Regional Reference Frames

Regional reference frames cover an entire continent and exist primarily to facilitate accurate and convenient connections to the global frame. This is achieved through including a much higher density of GNSS stations than is included in the ITRF. The regional frame is closely aligned to the ITRF through the inclusion of a global subset of IGS stations in the regional reference frame processing. From a user perspective, the advantage is that the nearest regional reference station might only be several hundred kilometres distant, while the nearest IGS station could be over 1000km away. From the perspective of a national datum manager, there are two clear benefits to utilising a regional reference frame.

Firstly, by submitting data from some or all of the nation's CORS to the regional frame, that data is processed in a consistent, systematic and well-documented manner, providing a valuable independent verification of the datum manager's own processing. For countries where there is limited capability or capacity to do GNSS processing at a

global scale, the coordinates and velocities produced for the regional reference frame can be used directly to realise the national datum.

Secondly, the higher density of GNSS CORS in the regional reference frame enables the datum manager to process their own data against a regional network of stations using shorter baselines than would be possible through direct connection to the ITRF. Because of the high degree of alignment of the global and regional frames, there is negligible loss of accuracy aligning to a regional frame compared with a global frame.

2.2.4. National/Local datums

The national or local datum exists primarily to support local positioning and data management activities. It is usually a static or semi-dynamic datum, meaning that coordinates do not change with time. Coordinates in terms of the national datum are effectively treated as a piece of static metadata describing the location of a ground-fixed object. A national datum enables the majority of users, working over relatively small areas, to ignore the effects of deformation in their work.

As well as static coordinates, national datums also provide increased densification of both control marks and deformation models. Computational and capability constraints mean that the global processing undertaken to realise global and regional reference frames does not incorporate highly localised deformation, such as that due to earthquakes and geothermal activity. Such deformation is primarily of local interest, so is most appropriately included within the national datum.

A national datum can also be far more responsive than a global reference frame. The ITRF is realised with ever-decreasing frequency, as the frame is now highly stable at a global level. It is produced by the global community and therefore is not set up to take

account of specific local drivers to compute another realisation. For example, after the 2016 Kaikoura earthquake impacted most of New Zealand at the level of at least a few millimetres, a substantial new realisation of the datum was required. There is no mechanism for making such an update to the global frame – at least not in the sense of publishing a new realisation of it. The national datum, however, can be updated at the discretion of the datum manager, whenever user demand makes this desirable.

So in the current environment, national datums are as important as they have ever been, but the reason for their value has changed. In the pre-GNSS era they were primarily needed for positioning. Now they are primarily needed for accurate data management over time, which means they need to be responsive to local phenomena that impact the accurate management of this data, such as earthquakes.

2.3. New Zealand Geodetic Datum 2000

New Zealand Geodetic Datum 2000 (NZGD2000) is the official geometric datum for New Zealand. Key parameters are shown in Table 1.

Reference frame	**Epoch**	**Ellipsoid**	**Semi-major axis (m)**	**Inverse flattening**
ITRF96	2000.0	GRS80	6378137	298.257222101

Table 1: NZGD2000 definition.

2.3.1. Realisation

In New Zealand, as in many other jurisdictions, the national datum is realised by maintaining close alignment with a realisation of the ITRF. When NZGD2000 was first developed in the late 1990s, it was aligned to ITRF96, this being the most recent

realisation of the global frame at the time. A regional network of stations was defined throughout Australasia, including (3) CORS stations operating in New Zealand. This regional network was used to calculate ITRF1996 epoch 2000.0 coordinates at 31 Order 1 stations throughout the country. These ITRF96 epoch 2000.0 became the official NZGD2000 coordinates for those stations (Pearse, 2000; Blick et al., 2005).

At this time NZGD2000 and ITRF96 epoch 2000.0 coordinates were identical. Thus the national datum was closely aligned with the global frame. A secular deformation model was used to ensure that observations made at epochs other than 2000.0 could be propagated to the reference epoch. In practice, it is often not necessary to apply the deformation model, as over small areas connections to passive control marks permit the user's survey data to be calibrated in terms of the local datum.

Since the calculation of the original NZGD2000 coordinates, there have been a number of earthquakes that have impacted significant portions of the country. These have been incorporated into the deformation model, as discussed in section 2.5.2.3. One of the impacts of incorporating these events is that the relationship between the global and local reference frames has become more complex, conceptually, and less accurate in terms of realisation.

While NZGD2000 is still defined through its relationship to ITRF96, in practical terms it is accessed via a more recent version of the reference frame. For example, critical GNSS processing products are currently provided in terms of IGS14, a global reference frame aligned to ITRF2014 and developed by the International GNSS Service (IGS) (Johnston et al., 2017). So processing is carried out in terms of the most recent global frame, then a transformation applied to convert the coordinates to ITRF96 at the

observation epoch. Finally, the deformation model is applied to propagate from the observation epoch to the reference epoch (Crook et al., 2016).

The process is described at a high level in Figure 1. These time-dependent transformations are a core component of datum operations in New Zealand and many other countries, including Australia and the United States.

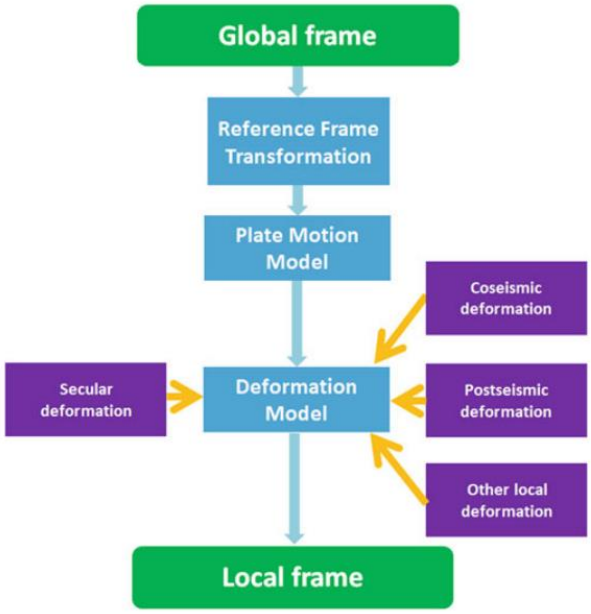

Figure 1: Generalised transformation path between global and local frames (national datums), assuming the plate motion model and deformation model are defined in terms of the national datum (Donnelly et al., 2014).

2.3.2. Active and Passive control

The fundamental, datum-realising, stations for the nation are comprised within the PositioNZ network of CORS (Gentle et al., 2016). The 37 stations in this network enable near real-time monitoring of the datum and provide key data to input into the national deformation model. Several of these stations are also part of the global network of the IGS. Thus they are the critical link between the global reference frame and the local datum, ensuring the relationship between the two remains well-defined and accurately realised.

On average, these stations are separated by approximately 120km, reflecting its primary purpose as a network supporting datum maintenance, rather than one that supports datum access. At this density, the PositioNZ network is only going to be able to detect long-wavelength deformation signals. These stations are therefore of little use when considering high-resolution deformation modelling in the spatial domain. Even considering other networks operated by GNS Science[4] and private providers, the minimum distance between stations is typically of the order of 30km. Again, not suitable for high-resolution modelling. Of course, in the time domain, the resolution of the CORS network is unparalleled, with measurements being made at frequencies of 1Hz.

Recognising this limitation of CORS, campaign GNSS data collected at passive control marks has long been a key component of New Zealand's geodetic system. Infill deformation monitoring at a national level is led by GNS Science and supported by Land Information New Zealand[5] (LINZ) and the University of Otago. This network of approximately 900 stations is surveyed approximately every eight years, on a rolling annual basis, splitting the country into 8 regions (Beavan et al., 2016). This dataset, in combination with the CORS data, is the primary observation dataset from which the national deformation model is calculated.

As **Error! Reference source not found.** shows, the density of this network varies, with g reater density where the strain is expected to be larger. On average, the separation between stations is approximately 20-30km. As is the case with the CORS, this density is not sufficient for high-resolution modelling. To obtain the higher density of passive control that would support deformation modelling at a far more localised level, passive

[4] New Zealand's geoscience research organisation
[5] The government department responsible for managing the national datum

control marks not intended for use as deformation monitoring or modelling marks need to be considered. These marks are typically contained within survey control networks designed primarily for cadastral, engineering and general spatial support purposes.

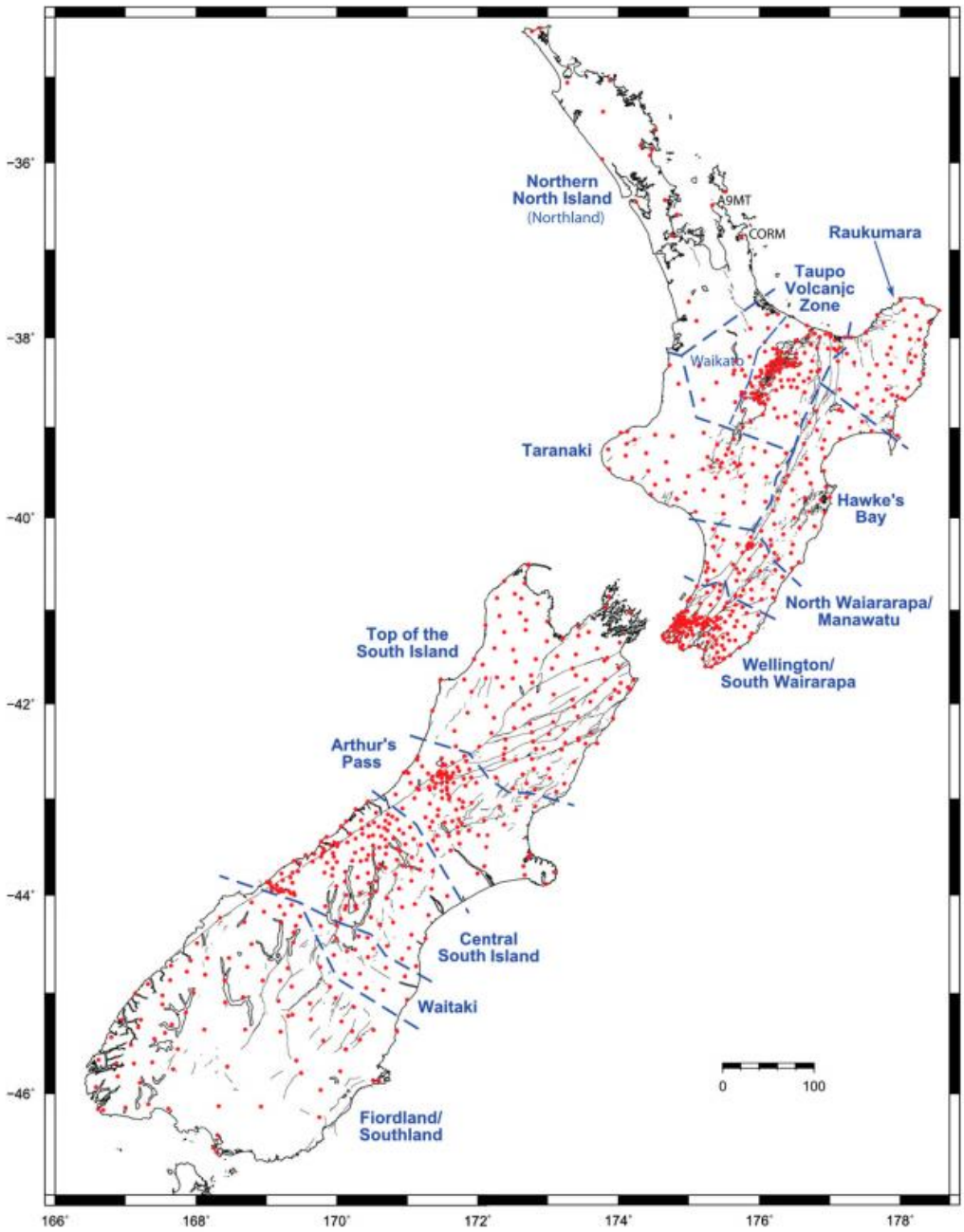

Figure 2: The passive control marks used in the generation of the national deformation model (Gentle et al., 2016).

Over the past twenty years, there has been a gradual shift in focus from passive control to active control in many jurisdictions, including New Zealand. This has led some countries to develop clear strategies to transition from passive control to CORS as the preferred means of datum access. For example, the United States is proposing that its new geometric datum, NAD 2022, will be accessed primarily via CORS and will *"change the overall reliance on passive control"* (Roman, 2015). Similarly, Japan has announced that due to the high density of their GEONET CORS network (average 20km spacing), it intends to stop maintaining passive control marks by 2024 (Miyahara et al., 2015).

While understandable, this move away from passive control does introduce risks, since the density of CORS would always be less than the density of the full passive control network. These risks primarily relate to the inability to use GNSS to measure fine-scale deformation, if there are not sufficiently dense passive control marks. It can be argued that techniques such as InSAR can provide this necessary densification, which is true to an extent. However, remote sensing techniques still have a strong reliance on GNSS, both for the horizontal component and for verification of the InSAR.

If national geodetic datums are to be accurate and accessible in areas of widespread local deformation, then reasonably dense passive control marks are still an important means of datum delivery. Some advantages of passive control marks are:

- Can still be used in the event of significant disruption to GNSS systems
- Provide a means of verifying that positions are in terms of the national datum to within required tolerances
- Provide marks at a density that is required for near-field deformation modelling in the aftermath of an earthquake

- Provide marks at a density that can support localised deformation monitoring

Particularly in areas of known localised deformation, a dense network of passive control is essential to the accurate modelling of both horizontal and vertical components.

2.3.3. Survey Control Networks

The *Standard for the New Zealand survey control system* describes various networks that together provide the nation's survey control system (LINZ, 2009b). Six networks are defined, with details provided in Table 2.

Control Network	**Purpose**	**Example**
National reference frame	Enables official national datums to be aligned to global reference frames, and this alignment to be monitored	GNSS CORS and VLBI radio-telescope co-located at Warkworth to enable NZGD2000 to be accurately aligned to the ITRF
Deformation monitoring network	Enables the determination and monitoring of land movement at national, regional and local scales	A regional network of passive marks at approximately 30km spacing exists to densify the national deformation model

Cadastral horizontal control network	Enables horizontal cadastral data to be connected to the geodetic system, to facilitate its accurate integration into the national cadastre	"Street-corner" survey control marks that cadastral surveyors connect to
Cadastral vertical control network	Enables vertical cadastral data to be connected to the geodetic system, to facilitate its accurate integration into the national cadastre	"Street-corner" survey control marks with a height that cadastral surveyors connect to
Basic geospatial network	Enables various government-directed activities to be referenced to geometric datums	Marks with beacons to enable remote observations to be made for orientation purposes
National height network	Enables various government-directed activities to be referenced to vertical datums	Precise-levelled benchmarks that provide vertical control for engineering purposes

Table 2: Control networks in New Zealand's geodetic system.

These control networks provide the national geodetic agency's view as to how a modern national survey control system should be constructed. The first two networks are internally-focussed; that is, they define networks that are required for the accurate and timely maintenance of the datum. The last four are focussed on the operational

requirements of users and recognise that different applications have quite different requirements of survey control marks.

The deformation monitoring networks are worthy of further explanation, as it is these networks that directly support the ongoing accuracy of the datum. They feed into the deformation models and patches. Associated with the standard is a guideline, which explicates the reasoning behind the various networks in more detail (LINZ, 2009a). While following a guideline is not compulsory, it provides a methodology, which if followed, will be considered to be compliant with the standard.

The National Deformation Monitoring Network (NDMN) consists of CORS, placed such that every point in the country is located within 100km of at least one station. The Regional Deformation Monitoring Network (RDMN) consists of passive control marks, nominally at two densities. Where the engineering shear strain[6] exceeds 0.2μrad/year, the network is to be of sufficient density to ensure that every point is within 20km of at least one such mark. In less rapidly deforming areas, where the shear strain is less than 0.2μrad/year, the density of marks is to be such that every point is within 35km of a RDMN mark.

Similarly, the Local Deformation Monitoring Network (LDMN) specifies two densities; one for high-deformation areas and one for low-deformation areas. But in addition, differing densities are also specified for urban and rural areas. The determination of whether an area is urban or rural is based on the predominant class of cadastral surveys in the area, which in turn is substantially based on the size of the land parcels being surveyed. Thus LDMN density requirements are related to parcel size. Table 3 is adapted from the guideline (LINZ, 2009b) and summarises the density requirements:

[6] The deformation perpendicular to the original length of a line.

Land use	Rate of deformation	Maximum distance from any point to one local-DMN mark (km)
Urban	>0.5 μrad/year	3
Urban	<0.5 μrad/year	5
Rural	>0.5 μrad/year	10
Rural	<0.5 μrad/year	n/a

Table 3: Local-DMN passive control mark densities for urban and rural scenarios.

The lack of a density requirement for rural areas with low deformation rates reflects the fact that in such areas no local deformation monitoring network is required. The regional network is of sufficient density in such cases. From Table 3, the maximum prescribed density is for marks to be at approximately 5km spacing ($3\text{km} \times \sqrt{2}$) in urban areas of high deformation. This guideline was driven by pragmatic considerations, recognising that the most common observation technique of static GNSS surveys becomes prohibitively expensive as passive control networks increase in density.

The guideline makes it clear that 5km spacing is not intended to indicate sufficiency, through clause 1.2.4(d) which states:

> *"It may be necessary to place additional marks where the magnitude of the expected or observed deformation cannot be modelled using the minimum density or configuration in [Table 3]"*

This immediately raises two questions: how can these areas of higher deformation be identified and what cost-effective techniques might exist to monitor and model such deformation? Certainly static GNSS campaign surveys undertaken at repeat periods of several years will not be sufficient to efficiently identify areas of highly localised

deformation, let alone enable accurate modelling. These alternative techniques are introduced later in this chapter.

2.4. New Zealand Vertical Datum 2016

New Zealand Vertical Datum 2016 (NZVD2016) is the official vertical datum for New Zealand (LINZ, 2016). It is the successor to New Zealand Vertical Datum 2009 (NZVD2009), the first official quasigeoid-based vertical datum to unify the 13 major levelling datums that provided the basis for heights in New Zealand for many decades (Amos & Featherstone, 2009). These 13 local levelling datums had been based on sea level measurements of varying lengths at individual tide gauges. They were then propagated along major roads and in major urban areas using precise levelling techniques.

The gravity data used in the computation of NZGeoid2009, the reference surface for NZVD2009, had a number of limitations. The distribution of terrestrial gravity measurements was very uneven, being heavily influenced by the accessibility of sites. They were also of varying and sometimes unknown quality, having been collected over a number of decades. In the near-coastal marine regions, where satellite altimetry produces lower quality results and shipbourne gravity is sparse, there were also challenges (McCubbine et al., 2018). To resolve these issues, a national airborne gravity campaign was undertaken to collect a single homogenous gravity dataset covering short to medium wavelengths. This new dataset was combined with existing gravity data to compute a new quasigeoid, New Zealand Quasigeoid 2016 (NZGeoid2016) over New Zealand's land and maritime area (McCubbine et al., 2018). This quasigeoid provides the reference surface for NZVD2016, which features normal-orthometric heights. NZVD2016 is not explicitly linked to tide gauges, which avoids the distortions that

would be present if the datum were fixed to multiple gauges around the country. Rather, the quasigeoid represents the mean sea level in the open oceans, in the absence of effects such as sea-surface-topography. Importantly, the normal-orthometric heights which this datum provides can be relied on to predict fluid flow, unlike the ellipsoidal heights of the geometric datum NZGD2000.

NZGeoid2016 has a well-defined relationship to the GRS80 reference ellipsoid, to which NZGD2000 ellipsoidal heights are referenced (Table 1). This makes NZVD2016 readily accessible via GNSS techniques. It also makes it far more resilient to vertical deformation events than the predecessor local vertical datums. This is because even substantial vertical uplift associated with large earthquakes, such as the 2016 Kaikoura Earthquake, has negligible impact on the quasigeoid reference surface. Thus at any given point, the ellipsoidal height change is the same as the normal-orthometric height change, for all practical purposes. Thus there is no requirement to re-measure gravity after a major earthquake. Heights can be re-established using GNSS only, or with local precise levelling connected to a framework of GNSS control. This obviates the need for extensive and expensive precise levelling to re-establish height control to support earthquake recovery.

The realisation of NZVD2016 is based on the realisation of NZGD2000 ellipsoidal heights, which then have the quasigeoid model applied to derive NZVD2016 normal-orthometric heights. In strict technical terms, the datum (that is, the quasigeoid reference surface and its relationship to the GRS80 ellipsoid) is independent of NZGD2000. But the reference frame realisation is derived from NZGD2000. As for the geometric reference frame/datum, from a user perspective, the vertical reference frame and datum can be considered synonymous.

An important consequence of NZVD2016 heights being derived from NZGD2000 heights is that any updates or additions to a vertical deformation model associated with NZGD2000 will propagate directly and (almost[7]) without error into NZVD2016.

Note that the forgoing discussion about the relationship to NZGD2000 ellipsoidal heights does not imply NZVD2016 heights can only be observed using GNSS techniques. If the quasigeoid model is incorporated appropriately into computational software, precise levelling height differences, vertical angles and GNSS-based ellipsoidal height changes can all be seamlessly brought into a homogenous frame using the quasigeoid model. For example, this approach is taken with New Zealand's National Geodetic Adjustment (NGA), where the high absolute accuracy of GNSS complements the high relative accuracy of precise levelling (Broadbent, 2018).

2.5. Deformation modelling

Modern national geodetic datums need to account for rigid plate motion and deformation as appropriate. Where the area of interest is entirely on the rigid part of the tectonic plate, a three-parameter plate motion model is sufficient to model national scale deformation. In Australia, for example, such an approach works well (Stanaway et al., 2014b). In contrast, countries such as New Zealand which sits astride a tectonic plate boundary experiencing significant deformation. In such circumstances, a gridded model of deformation values is required (Crook et al., 2016).

[7] A large enough vertical change will theoretically impact the quasigeoid, but as discussed previously this is unlikely to be of any practical importance

2.5.1. Global approaches

2.5.1.1. Australia and Europe

The official geometric datum for Australia is the Geocentric Datum of Australia 2020 (GDA2020). This static datum is defined in terms of its relationship to ITRF2014, with coordinates and velocities at a fiducial network of 109 CORS stations being mapped to the reference epoch of 2020.0 using a plate motion model (ICSM, 2018). A plate motion model works very well across the vast majority of Australia, which sits on the rigid part of the Australian plate. For example, at the 109 fiducial CORS, the individual station velocities differ by less that 1mm/yr relative to the Australian plate motion model (ICSM, 2018). Internal deformation of the majority of the Australian continent is estimated to be less than 0.2mm/yr (Tregoning et al., 2013).

This stability means that Australia does not currently utilise deformation models as part of its datum, let alone high-resolution local models. This is likely to change in the future as Australia seeks to maintain a centimetre-accurate datum. For example, Australia was impacted by small but significant post-seismic relaxation associated with the 2004 Macquarie Ridge earthquake (Tregoning et al., 2013). At a more local level, examples include subsidence due to coal seam gas extraction in the Surat Basin, Queensland and water abstraction from Perth. In both of these cases, local high-resolution deformation models would be required to maintain datum accuracy.

Europe has many of the same geodynamic characteristics as Australia, mostly sitting on the stable part of the Eurasian Plate. For the majority of the continent, deformation models are not needed, it being sufficient to model the movement of surface features using a plate motion model. This is the approach used for EUREF, the European

Reference Frame (Boucher & Altamimi, 2011). For countries, such as Great Britain, on the stable part of the plate, there is a two-step process to transform coordinates between a global datum (as used by GNSS) and a national datum, as described in Boucher & Altamimi (2011). Firstly, parameters published by the International Earth Rotation and Reference System Service (IERS) are used to transform current ITRF coordinates to ITRF89, the global frame to which EUREF is aligned. At this stage, the coordinates are still at the observation epoch. Secondly, a plate motion model (in the form of three rotation rates) is applied to bring the coordinates from their current epoch to 1989.0. They are now in terms of ETRF89. Finally, a transformation is applied to bring the coordinates in terms of the official national datum. In the case of Great Britain, this is Ordnance Survey Great Britain 1936 (OSGB36), which as the year suggests, is a datum based on triangulation. Due to distortions in the network, the accuracy of a standard seven-parameter transformation is no better than five metres. Consequently, a distortion grid is used to transform between ETRF89 and OSGB36 (Ordnance Survey, 2018).

While most of Europe may be considered to sit on a rigid plate, there are many countries in southern Europe that are very much on the deforming part of the plate. For example, the national datum of Greece is the Hellenic Geodetic Reference System of 1987 (HGRS87), a non-geocentric, static, local datum (Chatzinikos & Kotsakis, 2017) defined before the widespread availability of GNSS, similar in that respect to OSGB36. To accurately transform from an ITRF-aligned global datum, a velocity model is required. Even then, distortions in the national datum mean that across Greece, the average accuracy of HGRS87 is no better than 0.45m (Chatzinikos & Kotsakis, 2017).

2.5.1.2. Japan

In contrast to Australia, Japan's location in a zone of very high seismicity means that the country experiences extensive internal secular deformation, as well as regular significant earthquakes. The official geometric datum is the Japanese Geodetic Datum 2000 (JGD2000), published by the Geospatial Information Authority of Japan (GSI) in April 2002. The static datum is aligned to ITRF94 at epoch 1997.0 (Tanaka et al., 2007). Initially, no provision was made for secular deformation, the assumption being that the vast majority of surveys take place over local areas where such deformation is negligible. But within a few years, investigations were underway to investigate the use of semi-dynamic corrections to account for this (Tanaka et al., 2007). By 2015, these corrections had been introduced to enhance the long-term stability and accuracy of the datum (Miyahara et al., 2015).

The most significant earthquake in recent times was the M9.0 2011 Tohoku earthquake. In the wake of this event, the geodetic datum was disrupted across much of the country, requiring extensive GNSS and precise levelling surveys to re-establish the survey control system. Where marks were not directly resurveyed, transformation parameters were developed for local areas and used to update these non-surveyed marks. This resulted in the publication of a new set of coordinates across much of the country, referenced as "Geodetic Coordinates 2011" to distinguish them from the previous "Geodetic Coordinates 2000" originally published for the datum (Miyahara et al., 2016).

While some of the terminology and technical details differ, Japan's approach to datum management in a complex geodynamic environment is very similar to that of New Zealand. To some extent, Japan can leverage its very dense GEONET CORS network to

enable some localised deformation to be easily monitored. But as discussed in section 2.3.2, even this very dense network, by CORS standards, is insufficient for highly localised deformation. Japan has therefore been actively investigating the use of InSAR, combined with field surveys, to identify and potentially model highly localised deformation. For example, after the 2016 Kumamoto Earthquake in southern Japan, InSAR was successfully used to identify highly localised surface displacements (Nakano et al., 2016). However, Japan is not yet incorporating models of highly localised, rapidly varying deformation into the national datum.

2.5.1.3. United States

The official geodetic datum in the United States is the North American Datum of 1983 (NAD 83). Realised just prior to the availability of accurate global reference frames and GNSS positioning, it is offset by approximately 2m from the ITRF (Soler & Marshall, 2003). Transformation parameters are published by the National Geodetic Survey (NGS) to enable users to account for this offset, as well as rigid plate motion (Soler & Snay, 2004). These transformation parameters were jointly determined by the United States and Canada, since both use NAD 83.

However, a three-parameter rigid plate motion model cannot accurately model the deformation experienced in the western third of the United States. To account for this residual deformation, the Horizontal Time-Dependent Positioning (HTDP) software has been developed to incorporate relevant earthquakes and crustal velocity models, facilitating more accurate transformations between the ITRF and NAD 83 (Pearson et al., 2010; Pearson & Snay, 2013).

Driven by changing technologies and greater accuracy requirements, the NGS is currently in the process of developing new geometric and geophysical datums for the United States, scheduled for implementation in 2022 (Roman, 2015). The four new terrestrial reference frames, one for each plate on which United States territory sits, will be aligned to the latest realisation of the ITRF and will use a plate motion model to rotate about an Euler pole with the stable part of the relevant plate (NGS, 2017).

While the final details of the new datum are not confirmed, the NGS has issued a blueprint describing the proposed implementation (NGS, 2017). The use of the plate motion model ensures that coordinates are static for the majority of users, in the eastern and central parts of the United States. However, unlike New Zealand, the United States is not proposing to formally account for secular deformation, earthquakes or other regional and local effects within the datum, noting that these will in many cases be provided as a separate product. In taking this approach, the NGS states that modelling all such phenomena to the level of accuracy that users typically expect of a datum would be technically challenging and fiscally irresponsible.

If this proposal is implemented in its current form, it would mean that the new datum presents as a static datum in the central and eastern parts of the country (in the absence of intra-plate deformation). But in the west of the country, in states such as California, the datum will present as dynamic, with residual deformation not accounted for by the plate motion model being reflected in coordinates that change over time. The blueprint recognises that dynamic coordinates are likely to be a complexity that many users are ill-equipped to manage. To address this, it is suggested that “epochs of convenience” might be defined every 5-10 years to enable static coordinates to be calculated using an intra-frame velocity model.

NGS (2017) makes a clear distinction between ‘geodetic’ accuracies and ‘surveying and mapping’ accuracies. The argument is that geodetic accuracies are only achievable through the use of a datum incorporating a plate motion model. If one defines geodetic accuracy to be at the level of 1-2cm, this would be true. In a practical sense, it is neither technically possible not fiscally prudent to model all deformation, right down to highly localised movements, to this level of accuracy.

But because the secular velocities and other deformation models are identified as a necessary product for the user community, it is clear that the NGS is not denying the importance of high-resolution modelling, merely indicating that it sees such models as an additional product supplied to those who need it, rather than being a core part of the datum. However this product might eventually be provided to users, the value of low-cost, high-resolution modelling to the new United States datum is clear.

2.5.2. New Zealand Deformation Model

The NZGD2000 standard defines the NZGD2000 deformation model, which enables transformation of coordinates to the reference epoch (nominally 2000.0) from any other epoch (LINZ, 2007). The standard anticipates that the deformation model will be updated as required, stating that *“coordinates at the reference epoch may be updated as required to account for new observations or localised ground movements”* and that the most current published version of the deformation model should be used.

When the standard was written in 2007, New Zealand had not experienced any earthquakes since the introduction of NZGD2000 that had significantly impacted the datum. Earthquakes in the southwest of the country in 2003 and 2004 had primarily

impacted the wilderness area of the Fiordland National Park, so there was no practical need to account for them in the deformation model.

2.5.2.1. Functional Model

The NZGD2000 deformation functional model is fully described in LINZ (2013). The model defines the offset at any given place and time between the NZGD2000 reference coordinates, nominally at 1 January 2000, and an ITRF96 coordinate at any other epoch. The deformation model consists of one or more submodels, each of which represents deformation related to certain geophysical phenomena/events.

For many years, the NZGD2000 deformation model consisted of a single submodel (Figure 3), a secular velocity model developed in the late 1990s from GPS data collected between 1990 and 1998 (Beavan & Haines, 1997; Beavan & Haines, 1998; Pearse, 2000). This secular model was significantly revised in 2011, based upon daily CORS processing from January 1996 to February 2011, as well as any campaign data occupation length greater than six hours. Data impacted by earthquakes were excluded. The data were processed by GNS Science against a network of Australasian IGS stations (Beavan, 2012).

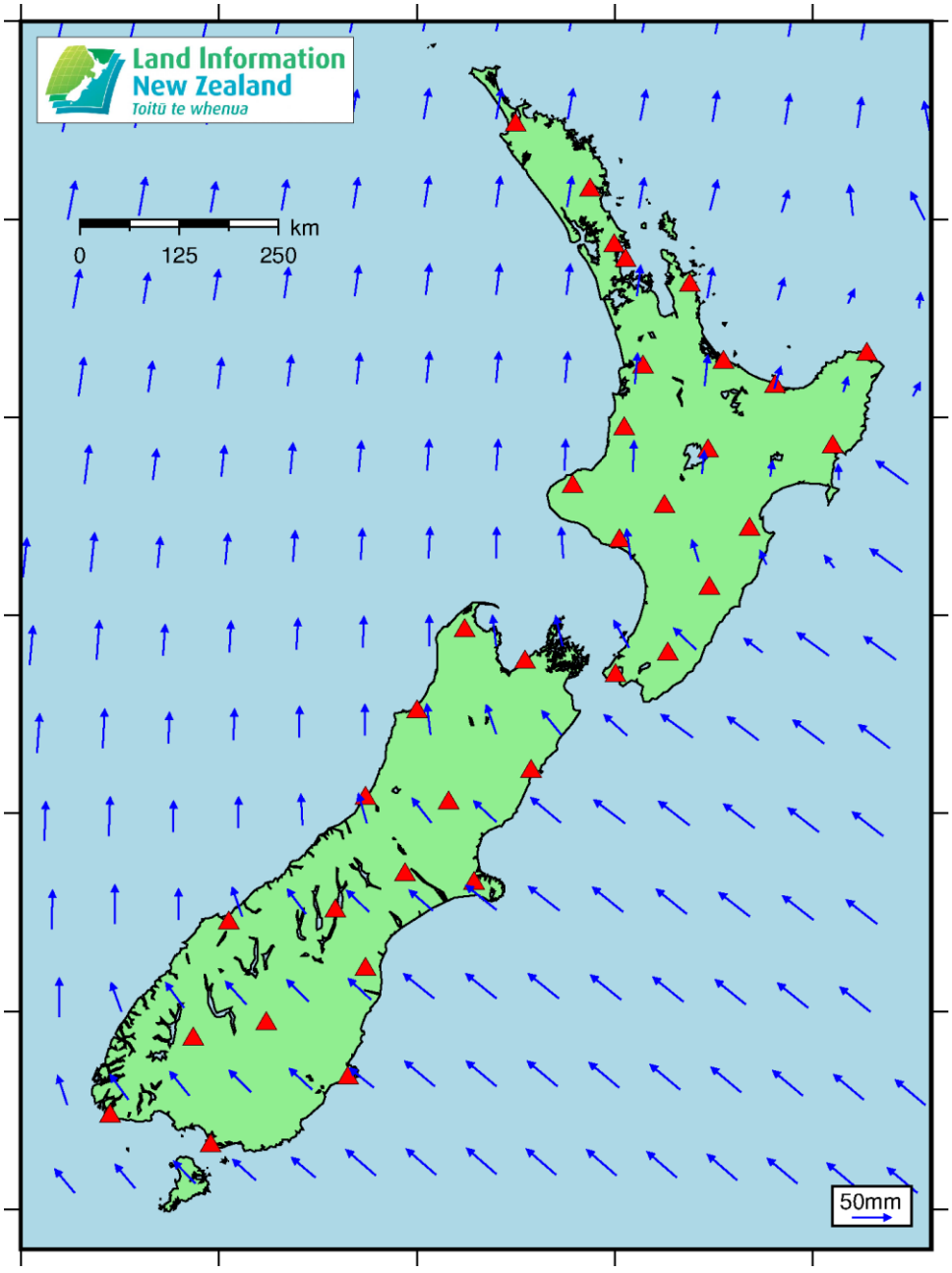

Figure 3: National secular deformation model.

Each submodel comprises one or more components, each of which represents the total deformation for that submodel. For example, for an earthquake there might be a component of coseismic deformation and another of post-seismic deformation. Each component defines a spatial extent and time function for the elements of deformation (horizontal and vertical) within that component. This enables the total deformation resulting from that component and therefore the submodel to be determined. Submodels

are either a national secular deformation model (of which there will only ever be one current version) or a patch. As the name implies, patches are used to account for movement that is not covered by the secular deformation model.

Figure 4 demonstrates how the secular deformation model is applied in practice to survey measurements.

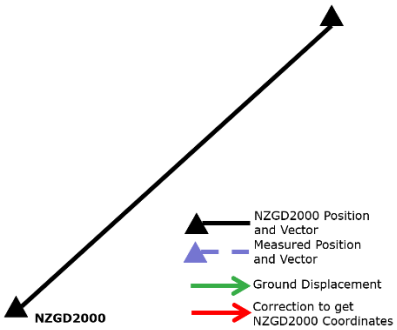

a) Black triangles represent two marks with NZGD2000 coordinates, and the black line the vector between them.

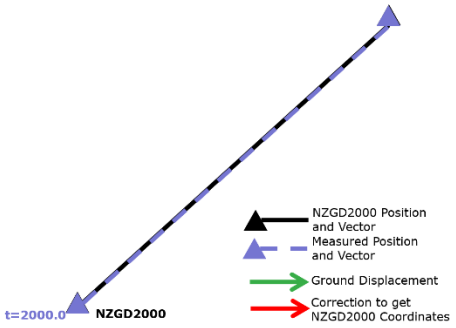

b) Measuring the line between these two marks in the year 2000 gives good agreement with the NZGD2000 coordinates.

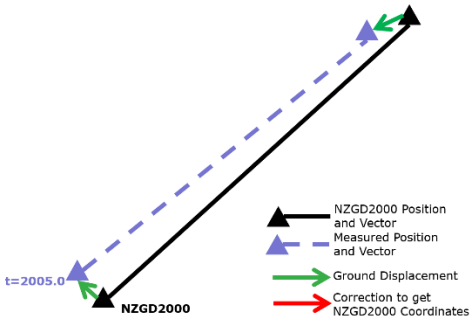

c) After 5 years the measured line is slightly different in both its length and direction. This is because each end of the line has been affected differently by the secular deformation, as indicated by the green displacement vectors.

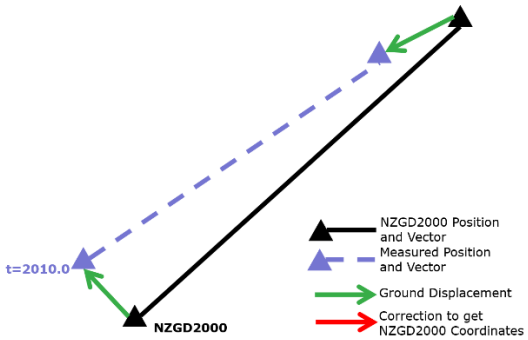

d) After 10 years, the measured line is different again.

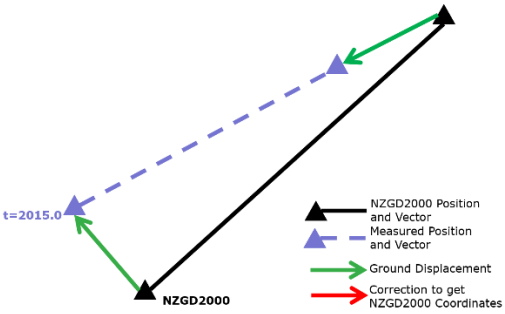

e) After 15 years the difference between the NZGD2000 and measured vectors has increased further. The size of this difference can be substantial

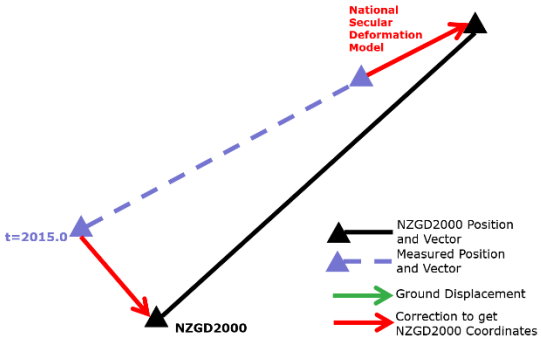

f) Applying the deformation model (specifically the national secular component), represented by the red vectors, ensures measurements made at any time can be used to produce NZGD2000 coordinates

Figure 4: Steps showing how real-world measurements diverge from the reference coordinates over time and how the secular deformation model enables reference coordinates to be generated from measurements made at any time.

Patches may themselves be one of two types: forward or reverse (Crook et al., 2016). These descriptors represent the time period for which the patch is applied relative to the deformation event. A forward patch is applied to all observations/coordinates ***after*** an event. It corrects those observations for the impact of the event and thus the NZGD2000 reference coordinates are the same after the event as before (within the limitations of accuracy of the model). Conversely, a reverse patch is applied to all observations/coordinates ***before*** an event, updating them for the impact of the event.

Forward patches are convenient in that they ensure the same reference coordinates are retained after the deformation event. There is no need to update geospatial databases to account for the earthquake. But forward patches lead to both conceptual and practical challenges. The conceptual challenge is that after an event such as an earthquake, users expect coordinates to change. In reality, the coordinates are just as able to fulfil their role as spatial references attached to ground-fixed objects after an earthquake, even with no change to the numerical values of those coordinates, but static coordinates after an earthquake are not intuitive. The practical challenge with forward patches is that they require all new data collected after the event to have the deformation model applied. This means that models need to be built into user devices and software, which is currently not the case. The steps for applying a forward patch, in conjunction with the secular deformation model are shown in Figure 5.

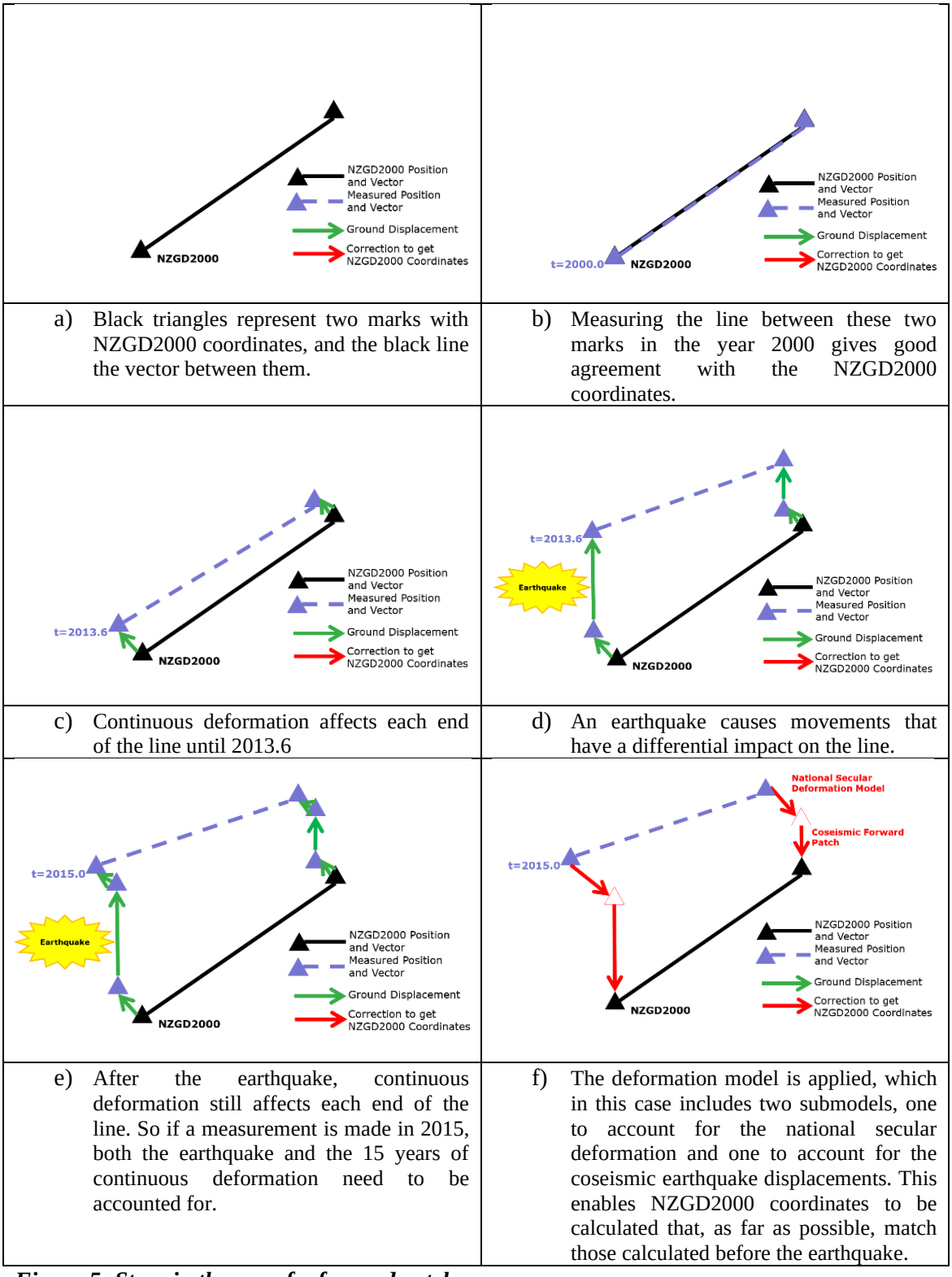

a) Black triangles represent two marks with NZGD2000 coordinates, and the black line the vector between them.

b) Measuring the line between these two marks in the year 2000 gives good agreement with the NZGD2000 coordinates.

c) Continuous deformation affects each end of the line until 2013.6

d) An earthquake causes movements that have a differential impact on the line.

e) After the earthquake, continuous deformation still affects each end of the line. So if a measurement is made in 2015, both the earthquake and the 15 years of continuous deformation need to be accounted for.

f) The deformation model is applied, which in this case includes two submodels, one to account for the national secular deformation and one to account for the coseismic earthquake displacements. This enables NZGD2000 coordinates to be calculated that, as far as possible, match those calculated before the earthquake.

Figure 5: Steps in the use of a forward patch.

Reverse patches are much more convenient from the perspective of the general user, as they only require the one-off application of the deformation model to the user's spatial data. This one-off update is applied by the geospatial data supplier/manager. Normally

the gridded patch model is applied through the GIS software being used to manage the data, for example as an NTv2 formatted grid (see section 2.5.2.2). The corrected data can then be fed to the general public.

<table>
<tr><td> 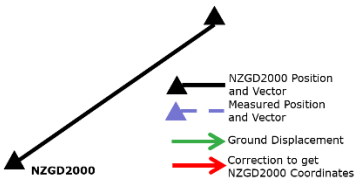
</td><td> 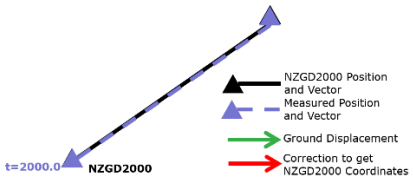
</td></tr>
<tr><td>a) Black triangles represent two marks with NZGD2000 coordinates, and the black line the vector between them.</td><td>b) Measuring the line between these two marks in the year 2000 gives good agreement with the NZGD2000 coordinates.</td></tr>
<tr><td> 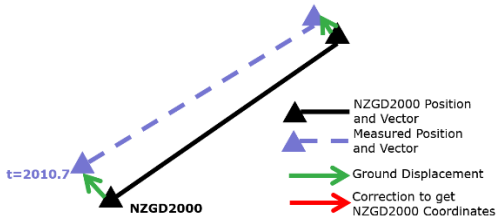
</td><td> 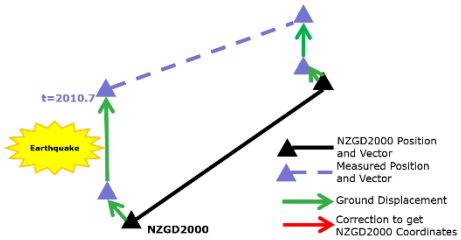
</td></tr>
<tr><td>c) Continuous deformation affects each end of the line until 2010.7</td><td>d) An earthquake causes movements that have a differential impact on each end of the line.</td></tr>
<tr><td> 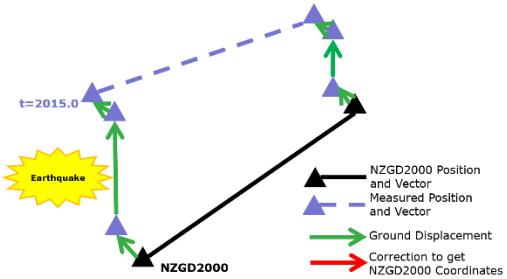
</td><td> 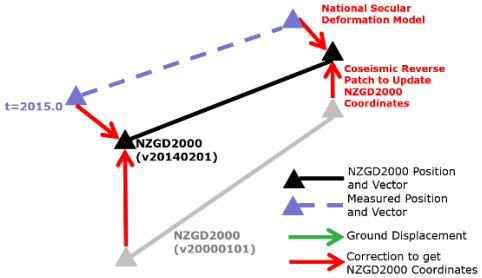
</td></tr>
<tr><td>e) After the earthquake, continuous deformation still affects each end of the line. So if a measurement is made in 2015, both the earthquake and the 15 years of continuous deformation need to be accounted for.</td><td>f) In this case the earthquake patch has already been used to update all the NZGD2000 coordinates existing at the time of the earthquake. This ensures that the official NZGD2000 coordinates reflect the earthquake movements. As a consequence, there is no need to apply the earthquake submodel to measurements made after the earthquake. However, the secular model still needs to be applied.</td></tr>
</table>

Figure 6: Steps in the use of a reverse patch.

The spatial representation for a deformation model often consists of a set of nested grids to recognise that a greater density of grid nodes is required where the deformation is greater (such as near a fault rupture). The time function can be a velocity, step, ramp or exponential decay function.

2.5.2.2. Format and Versioning

The full format of the NZGD2000 deformation model is detailed in LINZ (2013). It is published as a series of csv files in a nested folder structure. Each time the NZGD2000 model is published, the version is incremented by encoding a date within the model name. Each version of the model effectively corresponds to a new version of the datum. This is a consequence of the way in which NZGD2000 is implemented, through its defined relationship to the ITRF described in section 2.3.1. Since the definition of the ITRF does not change, applying the dynamic datum transformation which includes the new model will lead to the calculation of new and different NZGD2000 coordinates. These coordinates can be referenced unambiguously by including the version number.

An important component of the model format is that it includes all previous versions of the model, not just the current version. This means that existing NZGD2000 coordinates can be easily upgraded to a new version of the datum, so long as those coordinates have an epoch and the version of the deformation model used in their original calculation.

One of the biggest downsides of this format is that it is currently not supported by any commercial surveying or GIS software. Deformation models in general are not well-supported in commercial software, despite being an increasingly important part of many geodetic datums. It is unsurprising that a New Zealand-specific format is not supported in globally distributed software. However, this format has been created in the absence of

an international standard defining a format for deformation models that can incorporate the full range of requirements of a modern dynamic or semi-dynamic datum. As a practical measure, specific submodels of the NZGD2000 deformation model are converted to the NTv2 format developed by Natural Resources Canada. The NTv2 grid format is widely supported in software, and while it cannot incorporate the full information required for coordinate management using a versioned deformation model, the format works well in scenarios that solely utilise a step for the time function, as is the case for coseismic displacement. For many mapping and GIS applications, the accuracy is low enough that applying submodels for significant earthquakes via an NTv2 grid is sufficient to maintain the accuracy of that data. The current version of the deformation model is published on the LINZ website.

2.5.2.3. Current Components

Table 4 describes the 13 submodels that comprise the NZGD2000 deformation model.

Submodel	Description	Version added and updated
ndm	National secular deformation model	Added in version 20000101 based on igns1998b secular model. Updated in version 20130801 from igns2011 model for land and Nuvel1A for exclusive economic zone (which includes several offshore island groups not previously included in the model)
patch_c1_20100904	Darfield earthquake 4 September 2010	Added in version 20130801 as reverse patch
patch_c2_20110222	Christchurch earthquake 22 February 2011	Added in version 20130801 as reverse patch

patch_c3_20110613	Christchurch earthquake 13 June 2011	Added in version 20130801 as reverse patch
patch_c4_20111223	Christchurch earthquake 23 December 2011	Added in version 20130801 as reverse patch
patch_ch_20160214	Christchurch earthquake 14 February 2016	Added in version 20160701 as reverse patch
patch_cs_20130721	Cook Strait earthquake 21 July 2013	Added in version 20140201 as forward patch Updated to reverse patch 20160701 (model otherwise unchanged).
patch_ds_20090715	Dusky Sound earthquake 15 July 2009	Added in version 20130801 as reverse patch. Includes both coseismic and post-seismic components.
patch_gs_20071016	George Sound earthquake 16 October 2007	Added in version 20130801 as reverse patch
patch_ka_20161114	Kaikoura earthquake 14 November 2016	Added in version 20171201. Includes both coseismic and post-seismic components. Implemented with forward and reverse patch parts for both components, based on estimated strain rate. Updated in version 20180701 with reverse patch refinement grids for both horizontal and vertical movement
patch_lg_20130816	Lake Grassmere earthquake 16 August 2013	Added in version 20140201 as forward patch Updated to reverse patch 20160701 (model otherwise unchanged)
patch_mq_20041223	Macqaurie Ridge earthquake 23 December 2004	Added in version 20130801 as reverse patch
patch_si_20030821	Secretary Island	Added in version 20130801 as reverse patch

	earthquake 21 August 2003	

Table 4: Submodels within the NZGD2000 deformation model as at March 2019.

Several of these submodels are worthy of further explanation as the technical implementation attempts to reflect user expectations of the datum. The Lake Grassmere and Cook Strait earthquake submodels were implemented as forward patches in February 2014, within six months of the earthquakes. This relatively quick implementation from event to model update (compared with most of the other submodels) is partly because a forward patch results in no changes to coordinates. The patch gets applied to post-earthquake observations to bring them in terms of the datum (Figure 5). While this enabled the datum in the affected area to be restored quickly, the lack of coordinate change is confusing for users, when they are aware there has been an earthquake.

For this reason, in version 20160701 of the model, the forward patch was changed to a reverse patch, which led to the updating of geodetic coordinates in the area to reflect earthquake movements (Figure 6).

The Kaikoura submodel features the most complex implementation, including both forward and reverse patch sub-components. This hybrid approach is based on that described in Winefield et al. (2010), where a forward patch is proposed for the large area for which the deformation is small. A reverse patch is overlaid on the forward patch in the smaller region where the deformation exceeds some tolerance, based on geodetic accuracy standards.

The Kaikoura earthquake impacted the entire country at the millimetre level. Updating coordinates for relatively consistent horizontal movements in the far field of the

earthquake would have been disruptive for users, for little benefit. For example, horizontal movements in Wellington were relatively consistent and relatively small, being approximately 10cm in most of the city. Movement of 10cm is certainly significant for surveying and mapping applications, so it cannot be ignored. Hence this horizontal movement was included as a forward patch in the deformation model.

In contrast, the vertical movement was not included in the forward patch, even where it was relatively small. This relates to the fact that gravity-based heights are critical to the design, installation and ongoing management of engineered infrastructure. Even relatively small changes might be of importance for some applications.

2.5.2.4. Current Limitations

The NZGD2000 deformation model is relatively complex, accounting for numerous deformation events as shown in Table 4. But it is by no means comprehensive. There are significant parts of New Zealand where deformation is not modelled, or the modelling is insufficient to meet user expectations of the datum's capability to support ongoing management of accurate spatial data over time. Jordan et al. (2007) describe a conceptual model for including localised deformation within a national datum, using the August 2003 M7.2 Fiordland earthquake as an example of how the model might be applied.

For example, the Tahunanui Slump is an active landslide covering about 26 ha in the city of Nelson (Denton & Johnston, 2018). This complex rotation landslide is monitored by the local authority and regular resurveys have been undertaken over the decades. While on a national scale, this area of deformation is small, it is of significance to the local community, especially the approximately 120 households living on the active

slump. This is an urban area where normally the datum would be expected to support centimetre-level data management, but this is currently not possible without a localised deformation model incorporated into the national datum in standardised manner. Jordan (2005) developed a model of this landslide for datum management purposes using data ten-yearly terrestrial control surveys of the slip.

On a larger scale, there are significant towns and cities in the central North Island that are impacted by geothermal-related deformation. For example, parts of Taupo experience subsidence of up to 5cm per year, which is not included in any current deformation model built into the datum.

2.5.2.5. Definition of Localised

Some clarification of the term localised deformation is required, as it can refer to deformation of many different types and at many different scales. For example, in some contexts an earthquake affecting a quarter of the country might be referred to as localised deformation (Jordan et al., 2007). In other contexts, the movement of a single geodetic mark due to the impact of heavy machinery used for road maintenance could also be classed as localised deformation.

In this research, the term localised is used to refer to deformation that affects areas as small as 500m by 500m (25 hectares), or as large as an entire city and its surrounding area. The value of 25 hectares, which represents several urban blocks, has been chosen based on experience working with spatial professionals in the aftermath of the Canterbury earthquakes. For areas smaller than this, the deformation can be treated as an anomaly and there is little overall impact on district or city-wide data management. Beyond 25ha, the deformation is an integral part of the spatial reality for that area. It

becomes challenging and potentially expensive for surveyors to find stable survey control marks upon which to base their measurements. For spatial data managers, the size of the area where they cannot accurately manage spatial data becomes such that decision-making and efficient asset management is impeded.

2.6. Synthetic Aperture Radar

One promising observation technique for the modelling of deformation to high spatial resolutions is Synthetic Aperture Radar (SAR). This section describes the use of Interferometric Synthetic Aperture Radar (InSAR) to measure deformation. Details of the technique are available from several review papers that cover the topic (Bürgmann et al., 2000; Rosen et al., 2000; Simons & Rosen, 2015). Unless otherwise stated, this section is based on material in Simons & Rosen (2015).

2.6.1. Overview

The first use of InSAR for deformation studies occurred in 1993, when it was used to map deformation resulting from the 1992 Landers earthquake in California (Massonnet et al., 1993). For the first time, highly detailed visual representations of an earthquake were available. But the technique also provides quantitative information on the magnitude of surface displacements, in the direction of the line of sight to an overhead satellite orbiting at approximately 800km.

2.6.2. InSAR Data Processing

SAR systems operate at microwave frequencies (some of which are similar in frequency to GNSS). As an active remote sensing system, it provides its own illumination, sending

out pulses of electromagnetic radiation which reflect off “scatterers” on the surface of the Earth and back to the satellite-based sensor. The precision of radar measurements relates to the size of the aperture, which traditionally is limited to a few metres by physical constraints of the system. With an aperture of a few metres, the precision is very low and would be unsuitable for deformation modelling. However, a synthetic aperture can be created by combining a series of radar pulses as the satellite moves in space. This aperture can effectively be several kilometres in size, which with repeat passes and interferogram-formation, enables deformation measurements to be made at the level of a few millimetres. The radar sensor measures both the amplitude and phase of the returned signal.

Interferograms for deformation measurements are formed using two images collected from the same observation point at different times. These images are referred to as single-look complex (SLC) as the reflected data is a complex-valued quantity consisting of amplitude and phase information.

After resampling and co-registration so that pixels of the SLC images can be directly compared, an interferogram is formed which encodes the phase differences between the coherent pixels of two images. The interferogram is typically visualised as a series of interference fringes, each of which represents 2π radians of phase difference. This can be converted to a difference in metres using the wavelength of the signal, since each 2π radians of phase represents half a wavelength of displacement. The reason for the factor of 0.5 is that the full path of the signal requires it to travel both from and to the sensor. So, if the displacement is 10cm, then the signal travels an additional 20cm: 10cm extra on the way to the ground and 10cm extra on the way back. Figure 7 shows a typical interferogram generated using data from the Sentinel-1A satellite.

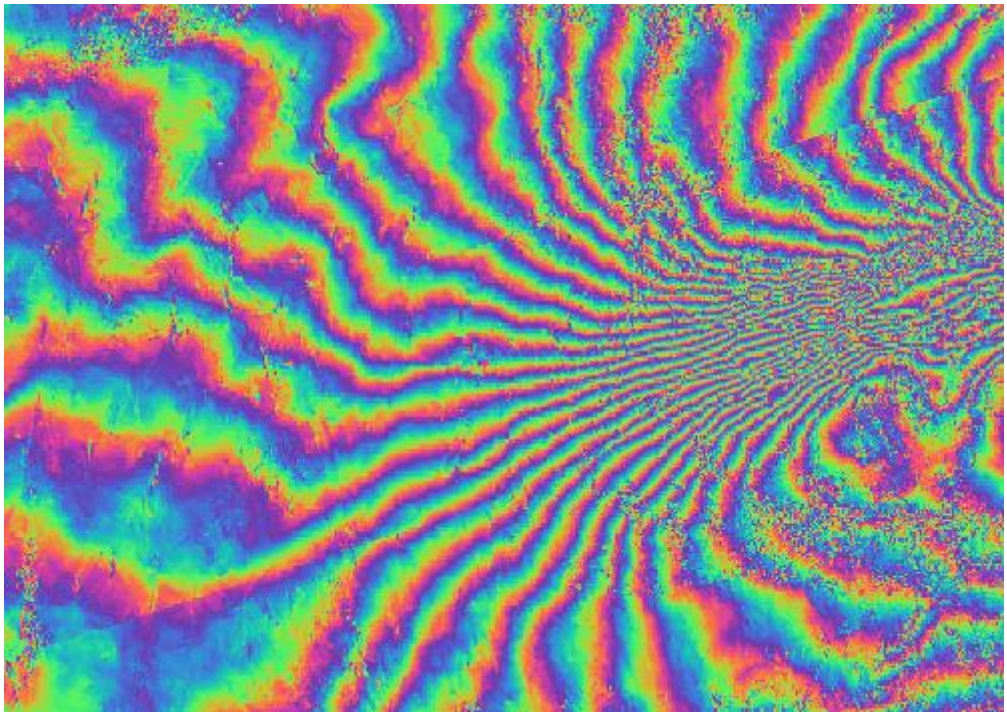

Figure 7: Typical interferogram (processed for the 2016 Kaikoura earthquake), with each interference fringe representing 2π radians of phase change. Data is from Sentinel 1A, so each fringe represents 2.8cm[8] of movement in the direction of the line of sight to the satellite.

Any difference in the phase is expected to be due to deformation if the sensor was in the same location when each image was captured. In reality, it is difficult to control the satellite track to the extent that observation points can be considered identical. The orbits may differ by hundreds of metres. This separation in space is useful for determining topography, enabling the images to be analysed in a manner analogous to the stereoscopic analysis of aerial imagery. But it is an additional source of phase change that needs to be removed for deformation analysis. This is typically done by using a Digital Elevation Model (DEM) to calculate the impact of topography on the total phase so that it can be removed, leaving only the phase component that is due to deformation. Techniques that involve removing the topography in this manner are typically referred to as Differential InSAR (DInSAR).

[8] This being half the wavelength of the Sentinel radar (5.6cm)

Once the topography has been removed, various filters may be applied to reduce the noise of the resultant image. The image is then converted from the radar coordinate system to a geodetic coordinate system by applying a terrain correction.

One of the key quantities computed during SAR analysis is the correlation or coherence of each pixel (the coherence is simply the magnitude of the correlation value). The coherence is 1 where the scatterers in the two pixels are completely coherent. For example, if there is a ground-based radar reflector in the pixel, then the coherence would be close to 1. Conversely, a value of 0 indicates that the scatterers in the two images are completely independent of each other. For example, where there has been major land damage due to liquefaction[9], totally changing the nature of the reflective surfaces between image acquisitions.

Figure 7 shows a "wrapped" interferogram, with the interference fringes clearly visible. This is very useful for visualising the location and magnitude of the most significant movements in an area. But the numerical values of the phase change at any point on that interferogram have a modulo-2π ambiguity. For most quantitative analysis, this ambiguity needs to be resolved so that the total or "unwrapped" phase change across an image can be found.

At a conceptual level, phase unwrapping first requires differencing the phase at each point of the image in each direction. Integrating over the entire image would then provide the total phase at each point. In practice, this approach would cause any errors to be propagated through the image, resulting in errors across the entire scene. Numerous approaches to unwrapping have been developed, in an attempt to solve this issue. But fundamentally, unwrapping is challenging or impossible when the phase has

[9] The loss of strength in solid material due to applied stress, such as during an earthquake, causing it to behave like a liquid

low coherence values. Figure 8 summarises the forgoing discussion, outlining a typical DInSAR processing sequence.

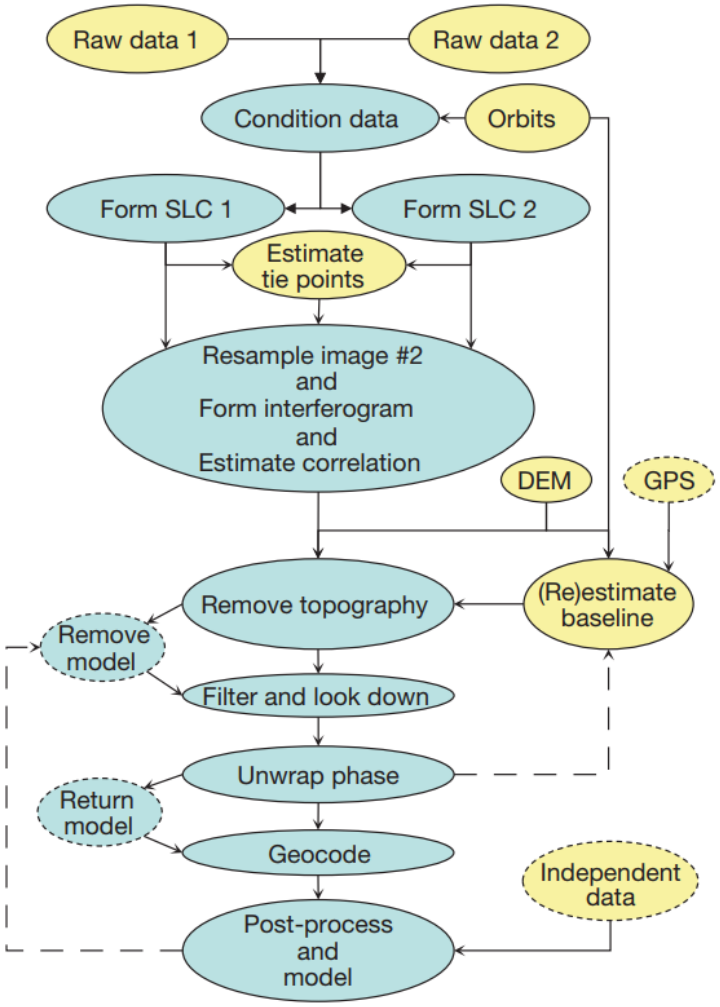

Figure 8: Typical DInSAR processing chain (Simons & Rosen, 2015).

2.6.3. Persistent-Scatterer Interferometry

As discussed previously, decorrelation (or incoherence) is a major challenge to successfully measuring deformation using SAR. One of the major causes of decorrelation is path delay resulting from variations in the atmosphere. As well as decorrelation, atmospheric effects can sometimes result in fringes being generated that

appear to be deformation, even though in reality there is none. The impact may not be so significant where the deformations are large (eg decimetre-level). But where the deformation being measured is smaller than a few centimetres, this can be a significant error source.

Persistent (or permanent) Scatterer InSAR (PS-InSAR) utilises particular scatterers in a stack of images that remain coherent over time (Ferretti et al., 2001; Ferretti et al., 2004). These persistent scatterers are identified by measuring the brightness of pixels. This requires that each image is radiometrically calibrated to remove variations in brightness attributable to variations in the sensor over a series of images. A pixel that consistently has high brightness over time is likely to have small phase dispersion and therefore be suitable for PS-InSAR.

Having identified the persistent scatterer points, the stacked interferogram is analysed to determine a consistent phase solution for that point, under some assumption about the nature of the deformation (eg linear or sinusoidal). The stack of interferograms typically consists of more than 20 images acquired over several months. Over this length of time, atmospheric error is decorrelated so can be averaged out.

Persistent scatterers can be any stable reflective surface, such as roads or roofs. Such scatterers occur at a much greater density in urban areas, which makes PS-InSAR a particularly valuable technique for urban environments. It is also highly accurate due to the removal of atmospheric error, with results often being accurate to a few millimetres.

2.6.4. Applicability to Geodetic Datums

InSAR is a highly accurate geodetic imaging technique, capable of measurements at the millimetre level in ideal observing conditions. It is already used indirectly in New

Zealand's geodetic datum, as one of the input datasets to the dislocation models developed by GNS Science that are used to model earthquakes within the datum. Its use for this purpose is likely to increase over time.

Overall, however, SAR data is heavily underutilised within the national geodetic datum. For example, its very high resolution compared with GNSS and other techniques makes it a natural technology to utilise for high-resolution, cost-effective, localised deformation models. It also has potential to be used directly as an observation, particularly for the vertical component. For example, it could be used to monitor change at passive control marks.

2.6.5. Vertical vs Horizontal

One of the characteristics of SAR is that it provides a displacement value in the direction of the line of sight to the satellite. For many applications this is sufficient, for example, where the displacements are used as input into an inversion used to create a dislocation model. But for datum management purposes, having the ability to resolve the InSAR-derived vector into vertical and/or horizontal components is important. Since the SAR sensor is emitting the radar signal primarily in the vertical direction, it is more sensitive to vertical displacements.

With respect to the east and north horizontal components, InSAR has some ability to resolve deformation in the east-west direction due to its near-polar orbit. However, deformation in the north-south direction is very difficult to resolve accurately, occurring in nearly the same direction as the sensor is travelling.

2.6.6. Data Availability

SAR data has traditionally only been freely available to academic and scientific institutes for research purposes. The government geodetic agencies that manage the national datum would typically be expected to pay for the data. While this is reasonable and probably necessary for the satellite operators to recoup costs, it has no doubt been a barrier to uptake.

With the launch of the Sentinel-1A satellite in 2014 as part of the European Union's Copernicus programme, this situation changed significantly. SAR data is openly and freely available from *Sentinel Online*[10], a data portal operated by the European Space Agency.

2.7. Cadastral Data

As discussed in the previous section, InSAR cannot accurately resolve the north-south component of a deformation field. Other remote sensing techniques, such as LiDAR are also far stronger in the vertical component than the horizontal. Passive GNSS control at typical geodetic densities is insufficient to model rapidly varying deformation. A dense, but horizontally accurate, dataset is required, preferably one that is freely and openly available. Cadastral data in New Zealand meets these requirements. Unlike InSAR, which is globally available, the accuracy and availability of cadastral data will be highly country specific.

[10] https://sentinel.esa.int/web/sentinel/sentinel-data-access

2.7.1. Cadastral Survey Datasets

All cadastral survey data is required to be submitted in digital form to LINZ as a Cadastral Survey Dataset (CSD). Included in the CSD are all the marks used and observations made by the surveyor. This includes observations connected to cadastral control marks. Bearings are provided in terms of one New Zealand's 28 meridional circuit projections. Distances are reduced to the ellipsoid. For strata and other 3D cadastral surveys, heights are supplied as a set of reduced levels. The surveyor is not required to supply coordinates as part of the CSD, these are calculated by LINZ as part of the data integration process.

A CSD is required to be certified for accuracy and completeness by a Licensed Cadastral Surveyor (LCS). It is then submitted to LINZ for approval and integration into the cadastre. The validation checks carried out prior to approval mean that any gross errors in the supplied data are likely to be identified and returned to the surveyor for correction.

The combination of surveyor licensing and independent validation by LINZ provide a high degree of confidence that approved cadastral data is of high quality.

2.7.2. Cadastral Coordinate Generation

Every CSD submitted into the Landonline[11] system is required to be integrated into the cadastre. The aim of integration is to build a seamless digital cadastre that is kept updated as new data becomes available. An essential part of integration is the calculation of coordinates for every mark included in the survey. At LINZ, this process is known as Cadastral Network Maintenance (CMN).

[11] Landonline is New Zealand's survey and title database and dataset processing system

CMN uses the least squares adjustment method to determine an optimal set of coordinates given a set of observations, observation uncertainties and constraints. The observations are supplied by the surveyor as part of the CSD. The uncertainties are assigned automatically based on characteristics of the observations when they are captured into the LINZ system. These characteristics include observation type, length of line, equipment type and the characteristics of the marks at each end of the observation (Donnelly & Hannah, 2006). The constraints (fixed marks) are determined by the cadastral analyst undertaking the adjustment.

The marks held fixed in the adjustment are required to be Order 6[12] or better geodetic marks. To generate reliable coordinates, at least two such marks are required in the adjustment for redundancy. Where the CSD does not contain two such marks, the cadastral analyst will attempt to add cadastral observations into the adjustment to provide the required connections.

An initial minimally constrained adjustment is run to determine observation statistics and identify potential outliers. Any outliers are investigated for errors and any errors found are corrected where possible. Where there is no evidence of gross or systematic errors with the observations, they are down-weighted until they are no longer flagged as outliers. This process ensures that the coordinate uncertainties calculated in the adjustment are consistent with the observation uncertainties. The adjustment is then authorised, which makes the coordinates available in Landonline.

[12] Order 6 is typically ‘street corner’ control, often calculated from survey control traverses

2.7.3. Data Availability

Where there is an earthquake resulting in shallow ground movement due to phenomena such as liquefaction, many new cadastral surveys are likely to be carried out. In the years immediately following the Canterbury earthquakes, hundreds of new CSDs were lodged with LINZ. These were typically driven by the need to re-define boundaries prior to rebuilding a damaged or destroyed property. Significantly, they provide a far higher density of survey-accurate horizontal positions than the geodetic system alone can provide. For example, geodetic marks in urban areas are separated by about 300m on average. Cadastral marks are separated by 20-50m so the spatial resolution they can provide is an order of magnitude greater than geodetic marks alone.

The distribution of cadastral marks is not even; they will tend to be denser in areas where there is more land damage and thus greater numbers of surveys carried out. One advantage of this is that the data will tend to be denser in areas where it will be the most useful for the recovery effort.

All cadastral and geodetic data is freely available from the LINZ Data Service (LDS), with the exception of the *crs_adjusted_observation_change* table, containing adjustment statistics associated with individual observations, which is available on request from LINZ.

Thus this modelling can be carried out without any additional data capture, making it very cost-effective.

The major limitation of using cadastral data for high-resolution modelling is that it takes time for sufficient cadastral data to be collected to use in the modelling. This is not a dataset that will typically be suitable for the initial post-earthquake response and

recovery. However, full recovery of the spatial system is a process that usually takes several years, in which time there would normally be sufficient surveys to complete the modelling.

2.8. Summary

This chapter has clearly established the need for high-resolution deformation models within a national geodetic datum. Users increasingly expect consistent, accurate spatial data, especially in urban areas. This is irrespective of the challenges posed by localised deformation that might vary rapidly over short distances, of which the average user of spatial data is typically unaware. While this local deformation may be significant from a cadastral, engineering or geodetic perspective, it is often not noticeable on a day-to-day basis, even by those who live or work in the affected area. Professionals regularly working with spatial data and familiar with local conditions can be expected to make allowances for inaccuracies resulting from localised deformation. Others, including those trying to make decisions on a national basis, whilst still accounting for local conditions, expect that this deformation is accounted for appropriately.

National datums exist to support accurate positioning in local conditions and accurate management of spatial data. Without high-resolution modelling, these objectives cannot be met across substantial urban areas in New Zealand. But the challenge goes well beyond New Zealand. Any jurisdiction of a reasonable size will have areas of localised deformation. Countries including Australia, Japan and the United States have recognised this, although the challenge of how to construct such models and incorporate them into the datum remains.

Approaches based solely on GNSS data, whether CORS or campaign data, cannot provide the density required. Alternatives must be considered. Two data sources have been identified as having considerable potential to support high-resolution modelling: digital cadastral data and SAR.

3. Shallow Ground Movement Modelling of the Canterbury Earthquake Sequence

3.1. Introduction

As discussed in Chapter 2, deformation modelling within a national datum is increasingly recognised as essential to maintain the levels of spatial consistency and accuracy that users demand. These deformation models have spatial resolutions that are typically of the order of kilometres. Even higher resolution models close to a fault rupture have spatial resolutions measured in hundreds of metres. For many purposes, the resolution of these models is more than sufficient, as the deformation does not vary substantially between any two nodes on the grid. However, in areas where deformation varies rapidly over short distances, these national or regional models cannot sufficiently represent the changes to the land to support accurate spatial infrastructure.

This lack of spatial resolution is particularly a problem for urban areas, where land is more valuable and densely developed. Engineered infrastructure is often designed to tighter tolerances and spatial data is collected and managed to a higher degree of accuracy. This impacts surveyors, infrastructure managers and spatial data managers. For example, after an earthquake, a surveyor re-establishing a property boundary needs to understand the size and direction of the land movements affecting that property. An infrastructure manager needs to know where buried pipes are now located. A spatial data manager needs to ensure that hundreds of pre-earthquake spatial data layers are consistent with post-earthquake data layers. The accurate management, or otherwise, of spatial data by the aforementioned professionals directly impacts the general public. For example, a property owner looking at a webmap showing their property boundaries

overlaid on post-earthquake aerial imagery expects to see those property boundaries coincident with fences, walls and other structures which were known to be on the boundary prior to the earthquake.

After an earthquake, there are often areas of highly localised deformation, whether due to proximity to a fault rupture or associated geophysical phenomena such as liquefaction. In this chapter, the 2010-2016 Canterbury Earthquake Sequence is used as a case study to demonstrate the development of a high-resolution deformation model utilising geodetically-corrected post-earthquake cadastral data.

3.2. The Dynamic Cadastre and the Canterbury Earthquakes

It has long been recognised that New Zealand's tectonic setting means that a dynamic cadastre[13] is a physical reality that needs to be reflected in the design of the nation's geodetic and cadastral systems. Grant (1995) proposed a new dynamic datum which could be used to maintain the accuracy of key national datasets, such as the cadastre. Further refinement of this concept during the mid and late-1990s sought to balance the dynamic reality of a country on an active fault zone with the practical realisation that a fully dynamic datum, where coordinates are updated frequently to reflect tectonic changes would not be useable with the software available at the time.

Aside from the issue of user tools, there were doubts as to the user benefits of coordinates that change frequently, particularly for datasets such as the digital cadastre which represent an abstract concept such as property boundaries. Even for engineering applications, where an accurate representation of physical reality is paramount, typical

[13] "Dynamic cadastre" refers to the fact that land is subject to change, such as due to deformation or erosion, which means that cadastral boundaries are subject to change.

variation in interseismic tectonic motion is sufficiently low that it is well within the tolerances of the vast majority of projects.

In Figure 9, relative movement due to secular motion exceeding 0.5ppm/yr is shown, which is equivalent to 5mm per kilometre over a period of ten years. By comparison, the most demanding cadastral relative tolerance is 100mm/km – it would take approximately 200 years for this standard to be breached, even in high-deforming parts of New Zealand, such as Wellington city. In this context it is difficult to see the value of updating cadastral coordinates to account for interseismic tectonic motion.

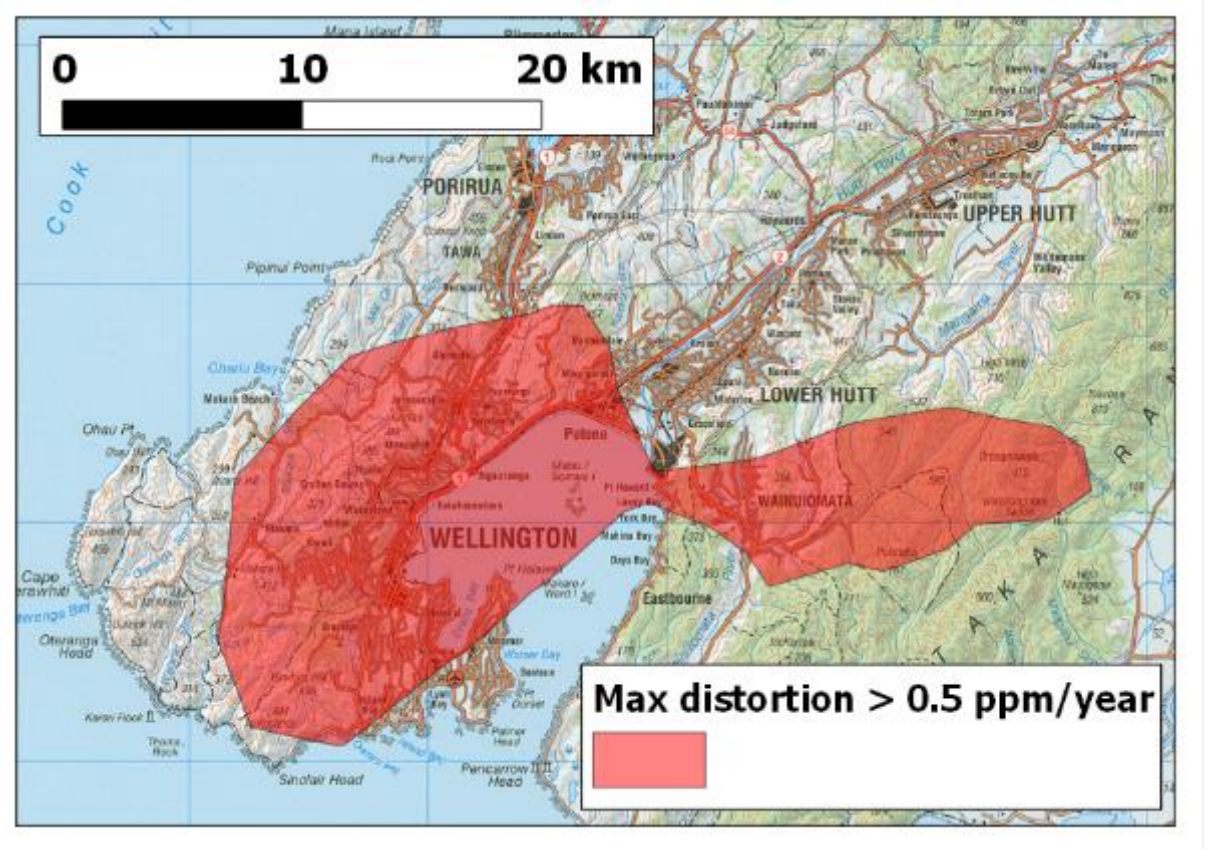

Figure 9: Relative secular deformation in Wellington.

Thus by 1998, LINZ had decided that a semi-dynamic approach to managing the geodetic datum and geospatial data would be optimal. The pragmatic semi-dynamic approach means that the spatial digital cadastre need only have its coordinates updated

when such an update would be of benefit to users of those coordinates. Earthquakes are a prime example of such a situation. Unlike typical interseismic motion, coseismic surface displacements often vary significantly over relatively small areas, particularly close to the fault planes. The semi-dynamic datum includes provision for coordinates to be updated in such situations (LINZ, 2007). For example, Figure 10 below shows areas (shaded red) where the maximum deformation exceeds 100ppm due to deep-seated tectonic movement. In this area, surveyors and others can expect to measure differences in excess of 1cm/100m, even in the absence of shallow ground movement.

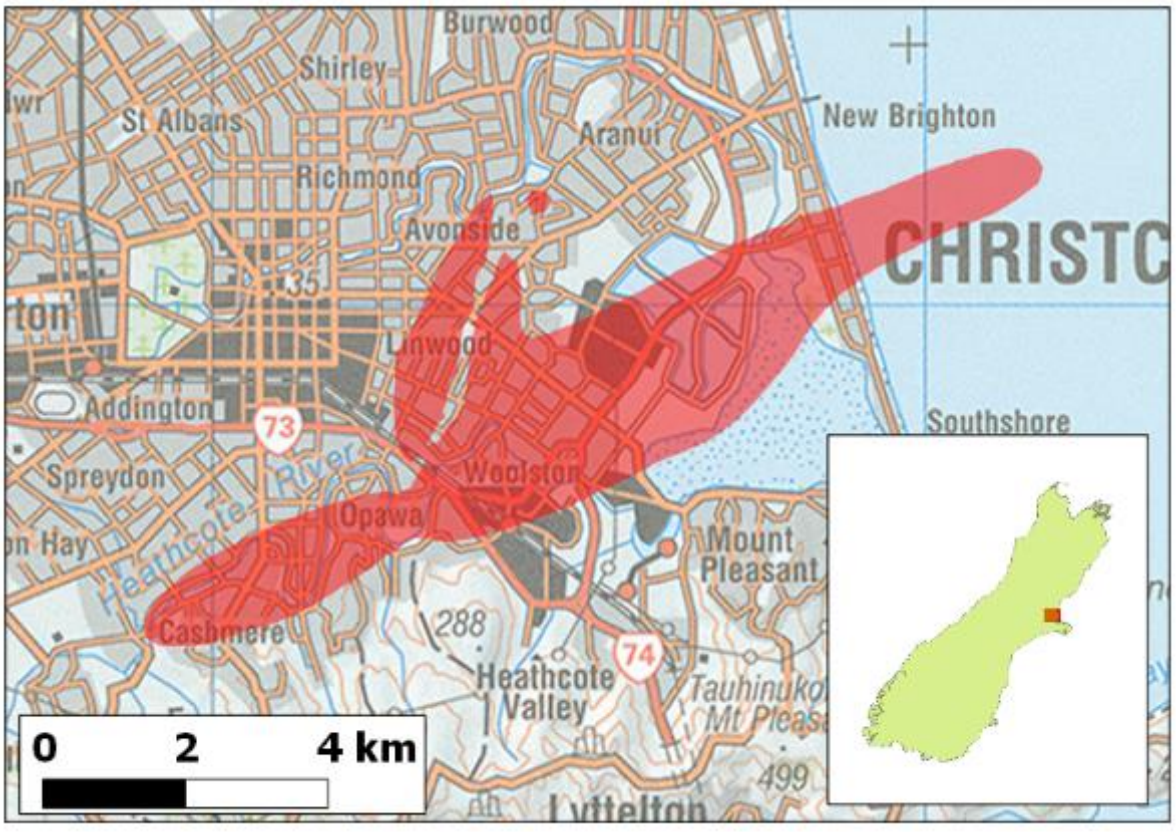

Figure 10: 22 February 2011 earthquake – area of deformation exceeding cadastral accuracy tolerances (100ppm) shaded red.

Grant et al. (2014) point out that to fully realise the concept of the dynamic cadastre requires due consideration of highly technical, but disparate areas of expertise: solid earth geophysics; geodesy; cadastral data management and land law. In the case of an

earthquake, solid earth geophysics is used to develop the dislocation model. Geodesy ensures that model has an accurate an unambiguous relationship with the real world. Cadastral data management expertise is required to manage the (potentially) millions of affected coordinates and land law specifies which types of movement should be reflected in cadastral updates.

The land law area of expertise is particularly challenging, relying as it does on abstraction of legal principles from limited statutes and case law and application of these principles to new situations, such as the large-scale shallow ground movement in Christchurch. Grant et al. (2014) details eight movement categories, remarking whether boundaries move with each category. It is concluded that boundaries move with deep-seated tectonic movement. This is self-evident in the case of secular motion, where there is clearly no value to updating the legal definition of property boundaries to reflect this gradual and imperceptible movement. Deep-seated earthquake movement is conceptually similar – the movements simply occur in a much shorter timeframe: seconds or minutes rather than hundreds or thousands of years.

In the case of liquefaction, the question of whether boundaries move with the ground movement is described as complex and Grant et al. (2014) make no firm conclusion. However, it is noted that New Zealand's cadastral coordinates are only updated for deep-seated movement using the deformation model (Crook et al., 2016).

Ballantyne (2016) suggests that an emphasis on the social dimension of the cadastre is required. He describes this in the context of the ongoing debate on the appropriate role of coordinates for boundary definition:

> "*The social dimension means that the parcel fabric is defined by coordinates only to the extent that they are efficient … are effective … are less invasive and are acceptable to those possessing and using the land"*

Adapting Ballantyne's concept to consider the social dimension as it relates to the Canterbury earthquakes, the dynamic digital cadastre should meet the following criteria:

Firstly, enable boundaries to be *efficiently* analysed and visualised with other spatial data. Landowners and infrastructure owners should be able to see at a glance how property boundaries relate to real-world infrastructure such as fences, buildings and utilities over large areas (eg all of Christchurch city).

Secondly, enable boundaries to be *effectively* analysed/visualised. Landowners and infrastructure owners need these relationships to be accurate. They want to understand whether their building that used to be on the boundary is likely still on the boundary, or is encroaching on the neighbouring parcel. While only a Licensed Cadastral Surveyor (LCS) can make this determination authoritatively, both the digital cadastre and other geospatial datasets need to have sufficient accuracy to make a reliable initial assessment, which could potentially lead to the engagement of an LCS.

Thirdly, enable boundaries to be analysed/visualised without recourse to *invasive* and detailed resurvey of every parcel.

Finally, enable boundaries to be depicted in a manner that is *acceptable to those possessing and using the land*. For the typical landowner, their only real exposure to the delineation of their property boundaries may be through web mapping provided by their local authority or some other entity that depicts their boundaries and buried utilities, overlaid on accurate aerial imagery. They need to be able to look at this web mapping

and have confidence that everything contained within the boundary lines is on their property, and everything outside the boundary lines is not. This criterion being successfully met is a logical outcome of meeting the first three criteria.

3.3. Motivation for High-Resolution Modelling in a Post-Earthquake Scenario

If the dynamic cadastre is to meet the four social criteria discussed in section 3.2, then a geodetic system capable of supporting these requirements is needed. This includes the deformation models upon which the cadastre and other geospatial datasets rely.

It is this social dimension that is the primary driver for the argument that a modern geodetic system must incorporate high-resolution deformation models. It is not sufficient for the geodetic system to simply provide a traditional network of active and passive control marks and models of deep-seated tectonic deformation. Note that this argument applies irrespective of whether or not property boundaries move with certain types of earthquake movement, a question that is far from settled in many jurisdictions. For example, if boundaries do not move with shallow ground movement, then the high-resolution model is required so that the location of engineered infrastructure can be accurately determined relative to those boundaries. If the boundaries do move with shallow ground movement, then the high-resolution model (see section 1.1) is required so that the digital spatial cadastre can be updated to reflect the legal reality as accurately as possible.

3.4. Canterbury Earthquake Sequence

3.4.1. Introduction

The Canterbury Earthquake Sequence commenced on 4 December 2010 with the Darfield Earthquake. This magnitude 7.1 earthquake was centred near Darfield, about 40 kilometres to the west of Christchurch. This was followed by earthquakes on 22 February 2011, 13 June 2011 and 23 December 2011. A further significant earthquake occurred on 14 February 2016.

The 22 February 2011 earthquake was particularly destructive, resulting in 185 deaths and widespread land and property damage, particularly in the eastern and southern suburbs of Christchurch city. Key details of the five major earthquakes are summarised in Table 5 and illustrated in Figure 11.

Date	**Magnitude (M_w)**	**Depth (km)**	**Distance from Christchurch CBD (km)**	**Reference**
4 September 2010	7.1	10	40	(Gledhill et al., 2011)
22 February 2011	6.2	5	10	(Kaiser et al., 2012)
13 June 2011	6.0	6	10	(Beavan et al., 2012)
23 December 2011	6.0	6	10	(Beavan et al., 2012)
14 February 2016	5.7	8	10	(Herman & Furlong, 2016)

Table 5: Major earthquakes in the Canterbury Earthquake Sequence

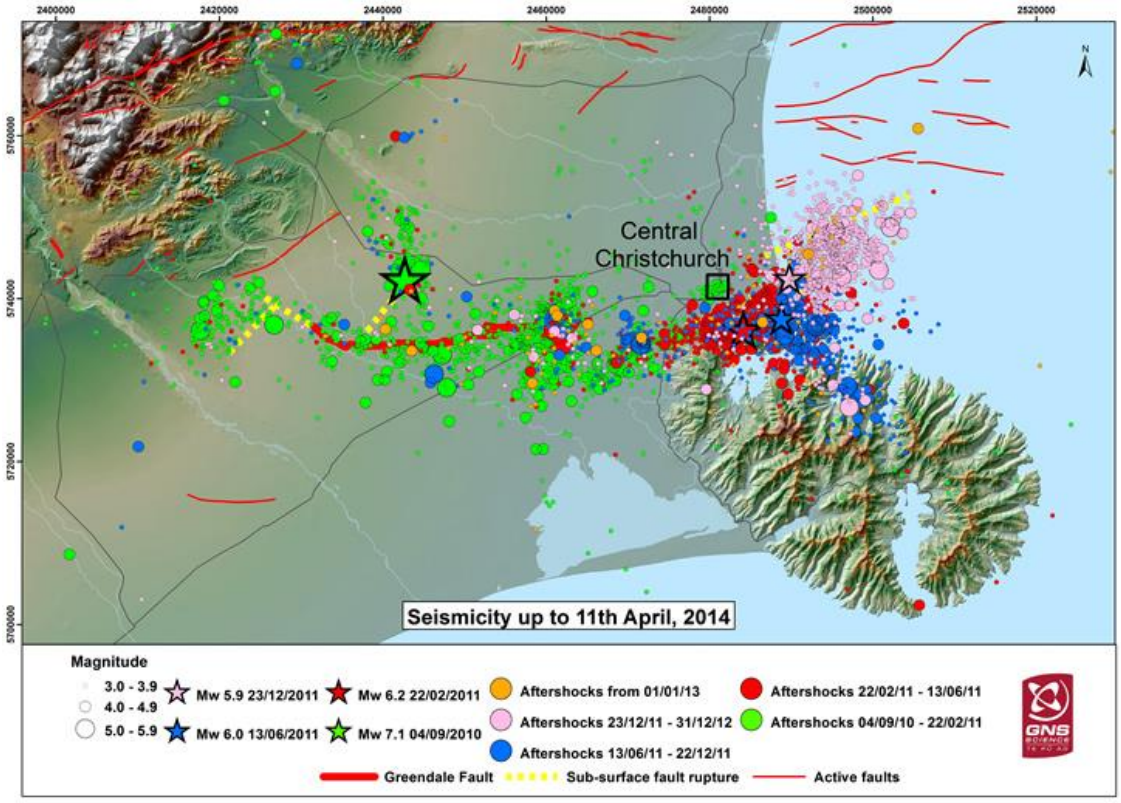

Figure 11: Location of earthquakes in the Canterbury sequence up to 11 April 2014. Supplied by GNS Science.

Figure 11 above shows the location and magnitude of the thousands of earthquakes that have impacted Christchurch since 4 September 2010. Note the west to east progression of the major earthquakes from 2010 to late 2011, as the crust was weakened and previously dormant faults were reactivated by the first earthquake in 2010 (Reyners et al., 2013). Of note for high-resolution modelling is that the fault traces of the three 2011 and the 2016 earthquakes coincide, at least in part, with Christchurch city. Thus as well as liquefaction, it is expected that there could be rapidly-varying deep-seated tectonic deformation in the city.

3.4.2. Deep-Seated Movement

There are two high-level categories of ground movement associated with earthquakes; deep-seated movement and shallow ground movement.

Deep-seated movement is driven by processes that occur at least several kilometres below the surface. This movement can be attributed to coseismic motion of the tectonic plates, which in turn drives the movement of deep sediments (Tonkin & Taylor, 2015b). This deep-seated movement is normally the dominant mechanism driving surface displacements over the extent of an earthquake-affected area. It is also well-modelled by geodetic dislocation models, particularly in the far field where lower seismic energy density makes the models less sensitive to assumptions about the structure of the upper lithosphere. For these reasons, it is deep-seated movement that the deformation models incorporated into geodetic datums seek to represent.

3.4.2.1. Data Collection

Three main datasets were collected for use in developing deformation models of the Canterbury earthquakes; seismic data, Interferometric Synthetic Aperture Radar (InSAR) and GNSS data. The GNSS data is particularly critical in the aftermath of an earthquake as it is also used to re-establish a network of passive control marks to support surveying as part of the recovery effort. The backbone of the post-earthquake GNSS data is provided by the CORS network owned by LINZ and GNS Science. These form an immediate post-earthquake fiducial network at which accurate post-earthquake coordinates in terms of the ITRF can be calculated within hours and updated as required to track post-seismic movements. The CORS in Canterbury have a typical spacing of

100km, although in urban areas, data was also available from CORS operated by private companies which increased the density.

While the temporal resolution of the CORS data is excellent,[14] the spatial resolution is insufficient for accurate modelling of deep-seated movement. It is also insufficient to re-establish a network of passive control marks at high densities. Therefore, in the aftermath of each major earthquake, GNSS survey campaigns led by GNS Science were undertaken. These surveys involved the collection of 48 hours of 30-second GNSS data at passive control marks throughout the affected region (Beavan et al., 2011). These marks are typically separated by 20km and are part of New Zealand's regional deformation monitoring network, which is resurveyed every eight years on a rolling basis by GNS Science, LINZ and the University of Otago (Beavan et al., 2016). In the Canterbury region, these stations had last been observed in 2008, so the pre-earthquake coordinates were still relatively recent when the first earthquake struck in 2010.

3.4.2.2. Dislocation Modelling

A number of published models[15] for one or more of the Canterbury earthquakes exist (Beavan et al., 2011; Beavan et al., 2012). These dislocation models are based on surface observations of ground displacements using GNSS and DInSAR. These observations are combined with *a priori* geological data about the location and characteristics of known faults that constrain the solution. Under the assumption that the earth can be treated is an infinite elastic half-space, the data are inverted to solve for nine key parameters of a fault plane. The *strike*, *dip* and *rake* describe the three-

[14] GNSS CORS data in the PositioNZ and GNS Science GeoNet networks is collected at 1 second intervals and permanently archived at 30 second intervals. See https://www.linz.govt.nz/data/geodetic-services/positionz

[15] All dislocation models discussed in this thesis were developed by GNS Science and are cited accordingly

dimensional orientation of the fault plane. The *slip* describes the magnitude of movement. The location is described by the parameters *latitude*, *longitude*, *depth*, *east relative location* and *north relative location*. A simple earthquake might be adequately modelled by a single rectangular fault plane, but it is often necessary to solve for many individual fault plane elements, particularly for complex earthquakes. For example, the dislocation model for the 2010 Darfield earthquake described eight separate faults using 974 rectangular fault elements. An example of these parameters is shown in Table 6 below and a visual representation of a dislocation model in Figure 12.

Parameter	**Value**
Strike (degrees)	86.1
Dip (degrees)	80
Rake (degrees)	159.431
Slip (m)	1.04731
Depth (km)	0.492504
Latitude (degrees)	-43.597473
Longitude (degrees)	172.076279
South (km)	-0.280986
East (km)	-9.96302

Table 6: Example 1km x 1km fault element parameters for the Greendale East-West fault from Model 8.2, developed 20 December 2011, GNS Science.

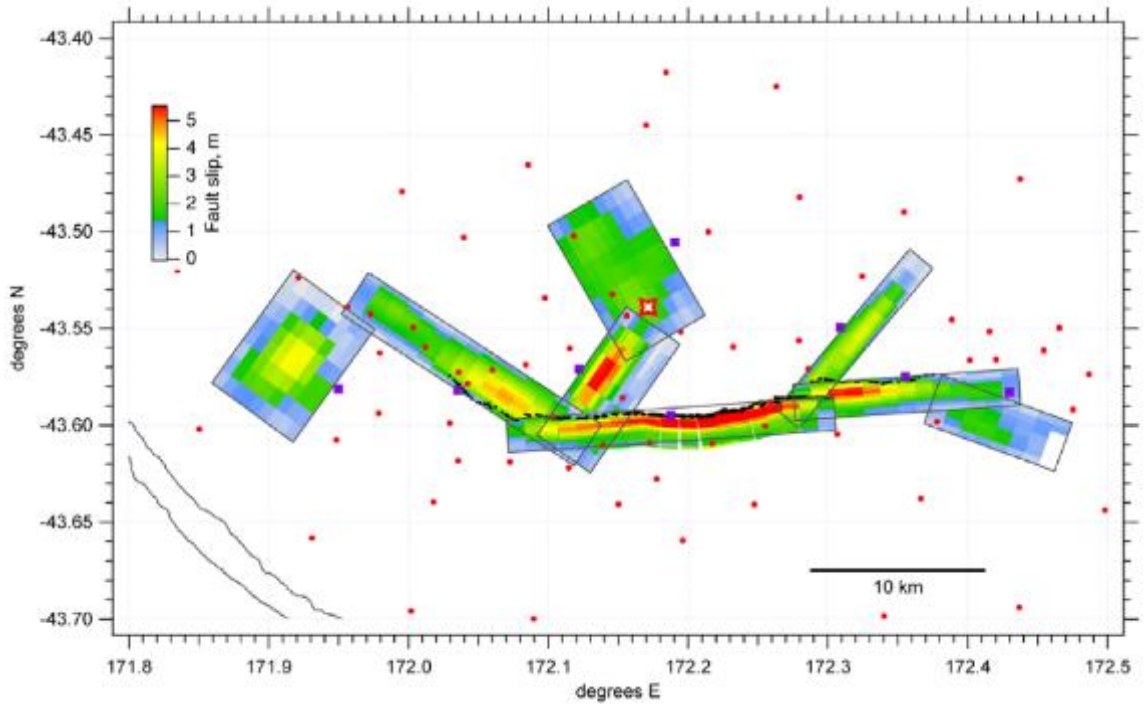

Figure 12: Geometry and slip distribution of Darfield earthquake dislocation model. Red dots are GNSS observation sites (Beavan, 2012).

Dislocation modelling is principally carried out for the purposes of understanding the geophysical mechanisms of a particular earthquake. They describe what is happening deep beneath the Earth's surface. This is of no direct relevance to the task of establishing or recovering a national datum after an earthquake. The real value from these models stems from the relationship to surface displacements, which can be calculated using Okada's equations (Okada, 1985). This means surface displacements can be calculated anywhere, even where surface data are sparse. In principle, this means that the datum can be re-established at all locations after an earthquake, once a dislocation model has been developed.

However, there are significant limitations to this approach when applied to real-world datum recovery situations. Figure 13 shows two common scenarios where dislocation modelling is not sufficiently accurate to recover the geodetic datum. Firstly, in areas close to the fault rupture, the dislocation modelling does not accurately predict surface

displacements. In the case of the Darfield earthquake, for the region within 15km of the fault ruptures, most residuals are at least several decimetres in magnitude. This provides a starting point for the analysis presented in Table 7 where analysis of residuals within various zones at increasing distance from the ruptures is used to estimate uncertainties in the model.

From a geodetic datum perspective, these discrepancies between observed and modelled deformation vectors can be treated as uncertainties and used to assess the accuracy of the datum if only dislocation models are used near a the fault. This uncertainty is inversely proportional to the distance from the fault, as shown in Table 7.

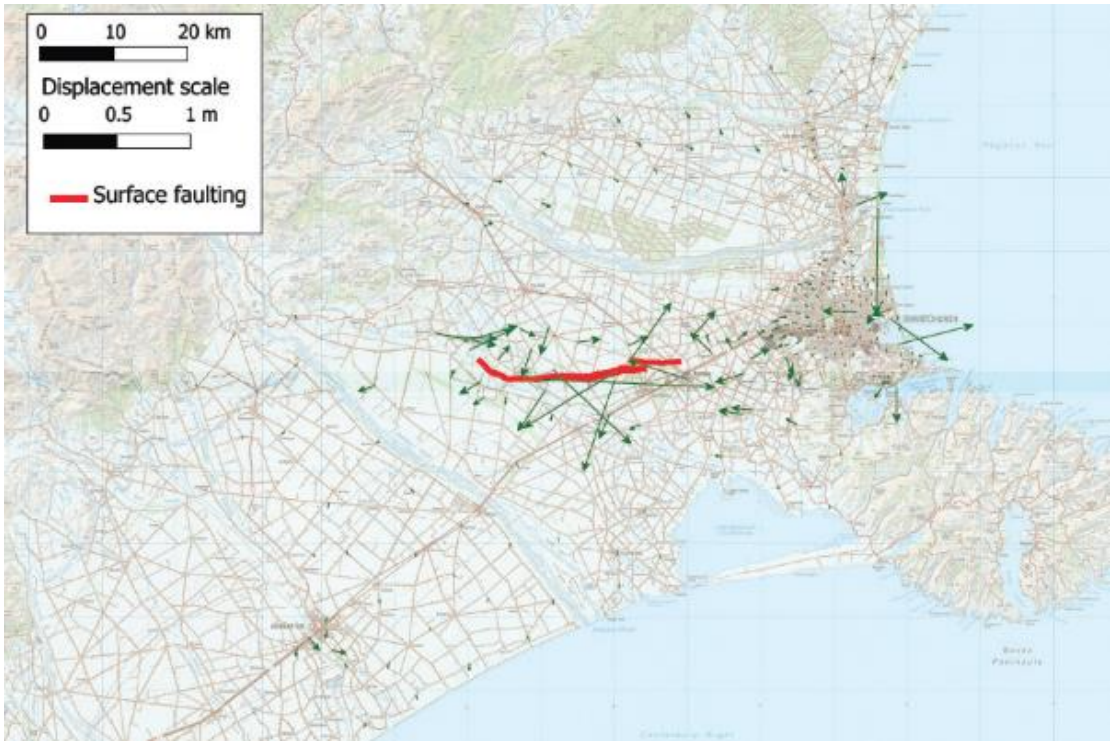

Figure 13: Difference between observed horizontal displacement from GPS and calculated displacement from dislocation model.

Description	Horizontal Uncertainty of Deformation Model (m) at 95% CI
Area up to 2500m from Greendale fault rupture	0.536
Area between 2500m and 7500m from Greendale fault rupture	0.251
Area between 7500m and 15000m from Greendale fault rupture	0.129
Area greater than 15000m from Greendale fault rupture, excluding south/east Christchurch (which is impacted by multiple earthquakes and shallow movements)	0.058

Table 7: Uncertainty estimates for the horizontal component of the Darfield deformation model.

Comparing the above table with the maximum absolute uncertainties as permitted for the least accurate level of cadastral control in New Zealand (0.15m), it is clear that dislocation modelling is not sufficient near the fault.

Secondly, a dislocation model does not account for highly localised effects such as movements due to liquefaction. In the case of the 2010 Darfield earthquakes, this liquefaction-induced deformation was relatively limited in extent. This can be seen by the fact that the large residuals in Christchurch were limited to individual geodetic marks, located near the estuary or rivers. The geodetic datum does not generally need to model such isolated instances of localised deformation, as there are still adequate stable and reliable geodetic control points near to the liquefaction-affected points.

In the February 2011 earthquake, the limitations of dislocation modelling were far more apparent, due to the widespread nature of the liquefaction-induced shallow ground movement.

3.4.3. Shallow Ground Movement

Tonkin & Taylor (2015b) identify five types of shallow ground movement, two impacting the Port Hills area to the south of the city and three impacting the flat land on which the rest of the city sits.

- Port Hills small-scale rockfall and ground movement.
- Port Hills large scale earthquake-induced landslides
- Flat land lateral spreading
- Flat land liquefaction-induced ground oscillation
- Area-wide ground stretching

Where these cover large areas, they impact on the geodetic system, which aims to provide an accurate and consistent datum over large areas. In practical terms, for a city such as Christchurch, a geodetically significant area is considered to be greater than 500m x 500m, approximately the size of a few city blocks. Where the shallow ground movement is more extensive, it becomes significantly more challenging and expensive for surveyors to identify and connect to stable control outside the affected area. This is also an area over which geospatial data managers are interested in being able to update their data, without needing to undertake additional post-earthquake surveys themselves.

3.4.3.1. Geophysical Mechanisms

The first type of movement, small-scale rockfall and ground movement is of little relevance to geodetic datum recovery, due to the limited extent of this type of movement. The other four are of interest as they have the potential to impact large areas of land, such that there are no unaffected geodetic control points within close proximity.

Large-scale earthquake-induced landslides were observed in significant parts of the Port Hills area to the south of Christchurch. One of the causes of these landslides is toe slumping, where failure of weak alluvial soils at the base of a slope leads to mass movement of land above the toe. These movements are typically up to 0.5m in magnitude (Tonkin & Taylor, 2015b). From a geodetic perspective, surface displacements are spatially correlated in the downslope direction, so there is potential for this to be modelled.

Flat land lateral spreading refers to the movement of land towards free faces such as water bodies (Tonkin & Taylor, 2015b). In Christchurch these water bodies were primarily the Avon River in the eastern suburbs and the Heathcote River in the southern suburbs. These parts of the city are nearly flat, with typically only gentle slopes towards the rivers. Again, there is a level of spatial correlation that suggests high-resolution geodetic modelling is likely to provide worthwhile accuracy improvements.

Unlike the two previously discussed mechanisms, liquefaction-induced ground oscillation is not so conducive to modelling. The reason for this is that ground oscillation results in movements that generally have low spatial correlation, because ground oscillation is caused by the shaking of the earthquake and is not related to free faces or slopes (Tonkin & Taylor, 2015b).

The final mechanism, area-wide ground stretching, is related to the large-scale topography of the city. Christchurch has an overall slope downwards from west to east, so in an earthquake, there is a tendency for the land to extend away from higher points in the city (Tonkin & Taylor, 2015b).

3.4.3.2. Impact on Geodetic System

The mechanisms of shallow ground movement are varied and complex. Where they cover only small areas, there is no need to incorporate them into deformation models, as it is possible to survey control points in nearby, more stable ground. But the ground deformation that results from many of these mechanisms extends hundreds of metres, or even kilometres. In these cases, the shallow ground movement needs to be accounted for in the geodetic datum, so that pre-earthquake spatial datasets can be appropriately updated to reflect real-world changes due to the earthquake.

3.4.4. Impact on Cadastral Boundaries

Shallow ground movement proved to be a particular challenge for the accurate re-establishment of cadastral boundaries. Extension and/or contraction of land over short distances meant that new measurements between survey marks often did not match those on the underlying CSD (Robertson et al., 2016). Prior to Christchurch, the assumption had been that individual parcels of land under survey moved as a block, and therefore the boundary dimensions would not need to change, with the exception of parcels at, or very close to, a major fault rupture. For parcels near the fault, new boundary dimensions might be required, which would be established in accordance with the long-standing principle that boundaries may change due to deep-seated tectonic movement. At an actual rupture, for example, this would mean that additional angles might be required in a previously straight boundary.

For shallow movement, the expectation was that boundaries would be re-established using a principle similar to that used for the re-establishment of boundaries after a landslide. That is, boundaries DO NOT move with the land and should be located such

that only deep-seated movement is accounted for. It is noted that while this was the LINZ opinion, it had not been tested in court and there were some in the surveying profession who disagreed with this approach. Those who disagreed often contended that adopting the landslide principle was not appropriate and that the position of monuments in the affected area should take precedence, irrespective of whether they had been affected by shallow ground movement. Ultimately, this legal issue was clarified via the enactment of legislation in 2016 that stated that in the case of shallow ground movement, boundaries move with the land. However, this question of deep-seated vs shallow ground movement was, for a time, of critical importance for surveying in Christchurch.

Numerous cadastral surveys were carried out in the years following the 2010 and 2011 earthquakes, primarily driven by rebuild requirements. Before construction work could commence on a new residential building in the most damaged parts of the city, the property would normally be resurveyed to provide confidence that the extent of land rights was consistent with the proposed new building and ensure compliance with local government planning requirements (Robertson et al., 2016). As these surveys progressed, it became clear that in a number of cases, the variation in land movements being measured across an urban-sized parcel were such that it was very difficult to confidently locate the boundaries using heretofore well-established principles of boundary definition. Furthermore, ambiguity in the available evidence of boundary location was leading to variations in determinations of the same boundary by different surveyors (Robertson et al., 2016).

From the above discussion, it is clear that the challenge was of a legal nature, rather than technical. With modern GNSS techniques, and appropriate recourse to the models

of deep-seated movement already published, it was possible to re-establish boundaries using either the “boundaries moved” or the “boundaries did not move” principle.

LINZ established a programme to develop a policy proposal for Government to consider a resolution to this issue. Given the high value of land and assets impacted by any policy proposals, as well as the impact on landowners and residents who had already endured many hardships as a result of the earthquakes, there was a strong requirement for the problem to be well-quantified and for the proposed solution to be backed up by strong technical evidence. An accurate model of shallow ground movements was essential to sound decision-making in this challenging situation.

3.4.5. High-Resolution Horizontal Modelling

Property boundaries in the parts of Christchurch that suffered the most serious damage were almost exclusively horizontal-only. Very few strata surveys were being undertaken. In any case, the nature of strata surveys is such that the risk of gaps and overlaps in the height dimension of the cadastre is low.

The two most obvious remote sensing techniques to consider for this high-resolution modelling were LiDAR and InSAR. In the vertical component, carefully processed LiDAR data, well-connected to the vertical datum, can achieve one-sigma uncertainties at the decimetre level or better (Tonkin & Taylor, 2015a). Horizontal positioning with LiDAR, however, is far less accurate. At one-sigma, the horizontal uncertainty of the Christchurch LiDAR data is 0.55m (Tonkin & Taylor, 2015b). While this level of accuracy is too low for many purposes, including cadastral analysis, LiDAR was considered to be one of the best options for developing a high-resolution model across the city.

Consequently, a sub-pixel correlation method was used by Tonkin & Taylor (2015b) to calculate a shallow ground movement model with a resolution of 56m. The relevant dislocation models published by GNS Science were used to remove the deep-seated movement to calculate a shallow ground movement model, an excerpt of which is shown in Figure 14.

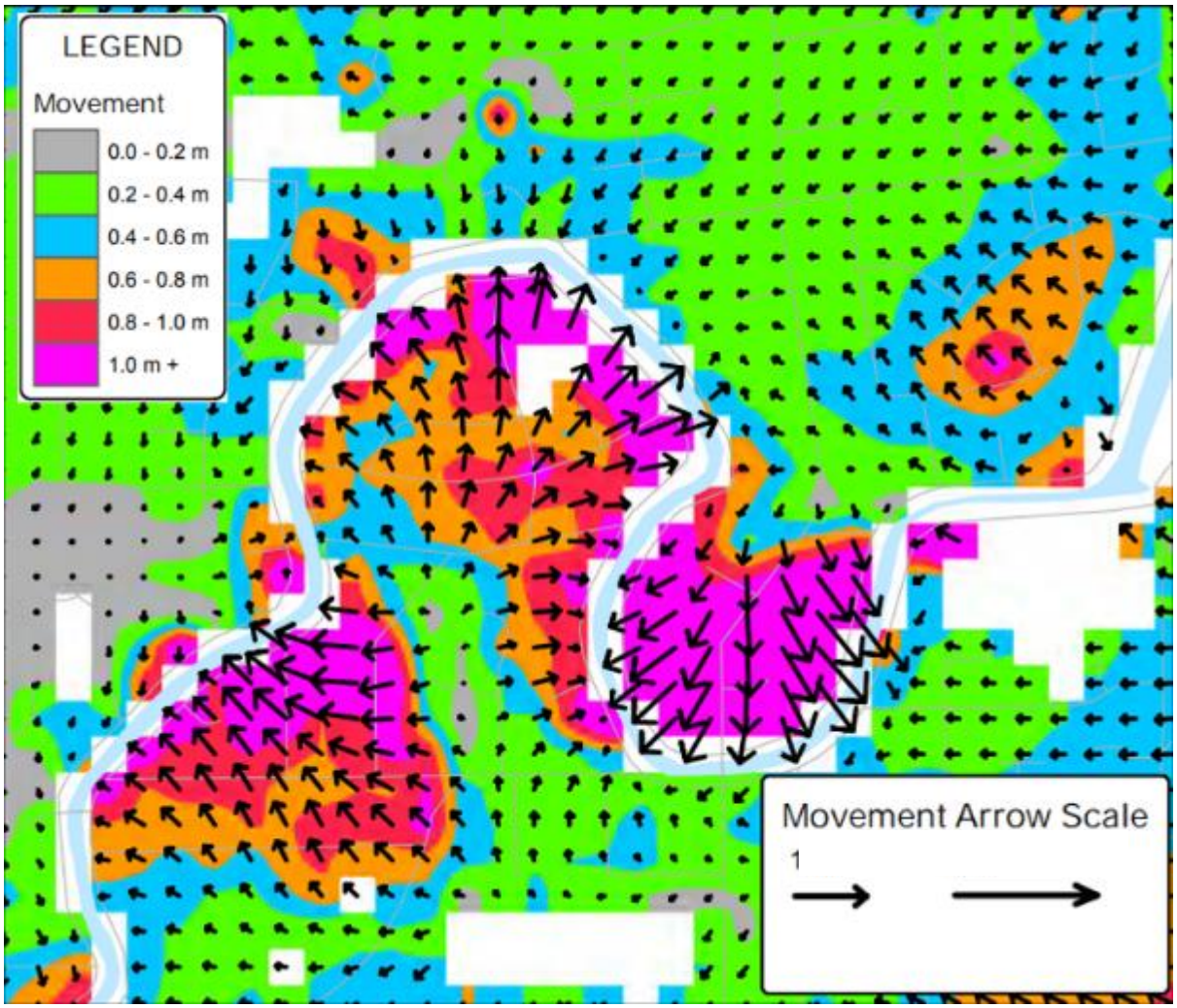

Figure 14: High-resolution horizontal shallow ground movement model derived from LiDAR showing Avonside and Dallington suburbs in Christchurch. Adapted from Tonkin & Taylor (2015b).

Figure 14 shows that while the modelled movements are large, they are relatively consistent. As would be expected, it shows the shallow ground movement vectors as

perpendicular to the Avon River (which runs through the centre of the image). This is entirely consistent with lateral spreading resulting from liquefaction and ground oscillation, where the land spreads on the downslope, towards free-faces such as river banks.

The high levels of consistency, however, are not expected and are at odds with the previous discussion about the significant challenges cadastral surveyors were experiencing in these suburbs and many others throughout eastern and southern Christchurch. This apparent uniformity is due to the large horizontal uncertainties in the LiDAR data. Therefore, while sub-pixel correlation of LiDAR provides valuable information about overall trends, it is not suitable for developing a high-resolution model suitable for inclusion in a national geodetic datum.

Another remote sensing option to consider is InSAR. There are two significant characteristics of InSAR that cast significant doubt on its utility in this particular scenario:

1) InSAR has poor horizontal accuracy, particularly in the north-south component. This is especially problematic in this scenario, due to the east-west orientation of the Avon River which means the greatest deformation is in the north-south direction.
2) The extensive land damage in the area of interest significantly reduces the chance of obtaining sufficiently coherent pre and post-earthquake images. Many scatterers are likely to have been destroyed or changed position in ways that have a significant component of apparent randomness. This is confirmed by radar analysis performed shortly after the February 2011 (Beavan et al., 2011).

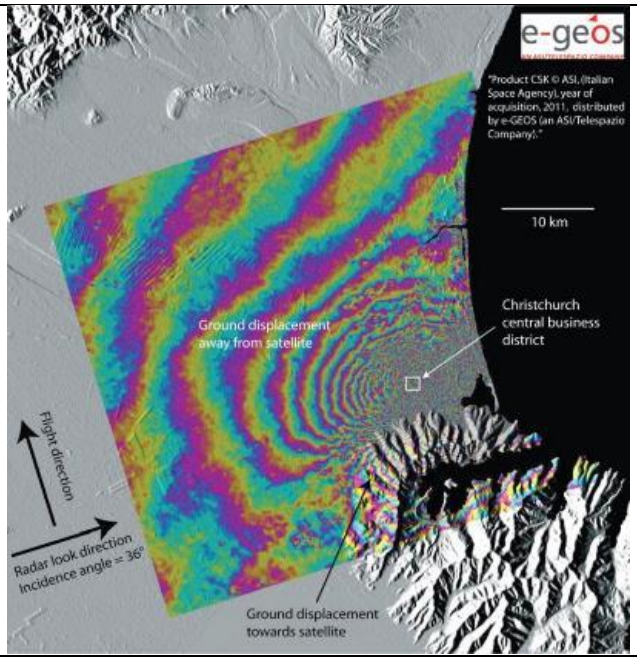

a) Interferogram for 22 February 2011 Christchurch earthquake (Beavan et al., 2011). Note the significant incoherence for the areas north, south and east of the central business district.

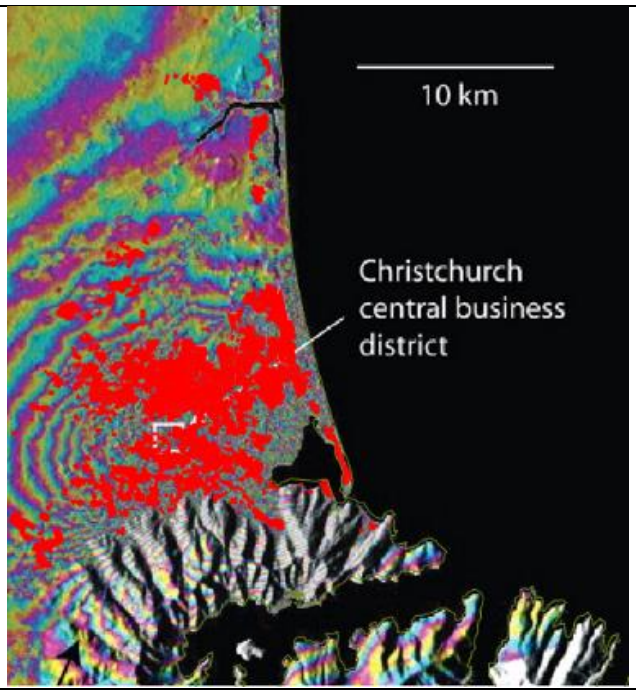

b) The interferogram from a) is enlarged around the Christchurch city area and overlaid with areas of land damage in red from Tonkin & Taylor (2012). The areas of land damage are correlated closely with the incoherent parts of the interferogram.

Figure 15: Interferogram over Christchurch showing the 22 February 2011 earthquake.

From these images, and the two points made above, it is concluded that in this particular case, InSAR is not an appropriate technique for high-resolution modelling.

At this point, it is useful to review the set of ideal characteristics for a high-resolution model:

- Dense dataset of pre and post-earthquake data
- Source data is free or low-cost
- High horizontal accuracy

Cadastral data meets these requirements. As discussed in section 3.4.4, numerous cadastral surveys were completed in the aftermath of the 2011 earthquakes. Cadastral data is highly accurate in the horizontal component, provides a high density of point observations in New Zealand, and is freely and openly available.

Cadastral data has not previously been used to develop a high-resolution model for incorporation into a national geodetic datum. However, there has been very limited use of cadastral data for geophysical analysis. For example, after the M7.6 Chi-Chi earthquake in Taiwan, pre and post-earthquake digital cadastral data was compared to determine coseismic displacements (Lee et al., 2011; Lee et al., 2010; Lee et al., 2006). From these displacements, various geophysical characteristics of the earthquake were inferred. The Chi-Chi scenario is very different to the Christchurch scenario. Firstly, the cadastral data used for the Chi-Chi analysis features consistent coordinates for pre and post-earthquake epochs, well-tied to the geodetic datum. For Christchurch the post-earthquake coordinates are highly inconsistent due to many of those coordinates being calculated prior to the geodetic control being updated, which occurred in December 2013. Secondly, the cadastral data for Chi-Chi was being used to calculate displacements due to deep-seated movement, and those displacements were almost identical over short distances. In Christchurch, displacements varied by several

decimetres over distances as short as 100m. Nevertheless, the Chi-Chi use of cadastral data demonstrates that it can be used for earthquake analysis.

3.4.6. Geodetic Refinement Model

It was essential to separate deep-seated and shallow movement in the Christchurch situation, due to the potentially differing impacts these types of movement have on cadastral boundary location. The four reverse patches for the 2010 and 2011 Canterbury earthquakes had been developed based on dislocation models and implemented into the deformation model. This section describes analysis carried out to identify and model additional deep-seated movement not included in these four official submodels.

3.4.6.1. GNSS Densification Data and Residual Deep-seated Movement

In 2012 and 2013, geodetic control surveys were carried out throughout Christchurch. Control marks were surveyed at intervals of approximately 300m using fast static GNSS techniques and the data published at the same time as the post-earthquake update to the deformation model and digital cadastre in December 2013.

In Figure 16, the difference between coordinates observed in this geodetic survey and those calculated by applying reverse patches to pre-earthquake coordinates is plotted. The reverse patches are derived from dislocation models, which only model deep-seated tectonic movement. Therefore, the vectors in Figure 16, are expected to represent only shallow ground movement. This is clearly not the case, as there are substantial areas in the plot where the vectors are highly correlated in both orientation and magnitude. For example, vectors throughout most of northwest Christchurch are oriented in a south-east

direction with a magnitude of 3-5cm. While small, this is significant at typical cadastral accuracies. A second, more significant, example occurs in the southeast of the city, where vectors across several suburbs are consistently oriented in a southwest direction, with a magnitude of 10-20 cm.

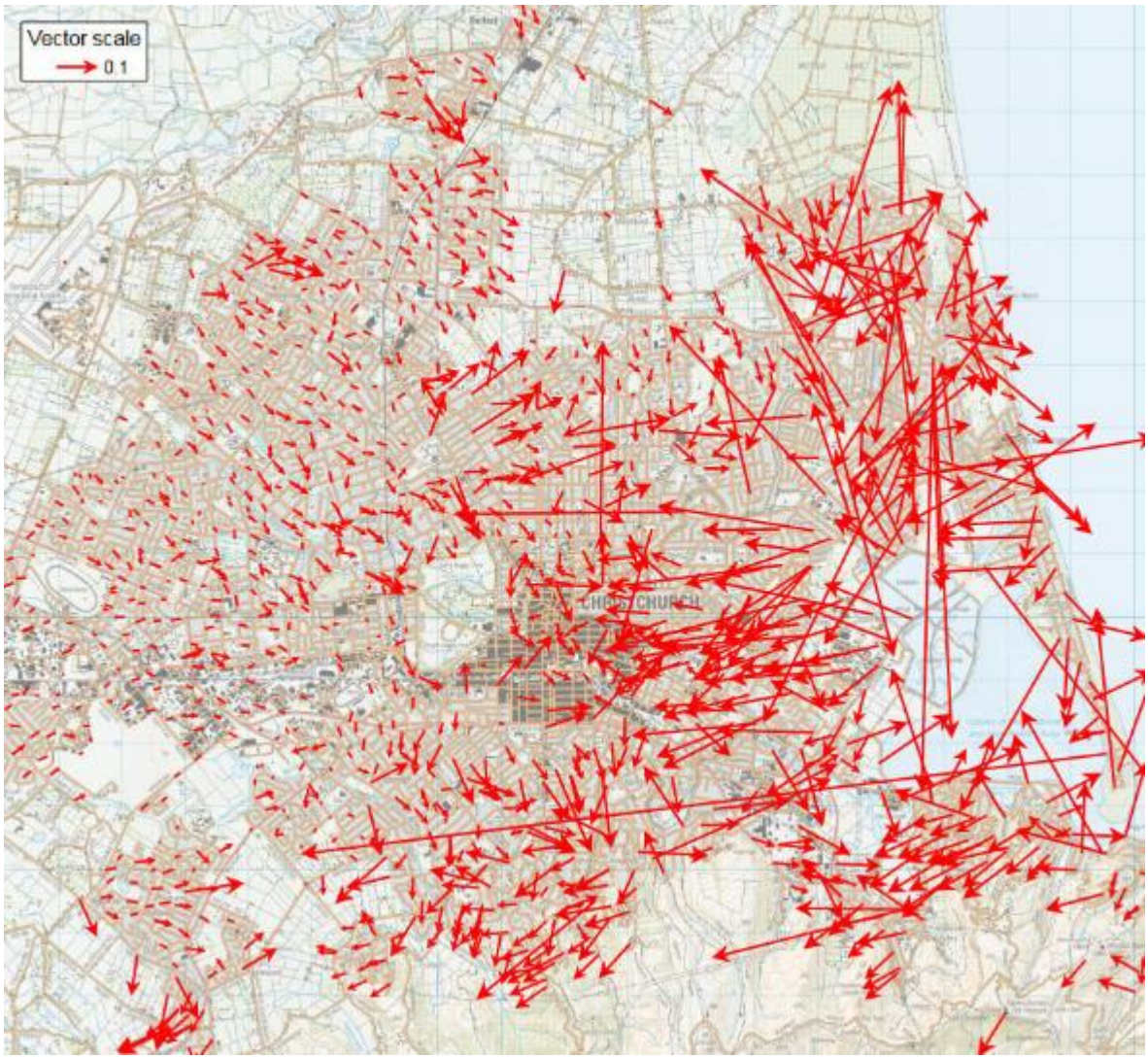

Figure 16: Difference in metres between observed horizontal coordinates and coordinates modelled using the four reverse patches for the 2010-11 earthquakes published in the NZGD2000 deformation model.

Thus, it is necessary to enhance the NZGD2000 deformation model to better account for deep-seated movement. The approach to doing this is to calculate a refinement grid based on the deep-seated movement residual displacement vectors in Figure 16.

3.4.6.2. Removing Marks Impacted by Shallow Ground Movement

The first step is to remove those displacement vectors that are affected by shallow ground movement. Due to the complexity of the factors determining whether movement should be considered deep-seated or shallow, the classification of vectors was done manually using several data sources. These data sources were:

1) Vectors of observed earthquake displacements, so that vectors could be compared with others nearby to assess levels of consistency
2) Vectors of residual earthquake movements (observed minus modelled, as in Figure 16), again so that vectors could be compared with others nearby
3) Topographic maps, so that elevation changes (potential for shallow landslides) and proximity to water bodies (potential for lateral spreading) could be assessed
4) Land damage mapping (Tonkin & Taylor, 2012)

In addition to the above four data sources, an algorithm was developed to quantitatively assess the likelihood that a mark was subject to shallow ground movement. The algorithm is as follows:

1) For each geodetic mark, find the nearest 5 geodetic marks
2) Calculate the vector to each of those 5 marks using only post-earthquake measured coordinates
3) Calculate the vector to each of those 5 marks using only post-earthquake modelled coordinates (ie deep-seated movement only is applied)
4) Calculate the difference between the observed and modelled vectors
5) If this difference is within the relative uncertainty tolerance for cadastral control marks, set status to ‘Pass’. Otherwise ‘Fail’

6) If all 5 vectors pass, then set the geodetic mark to ‘Pass’
7) Otherwise set to fail

Note that while this algorithm could be relied on when it assessed a ‘Pass’, it was less reliable at assessing failures. Some of these were false failures, as the algorithm did not adequately account for the possibility of differences caused by deep-seated movements near a fault, where deformation can vary rapidly over short distances. Therefore, it was not used to fully automate the process of identifying marks affected by shallow ground movement. But it provided a very useful filter to enable attention to be focussed on the more complex situations.

Using the four datasets above, plus the results of applying the above algorithm, the following factors were considered in making the final assessment:

1) Overall level of agreement with other observed earthquake movements within 1-2km (deep-seated movement is expected to be consistent (or gradually changing) over a fairly wide area)
2) Proximity to fault traces (further from fault, yields greater confidence that a discrepancy indicates shallow movement. Deep-seated movement varies more rapidly close to the fault)
3) Whether observation was in an area of known land damage

Marks flagged as being impacted by shallow ground movement were excluded from the modelling discussed in the next section.

3.4.6.3. Model Generation

To generate gridded models from dense datasets where the displacements can vary rapidly over short distances, such as near the fault, a modelling method which has high

fidelity to the observed data is required. The method selected was Inverse Distance Weighting (IDW), which weights all the data points within a specified radius of the grid node by the inverse of the distance to that point (or the inverse of the distance raised to some power):

$$\boldsymbol{w = \frac{1}{d^n}} \quad (1)$$

where:

w = weighting

d = distance from grid node to data point

n = power index (for example if n = 2, then the weighting is inversely proportional to the square of the distance)

This method puts greater weight on data that is close to the grid point being calculated. Use of IDW can sometimes lead to a "dimpling" effect as data points that are significantly different to other nearby points have an undue influence on the value at that grid point. To counter this, a filter can be applied to smooth the model, which averages data points within a user-specified radius.

The specific parameterisation of the IDW model will depend on the characteristics of the data and is typically determined by trial and error. For this refinement grid, the following characteristics were required:

1) Deep-seated movement is accurately represented at suburb scales (1-2km)
2) A smoothly varying model, as this is characteristic of deep-seated movement
3) Minimal influence of outliers
4) Minimal influence of data points on the 'other' side of the fault

The *gdal_grid*[16] open source raster analysis software was used to do the modelling by means of IDW. This is part of the *gdal* software stack that can be freely downloaded from the gdal website. The IDW algorithm included in this software includes a number of parameters, the most useful of which are:

- Search radius: Can set an elliptical or circular search radius
- Power: Set the power to which the distance is raised in the denominator of the IDW equation
- Smoothing: Width of the smoothing filter to be applied

Determining the most appropriate parameters to meet these four criteria was a process of trial and error. Finally, the following parameters were confirmed:

  - Search radius = 0.02 degrees (equivalent to 1600m east, 2200m north)
  - Power = 1
  - Smoothing = 0.005 degrees (equivalent to 400m east, 550m north)

The final grid had a resolution of 250m x 250m, this being chosen as the geodetic data used to create it had a typical density of 200m-300m.

3.4.6.4. Incorporation into the National Datum

Following the discussion in section 2.5.2.1 about the structure of the NZGD2000 deformation model, this model of the residual tectonic movement for Christchurch City becomes an additional submodel of the overall model. The question arises as to whether the model should be a forward or reverse patch. In this case, the decision is straight-forward, based on the fact that the model was calculated *after* the post-earthquake geodetic control coordinates in the city had been published and in use for several years.

[16] https://gdal.org/programs/gdal_grid.html

These published coordinates reflected actual earthquake movements. A key requirement for a submodel is that it can be used to produce coordinates that are consistent with official datum coordinates. Therefore, it must be published as a reverse patch. This means that if new post-earthquake observations are made between geodetic marks in Christchurch, the new submodel does not get applied, since those observations will already agree with the post-earthquake control. However, if pre-earthquake data is being updated, it does need to be applied. In the case of Christchurch, this submodel was developed after most spatial datasets had already been updated using a cumulative displacement NTv2 grid of the four submodels for the four major events. Spatial data managers would need to apply the additional deformation from the new submodel, being careful not to re-apply submodels they have already used. This highlights the importance of clear metadata when working in areas impacted by earthquakes.

All other submodels in the overall NZGD2000 deformation model (with the exception of the secular deformation submodel) relate to a specific earthquake, which leads to a logical naming convention using the event date in the name of the submodel. This new submodel relates to all four major earthquakes to impact Christchurch, since it was based on geodetic GNSS data collected after the last major earthquake of the 2010-11 sequence. Thus the name given to this submodel was “patch_cc_2010_11”.

If this submodel were to be officially incorporated into the national datum, then this would increment the version of the overall NZGD2000 deformation model. The naming convention is to choose the date of publication, rather than the date of the event to which the new version of the model relates. For example, if the updated deformation model were published in July 2015, the model would be named “nzgd2000_deformation_model_20150701”.

3.5. Cadastral Survey and Analysis

3.5.1. Earthquake Impact Zones

The deformation to be modelled has occurred as the result of an earthquake sequence, rather than a single event. This presents a particular challenge when attempting to derive a model within as short a timeframe as possible to aid the recovery effort. Each earthquake in the sequence has the potential to invalidate data collected prior to that earthquake. For example, land movements due to the 13 June 2011 earthquake could mean that observations made prior to that date are not reflective of the total movement due to the sequence. But in the case of an earthquake sequence, each earthquake will generally have an impact on a different part of the overall region. While it would be simple to exclude data prior to the most recent earthquake event, this approach would lead to the exclusion of significant amounts of data collected early in the sequence which provide valuable information. This is particularly true for the Canterbury sequence, where there was a significant earthquake on 14 February 2016, more than 5 years after the initial earthquake. It is therefore important to consider the extent of the impact of each major event in the sequence when deciding which data to include in the model.

Dislocation models are produced by GNS Science as part of their research into each earthquake (Beavan et al., 2012). From these dislocation models, LINZ derives grids of surface displacement and publishes these as one of the key products of its national geodetic datum (Crook et al., 2016).

The deformation grids for each of the five major earthquakes in the sequence were imported into the Quantum GIS software and contours of horizontal movement were

calculated at various intervals for each model. In choosing an appropriate contour for the extent of the impact of the earthquakes, the contours were cross-referenced with land damage data for each earthquake (where it existed[17]) (Tonkin & Taylor, 2012), as well as the results of geodetic surveys made after each event. By visual inspection, it was determined that using a contour of 0.02m for horizontal movement would encompass almost all the area where shallow ground movement might be expected.

Figure 17 shows the extent of the impact zones for each earthquake. The four post-2010 earthquakes in the sequence are similar in size and location and therefore have similar impact zones. However, for an urban environment, the slight differences in the size and location of the impact zones can be significant. For example, Figure 17 shows the February 2011 earthquake impacted the entire city significantly, so all cadastral data collected in Christchurch between the 4 September 2010 and 22 February 2011 earthquakes is unsuitable for inclusion in the modelling.

[17] Land damage assessments were not carried out after the 23 December 2011 and 14 February 2016 earthquakes as no major land damage was reported after these events.

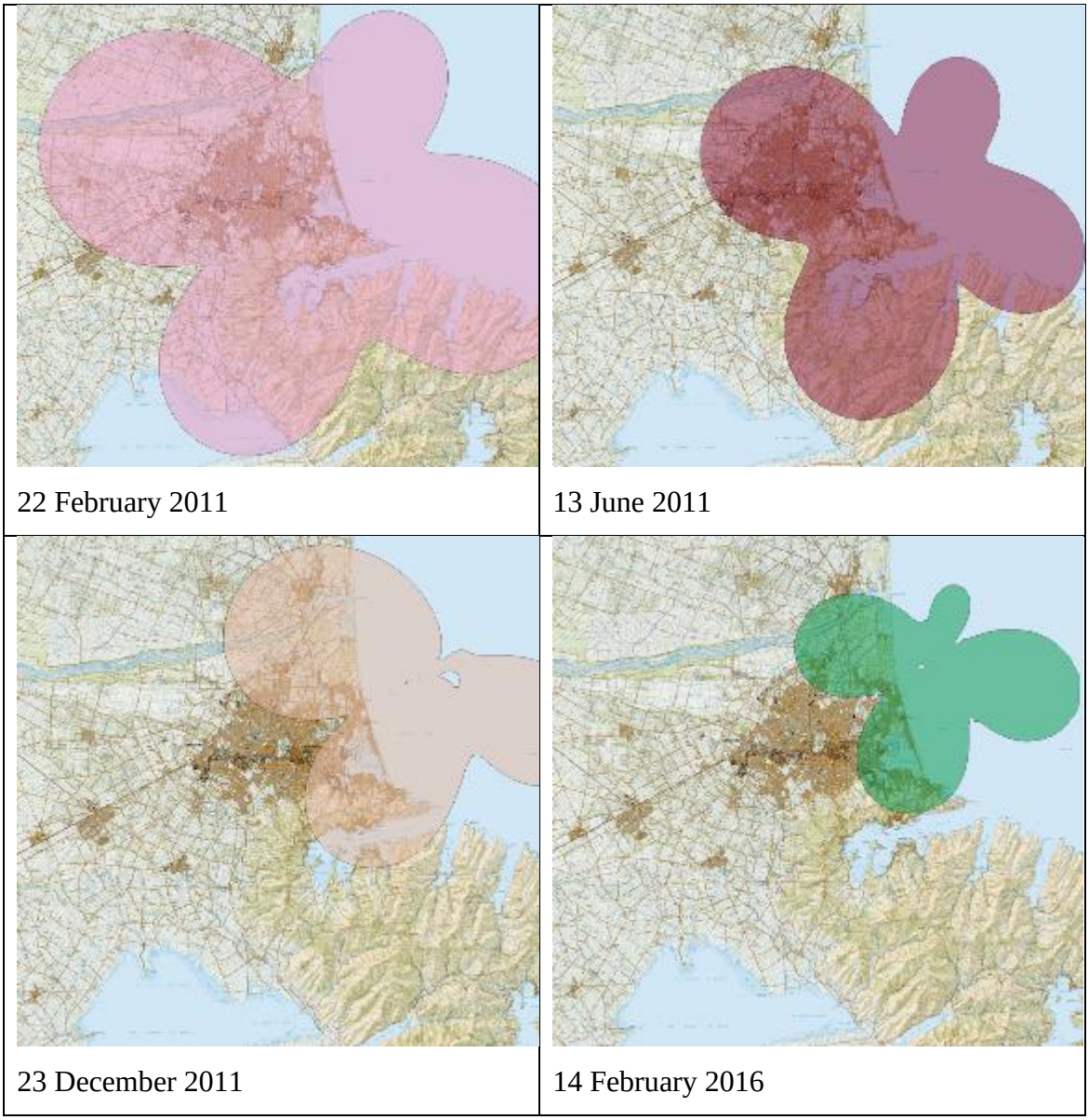

Figure 17: Impact zones (shaded area of at least 0.02m horizontal deep-seated movement) for the four major earthquakes subsequent to the 4 September 2010 earthquake.

Conversely, the 23 December 2011 earthquake significantly impacted only parts of the eastern and southern suburbs, representing about 30% of the total urban area. Thus cadastral data collected outside this impact zone in between June and December 2011 was unaffected and can still be utilised in the analysis, substantially increasing the number of data points available to the model, given that a lot of cadastral survey work had been completed by late 2011.

3.5.2. Processing

An initial inspection of the LDS/Landonline cadastral data tables might suggest that reliable earthquake related coordinate changes are directly available, generated upon authorisation of the cadastral adjustment. However, these coordinate changes do not reliably reflect earthquake movements, for a number of reasons. These include:

- The coordinates and coordinate changes recorded upon authorisation of an adjustment are relative to the marks held fixed in that adjustment. These fixed marks are almost certainly affected by earthquake movements themselves.
- Surveyors often found movements that were significant and inconsistent with nearby mark movements. In such cases, the surveyor may have treated the mark as disturbed, in which case a new mark was created in the cadastre[18] and therefore the recorded coordinate change is not related to the pre-earthquake position

The aim of the pre-processing phase is to identify the set of marks, observations and coordinates relating to post-earthquake cadastral surveys in the affected area.

A series of pre-processing functions were created to undertake the various tasks described below. All functions were implemented in a PostgreSQL database, which contained copies of the relevant tables from the Landonline system.

3.5.2.1. Data source

Cadastral data for New Zealand is held within the Landonline system. While the raw data in the Landonline system is not made directly available to users, full extracts of Landonline tables are available via the LDS, which is updated weekly. For this analysis,

[18] Rule 7.6 of the Rules for Cadastral Survey requires that a disturbed mark be treated as a new mark

the initial data was sourced from a data warehousing system available to LINZ internal users that contains the same data available via the LDS. This avoided the need to transfer large amounts of data over the internet when doing the initial setup.

Table 8 describes the tables used in the analysis. Full metadata for all tables used is available in the LDS data dictionary (LINZ, 2018).

Table	**Description**
crs_node	Nodes are an abstract entity associated with one or more coordinates, typically represented physically by a mark (such as a survey peg). Of interest is the identification of multiple nodes that relate to the same physical mark so that they can be treated as a single entity in the data processing.
crs_mark	Marks are the physical representation of a node. One node may have multiple marks over time, for example where a surveyor replaces a damaged mark in the same location. Of particular interest are marks recorded as "disturbed" after the earthquake, as these need to be dealt with carefully in the processing algorithm to avoid spurious results.
crs_mrk_physical_state	Contains details of marks pertaining to a specific CSD. For example, earthquake-related notes made by the surveyor about a mark are recorded here.
crs_ordinate_adj	Contains details of how the node was used in a particular adjustment, including coordinate change and uncertainty

	information. Note that these coordinate changes are relative to fixed control in an adjustment and are often not reliable in the aftermath of an earthquake.
crs_adj_obs_change	Contains details of observations used in a particular adjustment, including key adjustment statistics such as standardised residuals. Useful for filtering coordinates with potential errors from the analysis. This table is not provided in the LDS, due to its size, but can be requested from LINZ.
crs_adjustment_run	Details of adjustments run in the Landonline system. Provides a link between CSDs and adjustments.
crs_sur_plan_ref	Contains one or more spatial references (coordinates) to represent the location of a CSD
crs_survey	Contains key details of the cadastral survey, including the date of the fieldwork, needed to determine whether the CSD was earthquake-affected
crs_work	Contains status information about a CSD, such as whether it has been withdrawn from the system
crs_node_works	Provides the link between a CSD and the nodes on that CSD
crs_observation	Provides key metadata about observations in a cadastral survey, including the date of observation. Identifies whether the observation is newly measured or adopted from an older (possibly pre-earthquake) dataset

crs_setup	Links the observation and node tables
crs_vector	The spatial entity representing all observations between two nodes
crs_adjust_method	Identifies the type of least squares adjustment used to generate coordinates (eg cadastral or geodetic)
crs_cord_order	Identifies the order (accuracy class) of the coordinate

Table 8: Initial tables used in the processing.

3.5.2.2. Defining the Affected Area

Shallow ground movement in an earthquake context occurs primarily as a result of mechanisms such as liquefaction and lateral spreading. In the wake of the earthquakes, an extensive program of engineering assessment of residential areas was undertaken by the Earthquake Commission[19] (Tonkin & Taylor, 2012). These assessments identified the majority of land damage as occurring within the Christchurch City local authority, with more limited damage in the Waimakariri and Selwyn Districts to the north and south of Christchurch. Consequently, these three districts were chosen as the subject area for this analysis. These are shown in Figure 18.

[19] New Zealand's government-owned natural hazards insurer

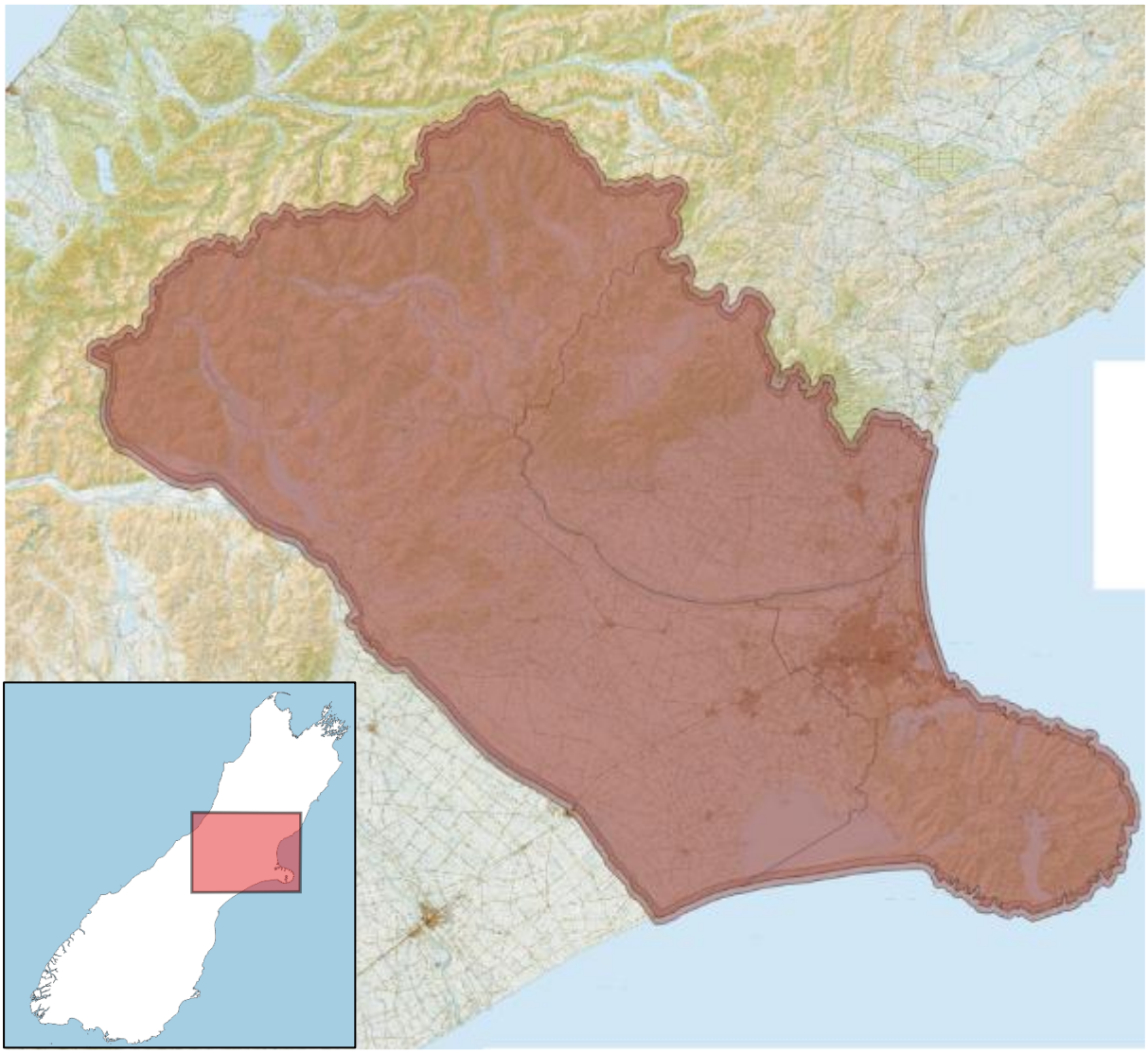

Figure 18: Extent of the analysed area, comprising the Christchurch, Waimakariri and Selwyn local authorities.

3.5.2.3. Get Affected CSDs

The *ceq_get_chch_selwyn_waimak_csds* function creates a table of CSDs in the affected area.

CSDs are located in Landonline by spatial references entered by the surveyor. A simple survey of limited extent might have a single spatial reference, typically located at the centre of the parcel(s) under survey. A CSD covering a larger area might have many spatial references. For example, a mark protection CSD covering several city blocks

carried out prior to major infrastructure repairs might have references at each road intersection.

Since classification of CSDs is needed to determine them as being affected or unaffected by shallow ground movements, these spatial references had their coordinates averaged to determine a single reference for each CSD. This averaged spatial reference was then used to determine which earthquake(s) in the sequence affected which CSDs. This was used later in the processing to exclude impacted CSDs and associated nodes and observations.

Post-earthquake CSDs were defined as those with a survey date after 4 September 2010, this being the date of the first earthquake in the sequence. Filters were applied to exclude CSDs created by LINZ staff to fix data errors and CSDs that had been withdrawn. As such CSDs may contain non-standard data or metadata that could bias the analysis.

The records of affected CSDs were inserted into the table *chch_selwyn_waimak_csd*.

3.5.2.4. Get Affected Nodes

The *ceq_get_chch_selwyn_waimak_nodes* function creates a table of nodes in the affected area.

Having created a table of post-earthquake CSDs in the affected area, this is used to identify nodes (and associated marks) connected to those CSDs. As part of this process, key metadata for each node was incorporated, including whether the mark was new, old, or adopted in the survey. This information enables an assessment to be made whether the coordinate changes for that node are relevant to the shallow ground movement

modelling. For example, an adopted mark does not have new observations connected to it in the CSD, so any coordinate change would likely not reflect earthquake movement.

The records of affected nodes were inserted into *chch_selwyn_waimak_node*.

3.5.2.5. Get Affected Observations

The *ceq_get_chch_selwyn_waimak_observations* function creates a table of observations in the affected area.

This was derived in a similar way to the nodes table, utilising the previously created *chch_selwyn_waimak_csd* table to identify observations associated with affected CSDs. Key metadata associated with the observations included whether the observation was measured, calculated or adopted and the equipment used to make the observation. In general, measured observations to nodes are required for the modelling, but an exception is made for calculated GNSS observations, as these are typically based on newly measured work.[20]

3.5.2.6. Get Observation Adjustment Statistics

The *ceq_get_chch_selwyn_waimak_aoc* function uses the *chch_selwyn_waimak_observation* table to insert relevant observation adjustment statistics into a table called *chch_selwyn_waimak_aoc*.

One key statistic is the accuracy multiplier, a value by which the assigned observation uncertainties are scaled to better reflect the actual accuracy of the data. Where an accuracy multiplier is significantly greater than 1.0, this indicates that the adjustment

[20] Whether to describe a GNSS observation is measured or calculated is left to the discretion of the surveyor.

analyst considered this observation to be of lesser accuracy than other observations of similar characteristics. The reliability metadata identifies where the adjustment has determined an observation is of uncertain reliability. For example, observations with a redundancy of less than 0.10, will be flagged as 'Low redundancy'.

3.5.3. Node Coalescence

Node coalescence is the process by which multiple nodes representing the same physical marks are identified and collated so that they can be treated as a single entity in the cadastral data processing.

3.5.3.1. Mark Name Standardisation

The *ceq_standardise_name* function enables marks with equivalent names to be linked, where they represent the same physical mark.

One particular challenge of using cadastral data is that mark naming conventions are not always consistent. Different surveyors may describe the same mark using different abbreviations and conventions may evolve over time. Table 9 below highlights some of the more common synonymous mark name components.

Standardised form	**Synonymous mark name components**	**Description**
PEG	P	A wooden peg, most often used as a boundary mark
BP	BRASS PLAQUE / BRASS PIN / BPIN	Circular bronze plaque with small divot punched in centre
SP	STEEL PIN / SPIN / SS PIN	Stainless steel pin with small divot punched in centre
DISK	ABD / ALD / BD /	Aluminium disk, primarily used as a

	DISC	boundary mark
UNMARKED	UNMK	Unmarked position, often used for easements or other non-primary parcels

Table 9: Synonymous mark name components requiring standardisation

In addition to the synonyms given above, existing marks used on a cadastral survey may occasionally have their names prefixed with ‘O’, for ‘old’. This naming convention was largely abandoned with the introduction of the Landonline system, but some marks using this convention remain in the system. Another challenge is that prior to the early 2000s, Roman numerals were typically used to identify the ‘number’ of a mark in a survey (eg IT IX DP 300000). But from the early 2000s, CSDs increasingly used Arabic numerals to identify mark numbers for new marks (eg IT 9 DP 300000). Then there are the more mundane discrepancies, such as differing amounts of whitespace between mark name components.

3.5.3.2. Reliable, Disturbed and Unproven marks

In the wake of the Canterbury earthquakes, there were three main ways in which a mark could be classified.

Firstly, a mark could be considered ‘reliable’, meaning that in the surveyor’s professional judgement, it was in its original position and could be used as part of the redefinition of boundaries. Where a mark is reliable, the surveyor connects any new observations they make to the existing mark in Landonline. If the mark does not yet exist in Landonline, then the surveyor will create it, but give it an appropriate state (adopted or old) to indicate that it is not a new mark in terms of the cadastre. So a reliable mark should only ever have a single node in Landonline.

Secondly, a mark may be considered ‘disturbed’, meaning that the surveyor judges it to be in a position other than which it was originally placed. Disturbed marks are not directly suitable for redefining boundaries, but assuming the cause of the disturbance is a discrete event, they can be used as new witness marks for boundary positions, once the new observations to them have been made and recorded into the cadastre. A disturbed mark will have a new node created for it and a new name assigned – effectively treating it the same as if it were a new mark placed by the surveyor. A mark might be disturbed a number of times during an earthquake sequence. In the case of the Canterbury Earthquake Sequence, there could be up to six nodes (a pre-earthquake node and one disturbed node for each of the five earthquakes in the sequence). In practise this did not occur, but there were several physical marks that had five nodes associated them.

The definition of a disturbed mark is provided in the *Rules for Cadastral Survey 2010:*

> *in relation to an old survey mark, means that the mark is in a position different from that originally placed and does not include a change of position due to deep-seated movement*

Deep-seated movement is defined thus:

> *ground movement caused by the deformation of bedrock which may be sudden, or slow and imperceptible, and excludes shallow movement that is limited to surface layers (eg, flow caused by liquefaction of soils, slumping, or landslip).*

The assessment of whether a mark was impacted by deep-seated or shallow-ground movement is challenging, hence there was significant variation in approaches taken by individual surveyors.

Thirdly, the mark could be considered ‘unproven’. This was a new status brought in after the earthquakes to pragmatically deal with the challenges of post-earthquake surveys. A mark was identified as unproven where the surveyor had connected to a mark that was not used for their boundary definition, and did not wish to define the mark as either reliable or disturbed. This might have been because they did not have sufficient evidence to make a determination, or might have been because the mark was not critical to their survey and they did not wish to spend time making the determination. These cadastral surveys were being paid for by clients, and determining mark disturbance was a complex and often ambiguous exercise, so the reluctance of surveyors to do this unnecessarily was understandable. Nevertheless, there was considerable value in having post-earthquake observations to these unproven marks in the cadastre, as they could provide valuable evidence to support boundary definition in the event that the unproven mark was subsequently destroyed (a common event in a city undergoing post-earthquake rebuild). From the Rules:

> ***18.3 Unproven marks***
>
> *(a) An old survey mark that the survey has not determined as being either disturbed or undisturbed may be included in a CSD where:*
>
> *(i) the mark has been affected by ground movement, and*
>
> *(ii) the mark is not being used to re-establish a boundary.*

Since an unproven mark is neither reliable, nor disturbed, it was not obvious whether new nodes should be created for unproven marks. Initially, this decision was left to the

surveyor, before LINZ provided guidance that unproven marks should have a new node created.

3.5.3.3. Identify Nodes for the Same Physical Mark

The next stage of the processing focussed on identifying which nodes are associated with the same physical mark and coalescing these into a single entity. The various coordinates associated with those nodes could then easily be tagged as relating to the same physical mark. Note that the 'physical mark' is not a logical entity in the New Zealand cadastral data model – if it were this coalescence would be straight-forward. Instead, an algorithm capable of dealing with the scenarios identified in section 3.5.3.2 is required.

Similar names, close proximity

Firstly, marks in close proximity with similar names were identified and had their names standardised using the *ceq_standardise_name* function described in section 3.5.3.1. In this context, close proximity was defined to mean marks within 2m of one another. This criterion was based on results of geodetic surveys, where the largest anomalous (ie shallow) movements were less than 2m. This subquery produced pairs of nodes that matched each other (each node could be in more than one pair, for example if there were three nodes in close proximity with similar names).

Disturbed based on nodes connected via calculation on CSD

Use of mark names to identify nodes that should be coalesced will only identify a small subset of nodes, since the Rules require that a disturbed node be given a totally new

name. These disturbed nodes are typically captured in a reasonably consistent manner on the CSD, as outlined below:

1. There will be two nodes included in the CSD, one representing the original position and one the disturbed position.
2. The node representing the original position will be captured as an adopted mark and will be connected to with adopted observations, since it is not possible to physically observe this original position.
3. The node representing the disturbed position will be captured as new mark, with a reference in the mark name that matches the CSD reference (ie if the CSD reference is “DP 500000” then the last two components of the mark name will be “DP 500000”).
4. There will be a short calculated vector between the original and disturbed nodes.

Disturbed node identified through digital linking of data

The simplest and only unambiguous disturbed node scenario is that which occurs where the surveyor provides a digital link between the original and disturbed position. Where such a link is provided, the relevant mark ids are captured in the *crs_mark* table. In this scenario, a recursive query can be used to combine a chain of disturbed marks into a single entity by tracing each disturbed node back to its previous node until it reaches a node that is not identified in the database as disturbed.

Combination

Based on the combined results of these three analyses above, the node representing the latest position for each mark was identified and populated in the *chch_selwyn_waimak_node* table.

3.5.3.4. Get Affected Coordinates

The next function in the processing chain, *ceq_get_chch_selwn_waimak_coordinates* links each node to the coordinate and the adjustment that generated that coordinate. Key metadata including the equipment type is also associated with the coordinate, based on the analysis carried out when creating the *chch_selwyn_waimak_observation* table.

3.5.4. Cadastral coordinate changes

The processing up to this point has focussed on identifying the most recent post-earthquake coordinate held in the Landonline database for each physical mark that has been resurveyed since the earthquakes. However, this coordinate still may not accurately reflect the post-earthquake location of the mark due to datum issues.

3.5.4.1. Geodetic Coordinate Update

On 14 and 15 December 2013, geodetic coordinates throughout the earthquake-affected region of New Zealand were updated (Crook et al., 2016). These coordinates were updated using new post-earthquake observations, where these existed. For nodes with no new observations, coordinates were updated using a new version of the NZGD2000 deformation model which included the 2010 and 2011 Canterbury earthquakes.

Prior to this update, only pre-earthquake coordinates were available for geodetic marks. Any cadastral coordinates generated up until this date would be in terms of those pre-earthquake coordinates, even though the new observations themselves represented post-earthquake relative changes across the extent of the survey.

3.5.4.2. Datum Inconsistencies Prior to the Update

One of the fundamental roles of a national geodetic datum is to enable data collected at various epochs and using various methodologies to be seamlessly combined to create a homogenous set of coordinates. For the New Zealand cadastre, the standards require that non-boundary marks have a positional uncertainty better than 0.15m at a 95% confidence interval. In reality, the digital cadastre is far better than this and with the ready availability of high-resolution aerial imagery and other high-precision datasets, errors in the digital cadastre of more than a few centimetres may be noticeable.

In the earthquake-affected area, prior to the geodetic coordinate update, coordinate inconsistencies were often far greater than a few centimetres. There are two main scenarios, outlined below.

Poor positional and poor relative accuracy - example

The geodetic mark IT I DP 72483 (geodetic code CML0) was observed to as part of SO 460787 in December 2012 and the cadastral coordinates were generated by LINZ in April 2013 (adjustment id 1733157). When the least squares adjustment was carried out, the analyst had difficulties with major inconsistencies among the fixed control marks in the adjustment, as rather than being held fixed, CML0 was free in the adjustment. The calculated coordinates differed by 0.95m from the existing, pre-earthquake, coordinates in the database. In fact, due to significant discrepancies, all but one of the control marks were freed up in the adjustment of this CSD, as no two control marks were related to each other. Thus the coordinates generated for this CSD have poor positional and poor relative accuracy.

Poor positional but good relative accuracy - Example

Another common scenario that occurs between the first earthquake and the December 2013 coordinate update is surveys where all of the connected control was impacted similarly by the earthquakes. All the control marks moved by the same amount in the same direction, at least within cadastral accuracy standards.

For example, geodetic mark BDYR (SS 658 SO 16236) was observed to on SO 461421 in February 2013. Coordinates were generated in a May 2013 cadastral adjustment (adjustment id = 1848141). In this case, all the control marks, including BDYR, were held fixed in the adjustment, indicating that the new observations were consistent with the pre-earthquake control coordinates, at least in a relative sense. In the December 2013 update, each of the control marks moved quite significantly, as shown in the table below.

Code	**dE (m)**	**dN (m)**	**dHz (m)**	**Observed post-earthquake?**
BDYR	0.230	-0.041	0.234	Yes
BK5C	0.220	-0.010	0.220	No
CMGB	0.237	-0.051	0.242	Yes
CMGQ	0.234	-0.038	0.237	Yes
CMJ4	0.242	-0.001	0.242	Yes
CMJ5	0.234	-0.040	0.237	Yes
DF5N	0.228	-0.026	0.229	Yes
Mean	**0.232**	**-0.030**	0.234	
Standard deviation	**0.007**	**0.018**		

Table 10: Coordinate changes in the December 2013 update for geodetic marks used on SO 461421.

From the above table, the total earthquake movement at each mark was reasonably consistent, being 0.232 ± 0.007m in the east component and -0.030 ± 0.018m in the

north component. The small standard deviations confirm that the movements are consistent (at a cadastral level).

Based on the movements at the control marks, it may be concluded that the cadastral coordinates generated in May 2013 could be updated to reflect the actual earthquake movements by applying offsets if 0.232m and -0.030m to the east and north coordinates respectively. In applying this offset, the relationships among the set of coordinates associated with this CSD are respected, so any shallow ground movement will still be reflected in the updated cadastral coordinates. But the coordinate set is in terms of the post-earthquake reference frame, so can be analysed with confidence alongside coordinates generated from adjustments carried out after the December 2013 coordinate update.

The above approach would only be necessary where there has been no cadastral adjustment of the data after December 2013. In some cases, cadastral adjustments of the same CSD were re-run after December 2013 to improve the coordinates. In other cases, later CSDs observed the same marks and therefore updated coordinates were available that were based on post-earthquake control. In such cases, the more recent coordinate would be used in preference to a prior coordinate updated using this process.

3.5.4.3. Post-Earthquake Coordinate Selection

The first step in correcting the pre-update coordinates was to categorise coordinates based on date and quality.

Coordinates calculated after the December 2013 update were identified based on the adjustment date.

Coordinates calculated between 4 September 2010 and 14 December 2013 were only selected where those coordinates had been calculated from surveys undertaken after the most recent earthquake in the sequence to affect that particular location. For example, a survey carried out in May 2011 would only have its coordinates included if the location was not impacted by the 13 June 2011 and 23 December 2011 earthquakes (see section 3.5.1 for discussion of how impact zones were determined).

3.5.4.4. Post-Earthquake Coordinate Quality Assessment

The next step was to carry out a quality assessment of all the selected coordinates. The aim was to filter out those coordinates where the accuracy was likely to be poor, or of unknown quality.

The following criteria were used to select high-quality adjustments, in terms of observation quality and connections to control[21], which in turn were expected to have produced high quality coordinates. Criteria used were:

- Connected to at least one existing Order 6 or better mark, held fixed in the adjustment
- Any down-weighting of the observations connecting to the fixed mark(s) is less than 3
- Observations connecting to the fixed mark(s) must not be identified as outliers in the adjustment statistics
- All Order 6 and better geodetic marks are either fixed, or the coordinate change upon freeing them up is less than 0.1m. This identifies situations where one or

[21] The fact that an adjustment was excluded does not imply that the CSD or adjustment was done poorly. In most cases, issues are due to poor historical data quality and a lack of good control in the vicinity of the survey.

more geodetic marks have coordinates that are inconsistent with others in the adjustment. For post-update adjustments, geodetic control should be consistent, but was sometimes not due to the impact of shallow ground movement which was not accounted for in control marks that had coordinates generated using only a model

As part of this query, the number of fixed marks with good connections was recorded for each adjustment. The results of this query were then used to classify each post-update adjustment as well-connected or poorly-connected.

A similar assessment was carried out on the pre-update adjustments to assess the quality of the connections to control. The only difference was that the fourth criterion (geodetic mark movements) was not used as large coordinate differences would be expected at some marks prior since the control had not yet been updated. Excluding these would exclude many of the cadastral coordinates in the areas of greatest interest (ie areas of significant shallow ground movement).

3.5.4.5. Correcting Pre-Update Coordinates

Prior to December 2013, when geodetic control was updated to reflect earthquake movements, the authoritative pre-update coordinates are not directly suitable for modelling earthquake movements, as they are based on pre-earthquake control. But in many cases, offsets can be applied to the coordinates to align them in terms of the post-earthquake reference frame.

Firstly, reliable post-update control coordinates were identified using the results of the connection quality analysis described above. Reliable post-update coordinates are those that are authoritative and were either fixed or freed up (ie a new, reliable coordinate was

calculated) in the cadastral adjustment. An equivalent process was carried out for pre-update coordinates.

There are two key subqueries to calculating the offsets.

The *max_adjust* subquery selects the largest adjustment id for post-update adjustments for a given node. This prevents duplicates from biasing results (ie where a coordinate has been used in multiple adjustments, it should only be used once for the purpose of calculating offsets). The maximum adjustment id is chosen as it is likely to be associated with the best coordinate (where there are multiple post-update coordinates for a node).

The *calc_offset* subquery selects nodes, coordinates and adjustment ids associated with each pre-update coordinate for which there is an equivalent post-update coordinate (using the adjustment ids in *max_adjust* to filter). It also calculates the offset (east and northing in Mt Pleasant 2000 projection) for each coordinate pair.

The main query then calculates the average east and north offset and standard deviation for each pre-update adjustment. Based on this analysis, the provisional pre-update reliability classes were updated as follows:

Reliability Class	**Criterion**
1	Standard deviation better than 0.05m
2	Standard deviation between 0.05m and 0.10m OR standard deviation cannot be calculated because offset is only calculated from a single mark
3	Standard deviation greater than 0.1m

Table 11: Reliability class descriptions.

The offsets were then added to the relevant coordinates to align all coordinates in terms of the same post-earthquake datum.

3.5.4.6. Pre-Earthquake Coordinates

The best pre-earthquake coordinates for each node were defined to be the most recent coordinates that had been calculated for that node, prior to the 4 September 2010 earthquake. Only coordinates of Order 7[22] or better were included, lower order marks not being considered sufficiently accurate.

3.5.4.7. Post-Earthquake Deep-Seated Movement Coordinates

In December 2013, LINZ applied corrections to all earthquake-affected coordinates to represent deep-seated movement (Crook et al., 2016). These corrections were calculated using reverse patches for the 2009 Fiordland earthquake and four Canterbury earthquakes. Once a denser geodetic dataset was available, it became apparent that there were deep-seated movements of up to 15cm in Christchurch City which were unmodelled by the official patches. This unmodelled deep-seated movement was probably not an issue for the spatial cadastre LINZ was seeking to maintain. But to achieve the objectives of this research, removal of any residual deep-seated movement was important so that the shallow ground movement model was not biased by it.

Therefore, the additional reverse patch was applied, derived from direct GNSS measurements of surface displacements (section 3.4.6). Application of the reverse

[22] Typical urban cadastral boundary accuracy

patches to the pre-earthquake coordinates was carried out using the CalcDeformation.py software provided with the NZGD2000 deformation model (LINZ, 2013).

3.6. Shallow ground modelling

With reliable pre and post-earthquake cadastral coordinates now available in the database, the shallow ground modelling was undertaken.

3.6.1. Modelling

The IDW method described in section 3.4.6.3 was adapted for the shallow ground movement modelling situation. Compared with the deep-seated movement refinement grid computed previously, there are a number of differences with shallow ground movement modelling that need to be considered when determining appropriate parameters for the model. Firstly, the deformation is expected to vary far more rapidly over shorter distances. Secondly, topographical features such as rivers are expected to have a significant impact on the direction and magnitude of the displacement vectors. For example, it is expected that vectors on opposite banks of a river will both be pointing towards the river.

As before, various parameter values were tried to determine an optimal set that resulted in a model which best represented the data. It was found that the distance in Equation (1) needed to be raised to the fifth power to avoid inappropriate smoothing of the data. For the same reason, no filtering was applied to smooth the model. For the shallow ground movement model, it was essential to have a high level of fidelity to the data points. Shallow ground movement is not typically smooth in nature, so a smooth model is not required.

To account for the impact of the rivers discussed above, break-lines were set along the Avon and Heathcote Rivers. This prevented the IDW algorithm from utilising points on the opposite side of a river to a grid point being calculated, even if they were within the chosen calculation radius.

3.6.2. Property Rights Impact Assessment

3.6.2.1. Rotation analysis

In the wake of the 2011 earthquakes, extensive resurveying was undertaken in the parts of Christchurch affected by shallow ground movement. For example, cadastral surveys to re-establish property boundaries and engineering surveys of damaged and new infrastructure. Horizontal cadastral survey observations are presented as projection bearings and ellipsoidal distances. In an urban environment, GNSS techniques may not work at some or all of the points in the survey, due to restricted sky visibility resulting from buildings, fences, trees etc. Thus many urban surveys are carried out using a total station. The total station can measure distances directly via EDM and independently of the datum. However, bearings are not measured independently of the underlying data. Any new survey requires an origin of bearings to determine its orientation. This typically involves the surveyor setting up over a mark and observing to a second mark at a known bearing (from a previous CSD). This bearing is then checked using a line to a third mark, ideally perpendicular to the first line.

Geodetic surveys of Christchurch undertaken by LINZ soon after the 2010 Darfield earthquake identified a clear rotational signal (Figure 19). While obvious at a citywide scale, at the typical scale of many surveys (ie a city block), the rotation is constant across the area of survey. Therefore, if orientation is set based on an underlying vector

from a previous survey, and checked to a third mark, in accordance with good survey practice, no error will be detected. Both bearings will differ by the same amount from the "true" post-earthquake bearing. In the absence of scale distortion, the surveyor might reasonably, but incorrectly, conclude that the local area is unaffected by anything other than a translation.

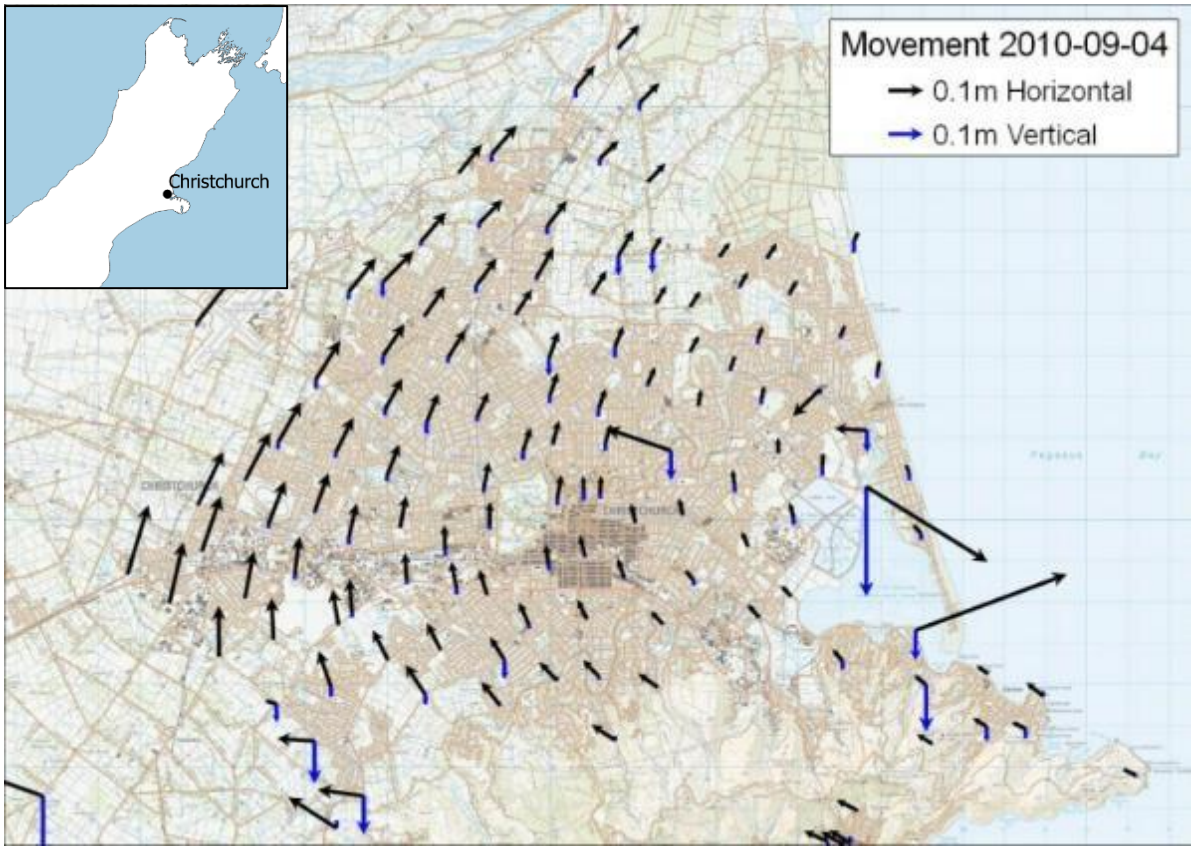

Figure 19: Horizontal and vertical coseismic displacements in Christchurch from the 4 September 2010 Darfield earthquake.

In Figure 19, the size of the rotation is approximately 2". This is well within the error tolerance of urban cadastral surveys featuring short lines, so is of no practical concern.

Such rotations are potentially present within the areas affected by shallow ground movement. In these areas, it is likely that any rotations would be significant at surveying levels of accuracy. Yet, if the surveyor takes an origin from three marks that are part of the same rotating block, even large rotations will be undetectable.

Failure to detect such rotations in a cadastral survey could lead to errors or inconsistencies in boundary determination. Thus, it is important to determine the extent of rotations within the area affected by shallow movement. Walcott (1984) provides a formula for the rotational strain rate of a velocity field:

$$\frac{1}{2}\left(\frac{\partial u}{\partial y} - \frac{\partial v}{\partial x}\right) \tag{2}$$

where u is the component of velocity along the x-axis and v is the component of velocity along the y-axis.

This formula is easily adapted for the case of a displacement field by replacing the velocity differentials in the numerators with displacement differentials:

$$\frac{1}{2}\left(\frac{\partial \boldsymbol{d}_x}{\partial y} - \frac{\partial \boldsymbol{d}_y}{\partial x}\right) \tag{3}$$

where $\boldsymbol{d}_x$ is the x-component of the displacement vector and $\boldsymbol{d}_y$ is the y-component of the displacement vector.

The partial derivatives of the displacement field were computed numerically from the gridded shallow ground movement model. The resultant strain field for part of eastern Christchurch is shown in Figure 20. The strain field is noticeably noisier than the original model from which it is computed, a consequence of the differencing required for its calculation. Despite this noise, it is clear by inspection of the Figure 20 that there is little consistency to the strain values, even over the small areas that would be typical of a cadastral survey. It can therefore be concluded that extensive systematic orientation errors in post-earthquake surveys is unlikely. The orientation check onto a third mark would almost certainly conflict with the initial orientation, which at least enables the issue to be identified at the time of survey.

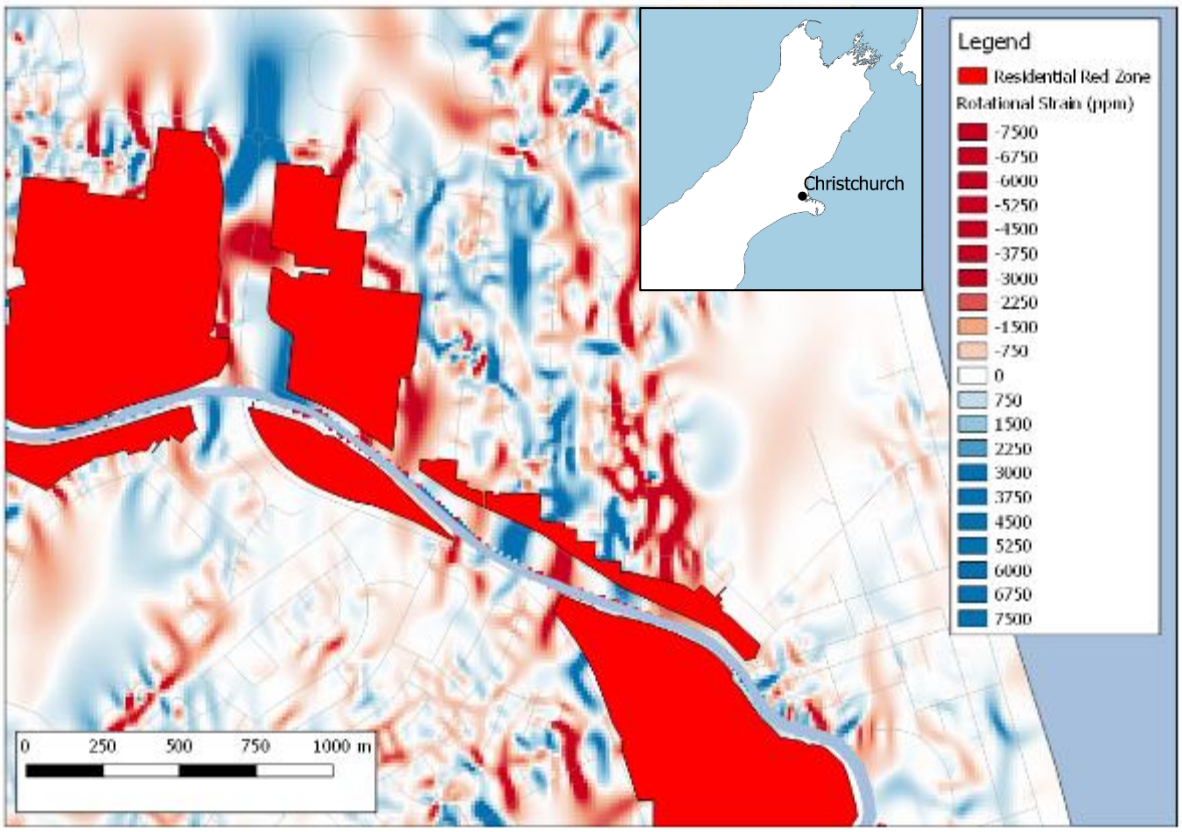

Figure 20: Example of rotational strain in eastern Christchurch calculated from shallow ground movement model.

3.6.2.2. Dilatation and Area Change Analysis

Another question of considerable practical and legal importance if property boundaries are to move with shallow ground movement is the potential for some landowners to have less land after the earthquake than before. Significant compression of a property has the potential to significantly reduce the value of property. Consider, for example, the minimum parcel size for which subdivision is permitted in accordance with planning rules. In an area of compression, it is possible that a property that was just above the minimum size before the earthquakes could be just below the minimum size after it.

Such a scenario could be catered for through a “grandparenting” rule within the local authority’s planning rules. However, this increases the complexity of the rules, which

from a policy perspective is undesirable. In deciding whether a rule change is justified, the local authority needs evidence as to the likely frequency of such a situation arising.

To answer this question, and other similar ones, it is necessary to compute the dilatational strain using the shallow ground movement model.

Walcott (1984) provides a formula for the dilatational strain rate of a velocity field:

$$\frac{1}{2}\left(\frac{\partial u}{\partial x}+\frac{\partial v}{\partial y}\right) \tag{4}$$

As for rotational strain, this is easily adapted for a displacement field:

$$\frac{1}{2}\left(\frac{\partial \boldsymbol{d}_x}{\partial x}+\frac{\partial \boldsymbol{d}_y}{\partial y}\right) \tag{5}$$

Again, the partial derivatives of the displacement field from the gridded shallow ground movement model were computed numerically.

Figure 21 is typical of the compression calculated from the model. It is small in both magnitude and area covered. Based on this, it was concluded that there was no significant, widespread, compression of private property and therefore no specific legislation or planning rules were required to deal specifically with compression-related issues.

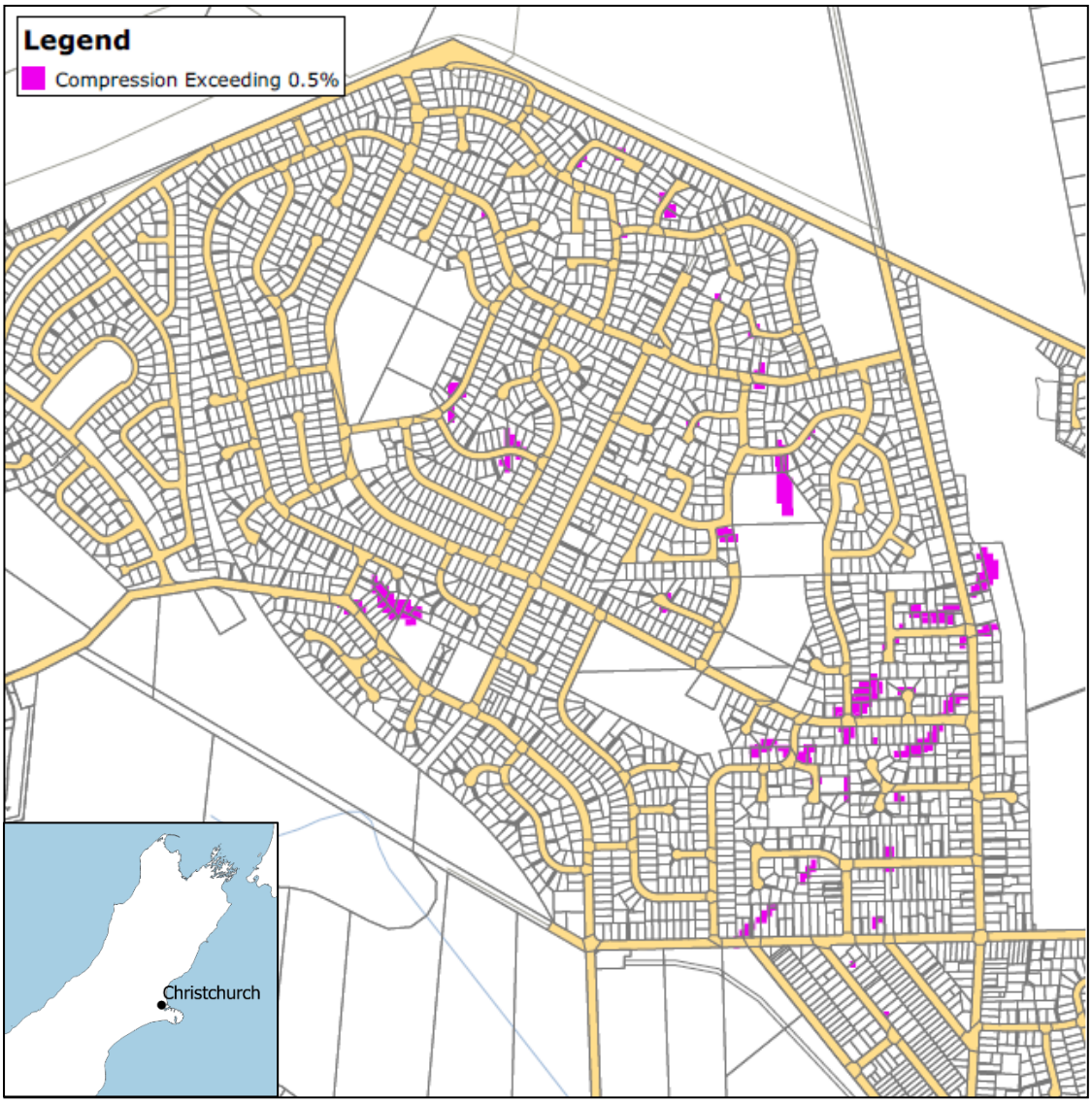

Figure 21: Ground compression exceeding 0.5% in a suburb of Christchurch.

3.7. Automated Monitoring

Often in datum management, it is desirable to monitor ongoing deformation in an automated way so that significant changes can be detected and assessed. In this case ongoing deformation was not the issue. Rather, the ongoing submission of new cadastral survey data as the rebuild progressed had the potential to significantly improve the model, particularly in areas where data was sparse.

The inclusion of additional data and recomputation of the model on a regular basis was important to maintain confidence with key stakeholders that the initial modelling had accurately described the problem. Significant policy recommendations had been made, including recommendations to introduce new legislation[23] to clarify the legal situation, based in part on the research described in this Chapter.

While those policy considerations were particular to this scenario, any models which are based on data collected over a long period of time are going to need to be recomputed (although not necessarily published) on a regular basis. For example, if a future earthquake results in substantial shallow ground movement over wide areas, an initial model can be produced within the first few months. This would be based on geodetic and the limited cadastral data collected up to that date. Publishing such an interim model, with appropriate qualifications as to its limitations, can be of great benefit to the ongoing recovery, as it enables potential problem areas to be identified and quantified. Once the interim model is published, regular recomputation of the model and comparison with the interim model enables decisions to be made as to when the improvements are significant enough to justify publishing an updated version.

Regular recomputation of models manually is time-consuming and there is risk of error due to the complexity of the process. Therefore, automation of the process is highly desirable.

Full automation of the data analysis and modelling process was achieved through developing the *ceq_calcs* software. Based on a Windows batch script wrapper, it utilises a mix of Python scripts and SQL functions to automatically analyse the cadastral data, produce the shallow ground movement model and a series of associated products,

[23] The *Canterbury Property Boundaries and Related Matters Act 2016* was duly enacted and came into force on 29 August 2016

including rotational strain and dilatation grids so that key areas of typical concern can be actively monitored. Figure 22 shows an example of two models produced three weeks apart, showing an area of significant difference due to the introduction of new cadastral data in the second model.

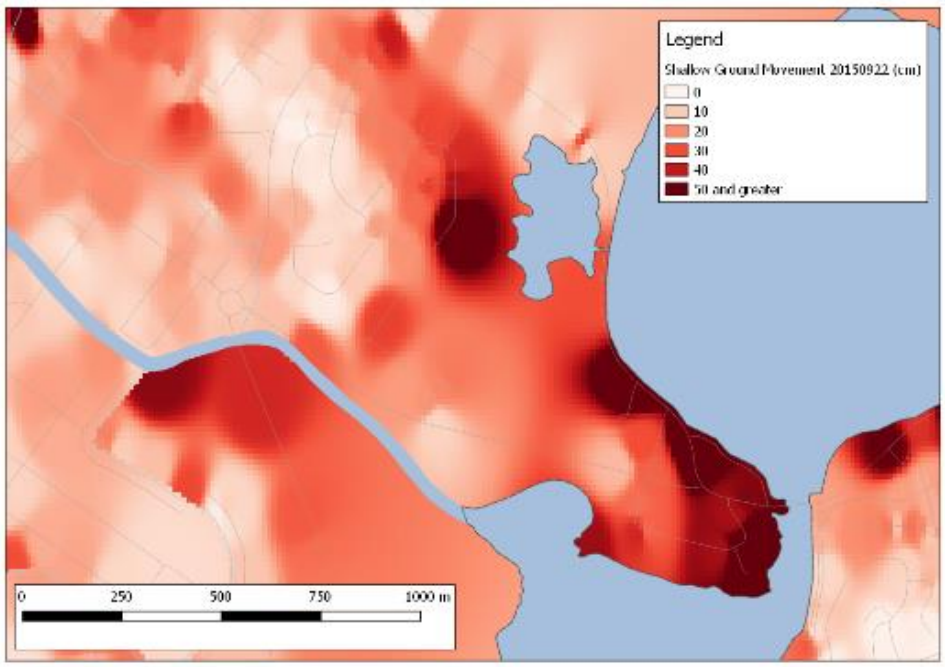

a) Shallow ground movement model computed 22 September 2015.

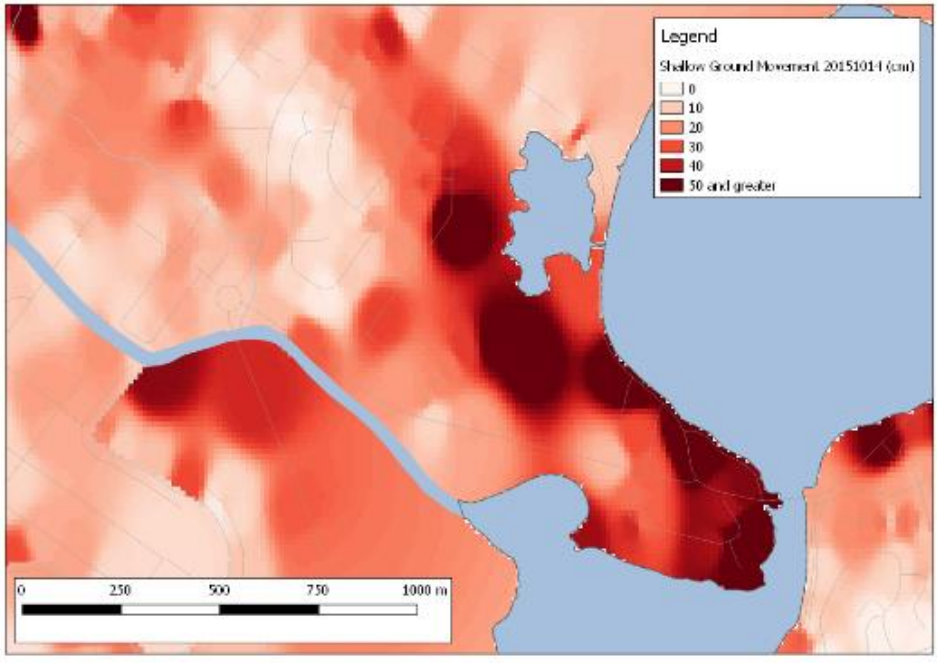

b) Shallow ground movement model computed 14 October 2015.

Figure 22: Shallow ground movement model at the mouth of the Heathcote River. Note the substantial additional ground movement identified in the 14 October 2015 model compared with the 22 September 2015 model.

An automated process is also essential in the situation where significant post-seismic deformation is associated with the earthquake. While this was not a characteristic of the Christchurch earthquakes, it cannot generally be assumed that post-seismic deformation is negligible. If there is significant post-seismic deformation, then the geodetic control coordinates may be periodically updated. After each geodetic update, the cadastral coordinates can be updated accordingly using this automated process, particularly the offset calculations described in section 3.5.4.5, and the various models regenerated.

3.8. Summary

This chapter has described a novel method of utilising dense, freely available digital cadastral data to calculate high-resolution deformation models in areas impacted by shallow ground movement, with the attendant high strains. After extensive processing, the cadastral data is brought into a form where it is in a consistent reference frame, despite in many cases having been collected prior to post-earthquake geodetic control coordinates being available. The key steps in this process are summarised in Figure 23.

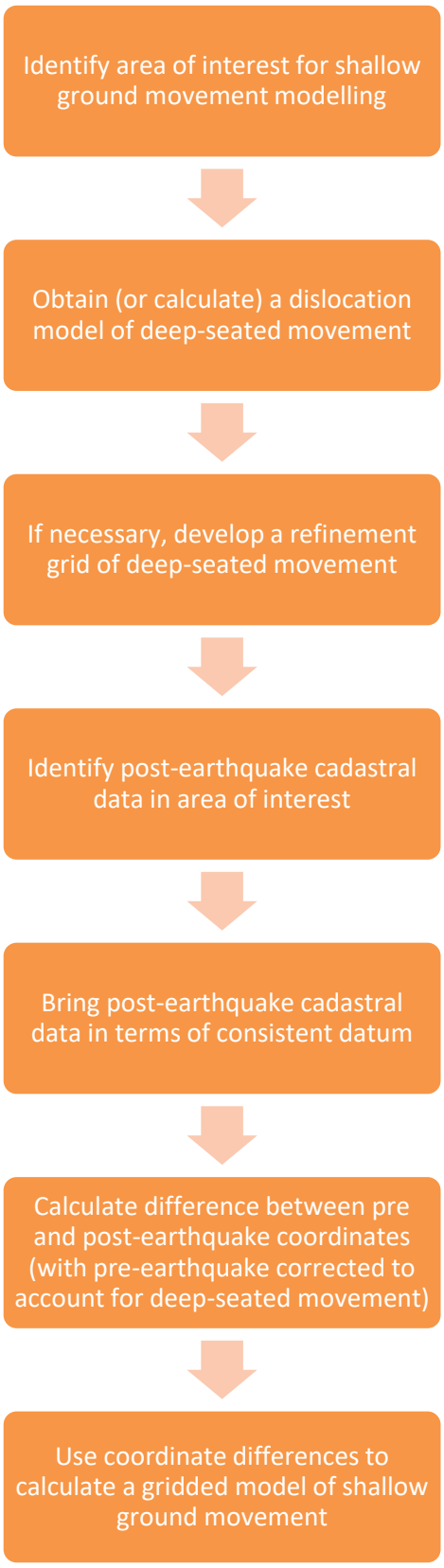

Figure 23: Key steps in the use of cadastral data to develop shallow ground movement models.

While aspects of the process are specifically related to Christchurch, the software could be easily adapted for another New Zealand-based scenario. Beyond New Zealand, the process outlined here can be adapted to other point datasets, whether cadastral or some other surveying data.

The data analysis and modelling process has been fully automated, such that all models and associated products can be calculated by running a single batch script. This automation enables regular recomputation of the model, meaning the latest information is available to help make decisions related to the recovery.

Finally, the benefits of high-resolution modelling have been clearly demonstrated through the application of the model to answer important questions that arise in an earthquake recovery situation.

4. Rapid High Resolution Modelling: Kaikoura Earthquake

4.1. Introduction

Chapter 3 showed how cadastral data can be used to develop a deformation model with high spatial resolution after an earthquake. One of the downsides of using cadastral data is that it takes months or years for significant amounts of data to be collected. Thus a different approach is required in the situation where rapid post-earthquake geodetic updates are required to assist with the recovery effort.

In the immediate aftermath of a major earthquake, updating the cadastre is a very low priority. Indeed, updating horizontal data layers generally is of less importance than updating vertical layers. This is because much of the key infrastructure requiring repair after an earthquake relies on gravity to direct fluid flow. For example, sewerage and stormwater networks.

This section describes a new approach using InSAR, in combination with targeted GNSS, to quickly re-establish accurate vertical control in terms of the official vertical datum after an earthquake.

4.2. Background

The M7.8 Kaikoura earthquake struck the upper South Island of New Zealand just after midnight on 14 November 2016. It is considered one of the most complex earthquakes ever to be recorded with modern instrumentation, with surface ruptures being recorded at over 12 separate faults. Horizontal movements of 6m and vertical movements of about 8m were observed with GNSS and radar (Hamling et al., 2017).

Post-seismic displacements were also significant. Analysis of CORS in the upper South Island reveals accumulated post-seismic displacement in the four months following the earthquake of up to 15cm horizontally and vertically (Jiang et al., 2018). In an event of this magnitude, it is reasonable to expect that post-seismic deformation might continue at detectable levels for several decades.

From a datum management perspective, there was immediate interest as to whether there was land damage with similar characteristics to the Christchurch earthquake. In particular, the Wairau Plain in the northeast of the South Island, which includes the small city of Blenheim, had some similar geomorphological characteristics to Christchurch. While liquefaction and associated lateral spreading were observed, the phenomenon was limited to areas in close proximity to rivers (Bastin et al., 2018). There was therefore no wide-scale impact of liquefaction on urban areas.

4.3. Synthetic Aperture Radar (SAR)

Based on CORS analysis, it was clear that this was the largest earthquake to impact mainland New Zealand in many decades. Significant horizontal movements had been observed over the top half of the South Island and bottom third of the North Island. Geodetic surveys using static (or even RTK) GNSS over such a massive area would take months, if not years to complete. From a national datum perspective, two things were urgently required after the Kaikoura earthquake:

1) Identify areas impacted by the earthquake so that GNSS surveys can be efficiently targeted
2) Quantify the vertical deformation resulting from the earthquake to support the immediate recovery efforts, including repairs to gravity-based infrastructure, such as sewers.

InSAR was identified as a key technique to answer these two questions as quickly as possible.

4.3.1. Imagery Sourcing

The Sentinel 1A and 1B SAR satellites were utilised for the analysis, based primarily on the free and open access of data to all users. This means it is readily accessible and any results of the processing can be made openly available, including to commercial parties who are assisting with the recovery.

Data from the European Space Agency's (ESA) Copernicus programme, including radar data from the Sentinel satellites, is available from the Copernicus Open Access Hub[24]. Perusal of the catalogue revealed that the affected region had recent pre and post-earthquake imagery on both ascending and descending tracks.

Radar images were downloaded using shell scripts via the Access Hub API, for both pre and post-earthquake ascending and descending tracks. A number of radar products are provided in the Hub. The products used for this processing are the Level 1 Single Look Complex (SLC) images. These images have already been pre-processed by ESA to focus the data and geocode it into radar coordinates (azimuth and range geometry). The acquisition mode used was Interferometric Wide (IW), which provides images with a resolution of 5m by 20m over a 250km swath. Each image consists of 3 subswaths, each of which is captured using the Terrain Observation with Progressive Scans SAR (TOPSAR) method. This method captures the data in a series of steered "bursts" which ensure uniform coverage and quality over the acquisition area.

[24] https://scihub.copernicus.eu/dhus/#/home

4.3.2. Processing Methodology

Processing was carried out using the Sentinel Application Platform (SNAP[25]). This software includes an Application Programming Interface (API) which enables processing chains to be set up and run via scripts. This has the advantage of ensuring consistency of processing, as well as the traceability of the parameters used in the processing. The high-level steps in the processing are described below. For more extensive details of any part of the processing, refer to the Sentinel Online User Guide[26]. The processing chain was split into the three sub-chains below to enable computer system resources to be freed up at the conclusion of the processing for each sub-chain. The first of these sub-chains is shown in Figure 24 and described in Table 12.

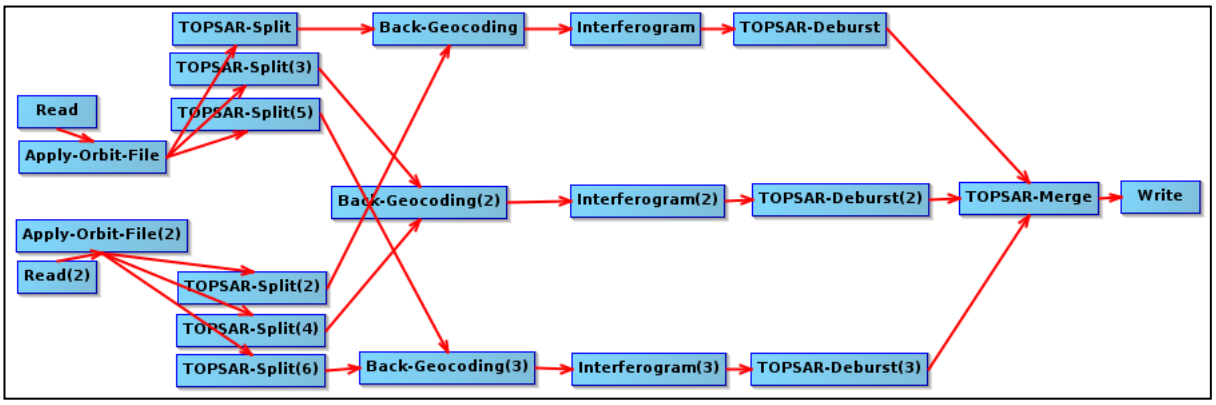

Figure 24: Kaikoura radar processing: From start to interferogram subswath merging.

[25] Not to be confused with the LINZ SNAP least squares adjustment software mentioned later in this Chapter

[26] https://sentinel.esa.int/web/sentinel/user-guides/sentinel-1-sar

Process	Description
Read	Import the Level 1 SLC images obtained from the Copernicus Open Access Hub. In Figure 24, the two separate "Read" processes reflect that pre and post-earthquake images need to be imported.
Apply Orbit File	Update orbit state vectors using precise ephemeris. The state vectors supplied with the downloaded SLC image are only predicted orbits, so where possible, the precise orbits should be used to improve the quality of the final interferogram (orbital areas can sometimes result in interference fringes that can be mistaken for deformation). It is usually at least several days before the precise ephemeris is available, so it is not necessarily available for urgent post-earthquake processing. However, even the predicted orbits are sufficiently accurate for urgent post-earthquake processing, where uncertainties in the low centimetres (rather than millimetres) are acceptable.
TOPSAR Split	Splits the subswaths into separate products for ease of processing. Radar processing is resource-intensive, so it is desirable to process as small an area as possible, whilst still ensuring the area of interest is covered. The Sentinel SNAP software has a viewer that can be used to select the relevant data to process. At this stage, certain bursts and/or polarisations can be chosen if processing data across the entire swath is not required. In this case, all bursts for all subswaths were processed. Since there are three subswaths, Figure 24 shows three "split" processes for each of the two imported images.
Back Geocoding	Co-registers the pre and post-earthquake images for each of the three subswaths. Co-registration is carried out based on orbit data and a

	Digital Elevation Model (DEM). Where available, the precise ephemeris is used. The DEM used is the Shuttle Radar Topography Mission (SRTM) 3-second (90m) product. One image is designated the master and the other the slave. The slave is resampled onto the master using bilinear interpolation. In Figure 24, there are three "back-geocoding" processes; one for each pre and post-earthquake subswath pair (there being three subswaths).
Interferogram	Forms complex interferograms for each of the subswaths. The flat-earth phase, which is a systematic phase signal related to the curvature of the Earth, is subtracted from the interferogram as part of this processing. The flat-earth phase is modelled using a degree-3 polynomial fitted to 500 points over the image. This is carried out for each of the three subswath pairs.
TOPSAR Deburst	Merges the bursts, of which there are typically 10 per subswath. This involves resampling pixels at the overlapping boundaries of each burst to produce a single value.
TOPSAR Merge	Merges the three subswaths to form a single interferogram of the entire swath
Write	Writes the interferogram to disk in preparation for the next stage of processing

Table 12: Description of steps in SAR processing – Part 1.

The second sub-chain removes the topographic phase and filters the interferogram, as shown in Figure 25 and described in Table 13.

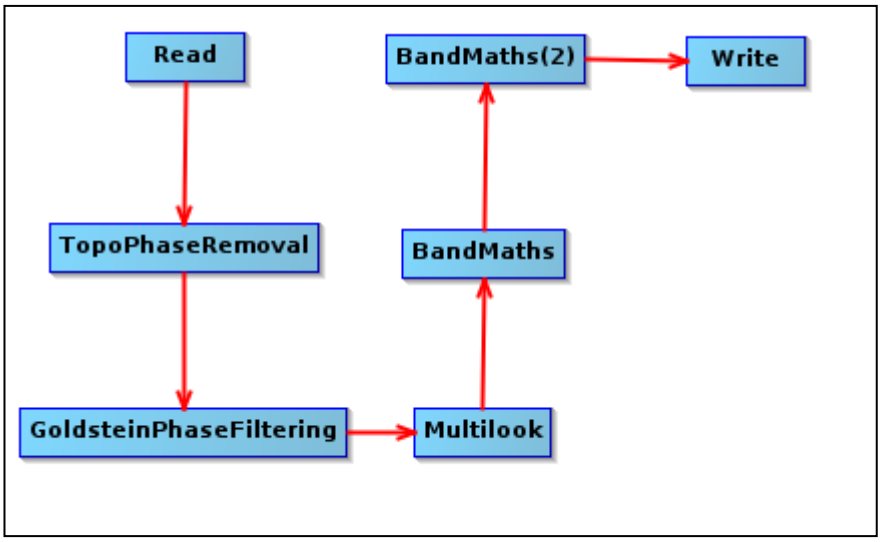

Figure 25: Kaikoura radar processing: Topographic phase removal to complex phase calculation.

Process	**Description**
Read	Import the merged TOPSAR interferogram
TopoPhaseRemoval	Some of the phase change in the current interferogram is due to topographic effects, which need to be removed. The SRTM DEM is used to remove the impact of topography from the phase. What remains is the phase due to deformation. It is this topographic phase removal that defines Differential InSAR (DInSAR).
GoldsteinPhaseFiltering	Filters the interferogram to reduce noise, which is particularly important if the interferogram is to be unwrapped, as high noise can adversely impact the numerical results.
Multilook	Further reduces noise by averaging neighbouring pixels. Multilooking is also used to generate approximately square pixels. For this process 10 range looks and 2 azimuth looks

	were used. Since the original image was 20m by 5m, this produces a multi-looked image of 40m x 50m (approximately square).
BandMaths	Replaces values of 0 in the real and imaginary part of the complex interferogram with nulls. This prevents artefacts in the data that are unrelated to deformation.
BandMaths(2)	Calculates the phase in radians from the complex interferogram.
Write	Writes the interferogram to disk in preparation for the next stage of processing.

Table 13 : Description of steps in SAR processing – Part 2.

The third and final sub-chain georeferences and reprojects the interferogram, as shown in Figure 26 and described in Table 14.

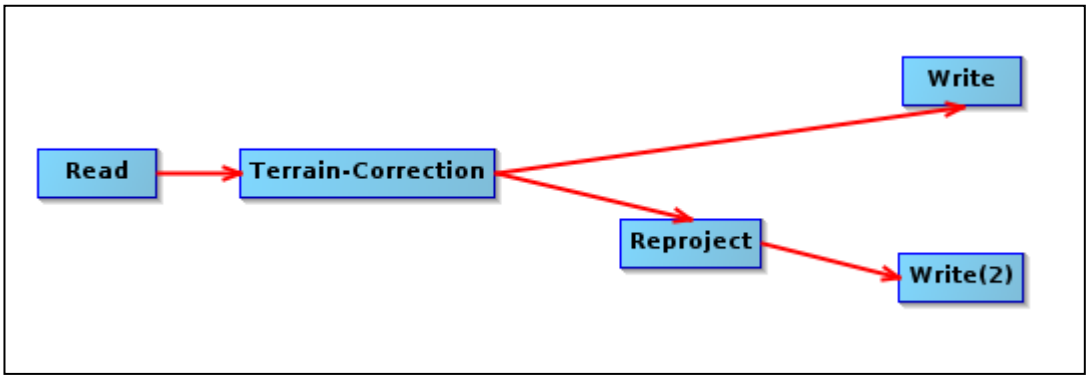

Figure 26: Kaikoura radar processing: Terrain correction and reprojection.

Process	Description
Read	Import the filtered, multi-looked, interferogram
Terrain Correction	Accounts for topographical variations which can cause distances to be distorted. Also georeferences the interferogram using Range-Doppler orthorectification. At this point a copy of the image is written to disk for potential further analysis. The reference frame is nominally WGS84.
Reproject	Reprojects the georeferenced interferogram into the national mapping projection, New Zealand Transverse Mercator 2000 (NZTM2000 or NZTM), for more efficient usage in GIS software.
Write	Writes the georeferenced interferograms to disk, one in terms of WGS84 and one in terms of NZTM.

Table 14: Description of steps in SAR processing – Part 3.

4.3.3. Interferogram Results

Wrapped interferograms (where the fringes are visible) are shown in Figure 27 and Figure 29.

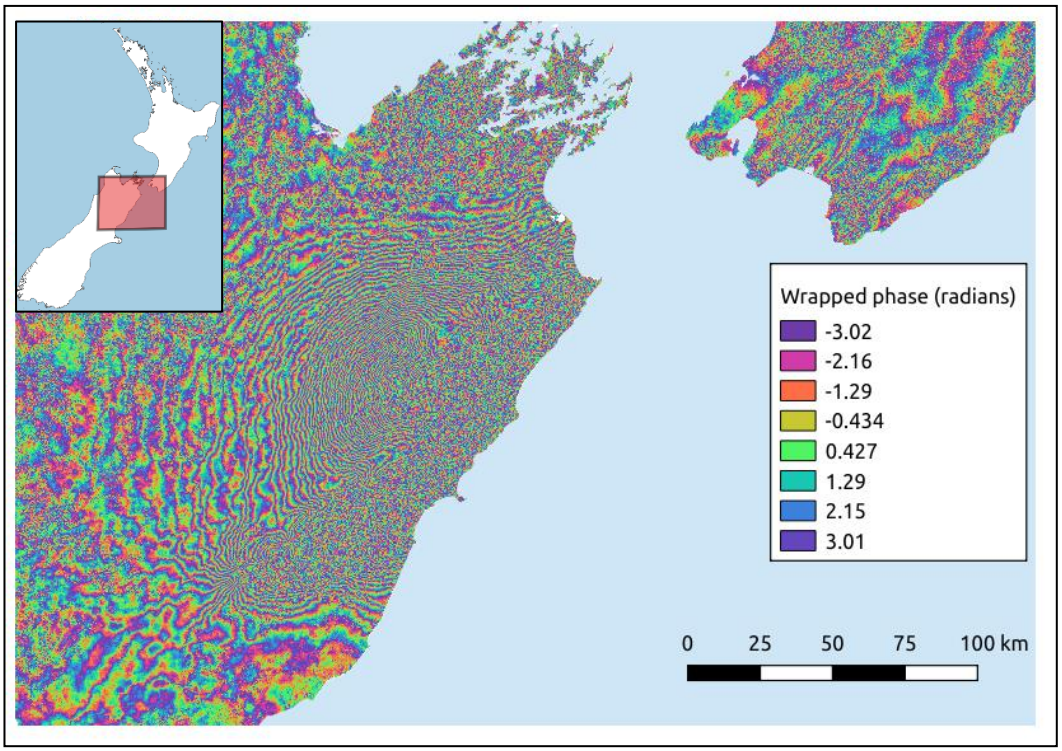

Figure 27: Interferogram of 2016 Kaikoura Earthquake from Sentinel ascending track images on 3 November 2016 and 15 November 2016. Each fringe represents 2.8cm of movement relative to the satellite.

In Figure 27 the primary impact zone of the earthquake is clearly visible, being the area in the northeast of the South Island where the fringes get closer together until they effectively "wrap up" on themselves and become indistinguishable due to the magnitude of the movements.

Outside of this area of extensive movement, areas of incoherence, which presents as random noise, are primarily due to the presence of forests. Figure 28 shows an enlarged view of one of these areas of incoherence, overlaid with forest boundaries. Clearly the amount of random noise is significantly increased in forested areas. This occurs because in a forested area, the radar signal is often reflecting off the trees, rather than the ground. Thus, natural change between image acquisitions, such as tree growth, is often sufficient to change the scatterers to the extent that a coherent image cannot be formed. This phenomenon of interaction with features other than the ground is related to the

wavelength of the radar signal. The longer the wavelength, the more likely the signal is to travel through obstructions such as branches and trunks and reflect off the ground. Thus in forested areas, the ALOS2[27] PALSAR[28] sensor, with a wavelength of 22.9cm, would be more likely to return a coherent image than Sentinel, with its wavelength of 5.8cm. However, in this case, the focus of the analysis is urban areas, where penetrating vegetation is not such a problem. Thus Sentinel is expected to work well in these urban areas and as discussed previously, has the significant advantage of the data being freely available. Nevertheless, it is important to acknowledge this limitation, which in some scenarios could prevent the necessary analysis.

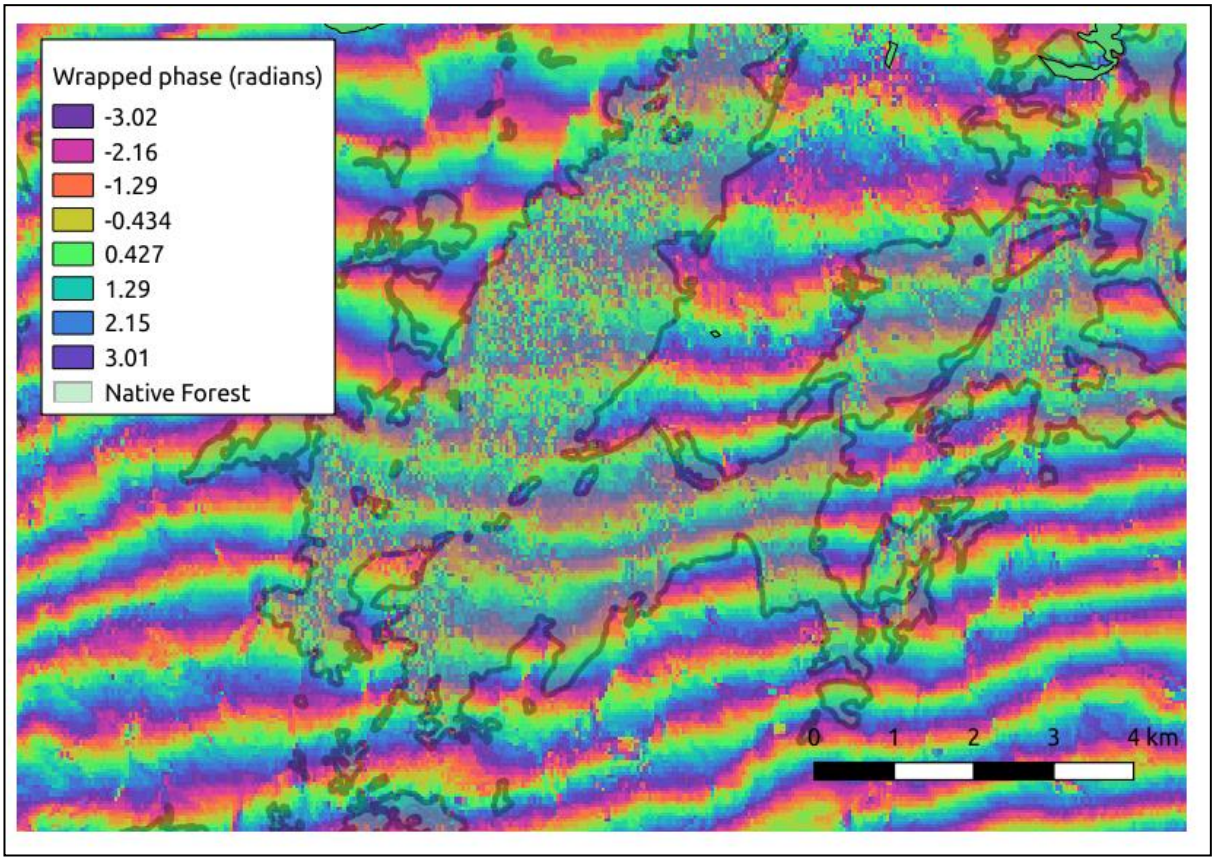

Figure 28: Example of decorrelation (incoherence) in forested areas (shown with black boundaries).

[27] Advanced Land Observing Satellite 2, a Japanese SAR satellite
[28] Phased Array type L-band Synthetic Aperture Radar, the SAR instrument on Japan's ALOS2 satellite

Compared with Figure 27, Figure 29 shows significantly increased areas of incoherence, to the degree that the extent of the earthquake is not readily discernible from the plot. In this case, the incoherence is due to temporal decorrelation. The ascending track interferogram (Figure 27) had pre and post-earthquake images separated by only 12 days. In comparison, the descending track interferogram is formed from images separated by more than two months. In this time, clearly there has been vegetation growth or other changes that have substantially changed the properties of the scatterers and impacted the quality of the interferogram. Atmospheric variations are also likely to be greater when images are separated in time.

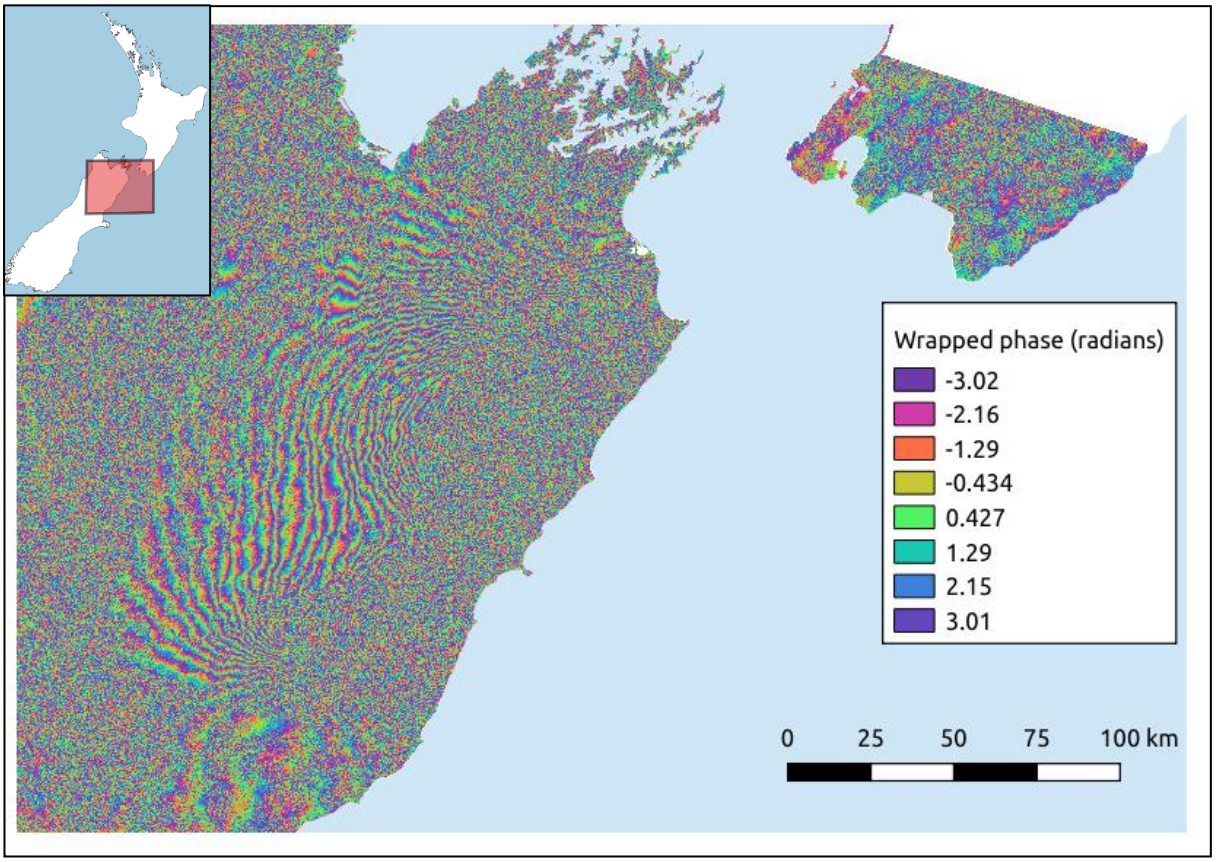

Figure 29: Interferogram of 2016 Kaikoura Earthquake from Sentinel descending track images on 5 and 10 September 2016 (pre-earthquake) and 15 and 16 November 2016 (post-earthquake). Each fringe represents 2.8cm of movement relative to the satellite.

In particular, the incoherence impacts areas of importance for this analysis, including the Kaikoura peninsula.

4.4. Rapid GNSS data capture

Radar cannot operate in isolation. It is a relative observation technique that needs to have datum established, which is usually done using GNSS. Where the CORS network is sufficiently dense, and the interferogram of sufficiently high quality, this may be done in reference to a CORS station or stations that are within the extent of the image. In the case of the Kaikoura earthquake, this is not the case. The CORS are too widely separated.

Secondly, as a consequence of the look angle and orbit of the radar sensor, when translated to local topocentric components, the resulting east-west component is less accurate than the vertical and the north-south component is weaker again, as discussed in section 2.6.5. While restoration of vertical datum is often more important than horizontal, some level of post-earthquake horizontal control is still useful. In the response phase, cadastral data used in Chapter 3 is not an option as such surveys take months or years to be completed in sufficient numbers, and then are only likely to occur at sufficient densities in areas affected by liquefaction or some other highly localised geophysical phenomena.

Thus rapid GNSS data capture is proposed as the best way to re-establish horizontal control, and provide necessary validation for radar in the vertical, in the event of an earthquake.

4.4.1. Use of Radar in Planning

Data from GNSS surveys is only useful for assisting recovery if it can be collected quickly and the results made available soon after data collection. Ideally this would occur within days of the earthquake, and certainly it needs to be completed within weeks. When an area as large as the top of the South Island is impacted by an earthquake, it is essential that these surveys are carefully prioritised and limited to the areas of greatest value if these timeframes are to be met.

The interferogram in Figure 27 can be used to carry out this prioritisation, as it clearly shows the area of decorrelation in the vicinity of the major faults (more so than Figure 29). The following four examples outline how the interferogram can be used to prioritise geodetic survey activities in the aftermath of an earthquake.

The *Rules for Cadastral Survey 2010* (LINZ, 2010) specify in section 4.2 that connections to control points in urban areas are required where such a point exists within 500m. Control marks for cadastral surveying are not the top priority in recovering from an earthquake. However, experience in New Zealand after the various earthquakes of the past decade indicate that a post-earthquake network of marks that is aligned with this cadastral standard works well for engineering purposes (given that there are no national engineering standards for control mark density). Based on this, a density of one control mark per square kilometre is used as a starting point for determining density for post-earthquake GNSS surveys. For areas less than three square kilometres, three marks should be surveyed to provide suitable redundancy for local surveys.

4.4.1.1. Blenheim

Blenheim was the largest urban area in the primary impact area. Examination of Figure 30 shows that the fringes are progressing across the town in a southeast to northwest direction. The three complete cycles covering the urban extents of the town represent 8.4cm (3 x 2.8cm) of displacement. In a flat urban area such as Blenheim, this magnitude of movement could cause problems for engineered infrastructure. In the rural area to the north and east of the town, there is potential evidence of liquefaction, as indicated by the areas of incoherent pixels. But within the town itself, the fringes have good coherence and fringes are fairly regular.

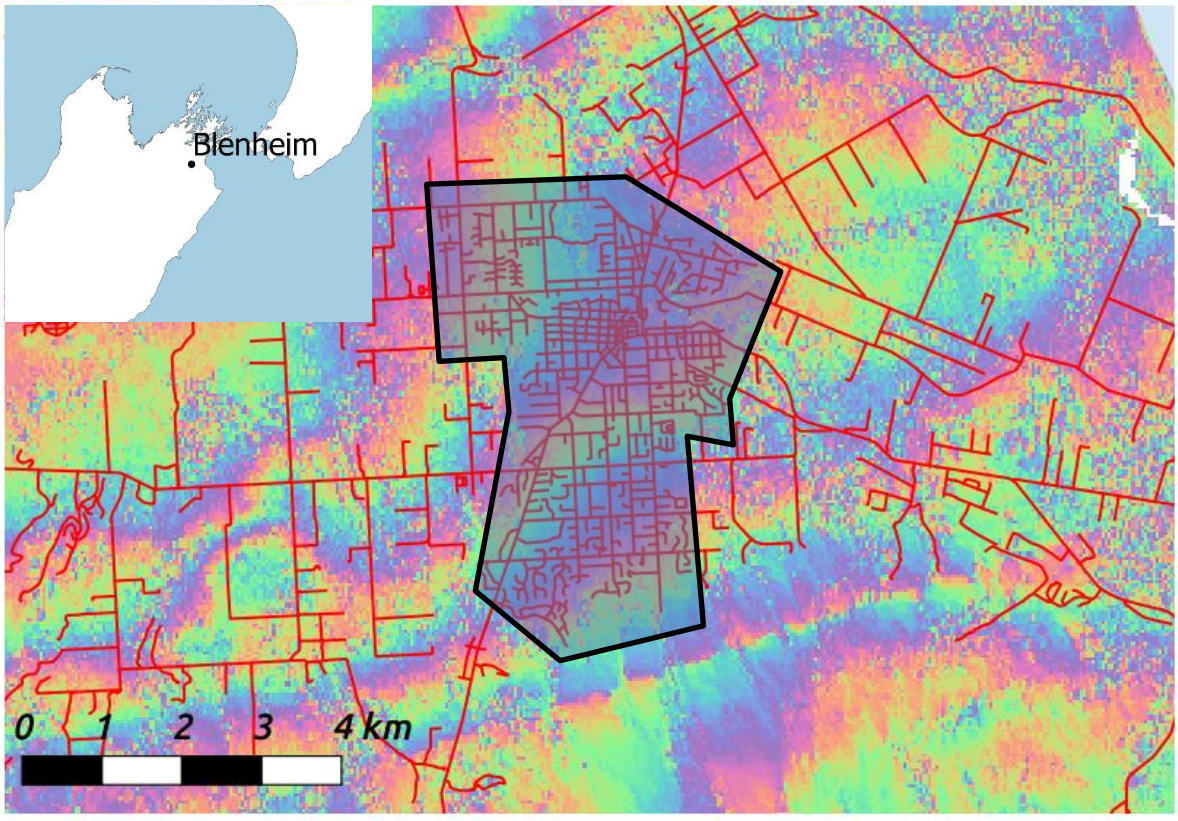

Figure 30: Blenheim interferogram with the extent urban area indicated by the black border with road network shown as red lines.

Blenheim has an area of about 20 square kilometres, thus the starting point is to require 20 marks. However, the high coherence and relatively low movement indicated by the

interferogram justifies a smaller number. This is important, as in an urgent recovery situation, geodetic survey resources need to be targeted where they will be most useful. Further densification can be carried out if the initial survey produces results that conflict with the interferogram.

So the conclusion for Blenheim is that it would benefit from GNSS control, but this does not need to be particularly dense. Four or five marks well-spaced across the town would be sufficient for urgent datum restoration.

4.4.1.2. Ward

Ward is a small town, about 45km to the south of Blenheim. It is closer to the major fault ruptures and this factor manifests itself in the interferogram in Figure 31. Coherent fringes are non-existent, indicating significant land damage, significant land movement, or both.

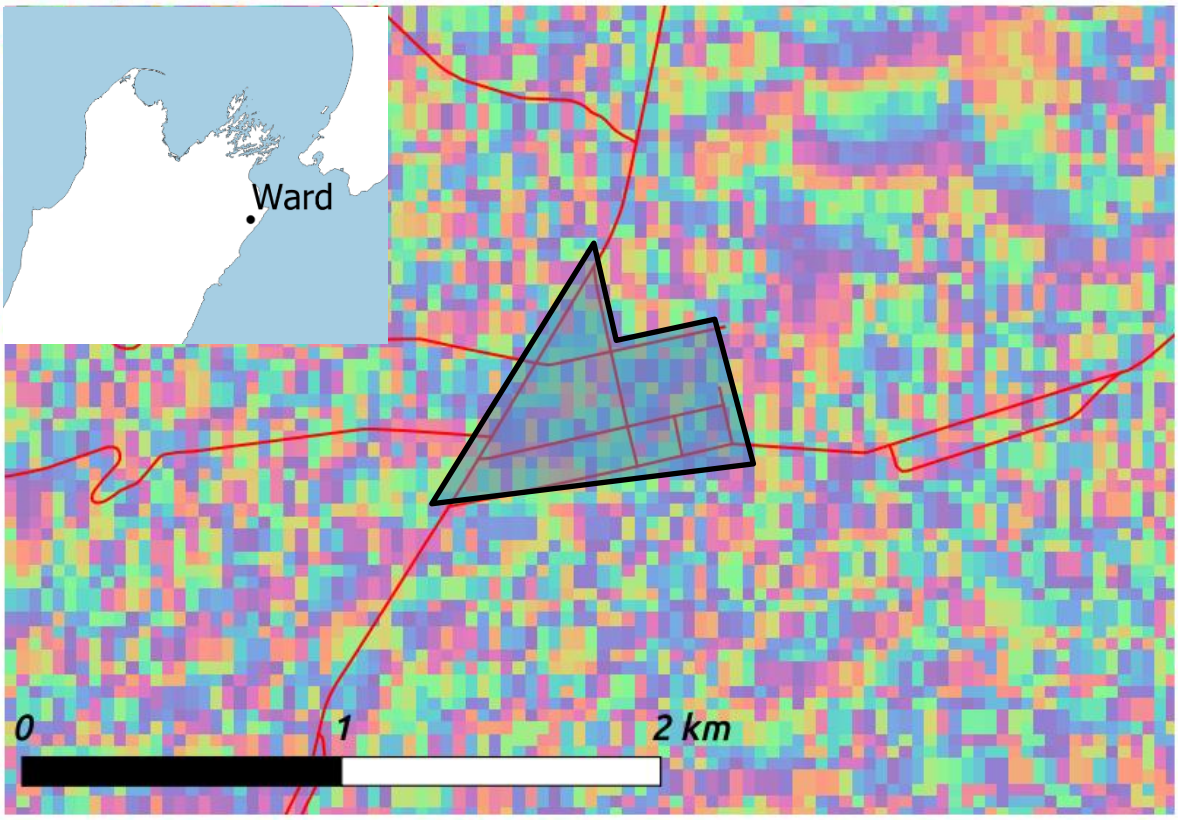

Figure 31: Ward interferogram with the extent urban area indicated by the black border with road network shown as red lines.

Again, it is concluded that urgent GNSS survey is required. In this case a much greater density than for Blenheim is justified based on the radar interferogram, since radar cannot be used to re-establish datum. Ward has an area of one square kilometre, so three marks are required to provide the necessary coverage to support post-earthquake activities in this area of significant movement and/or land damage. Note: The areal extent of Ward (Figure 31) is considerably smaller than that of Blenheim (Figure 30).

4.4.1.3. Kaikoura

In Kaikoura, the eponymous earthquake has clearly resulted in significant movement and/or land damage. Fringes are only partially coherent across the town, again indicating land damage and/or significant movement (Figure 32).

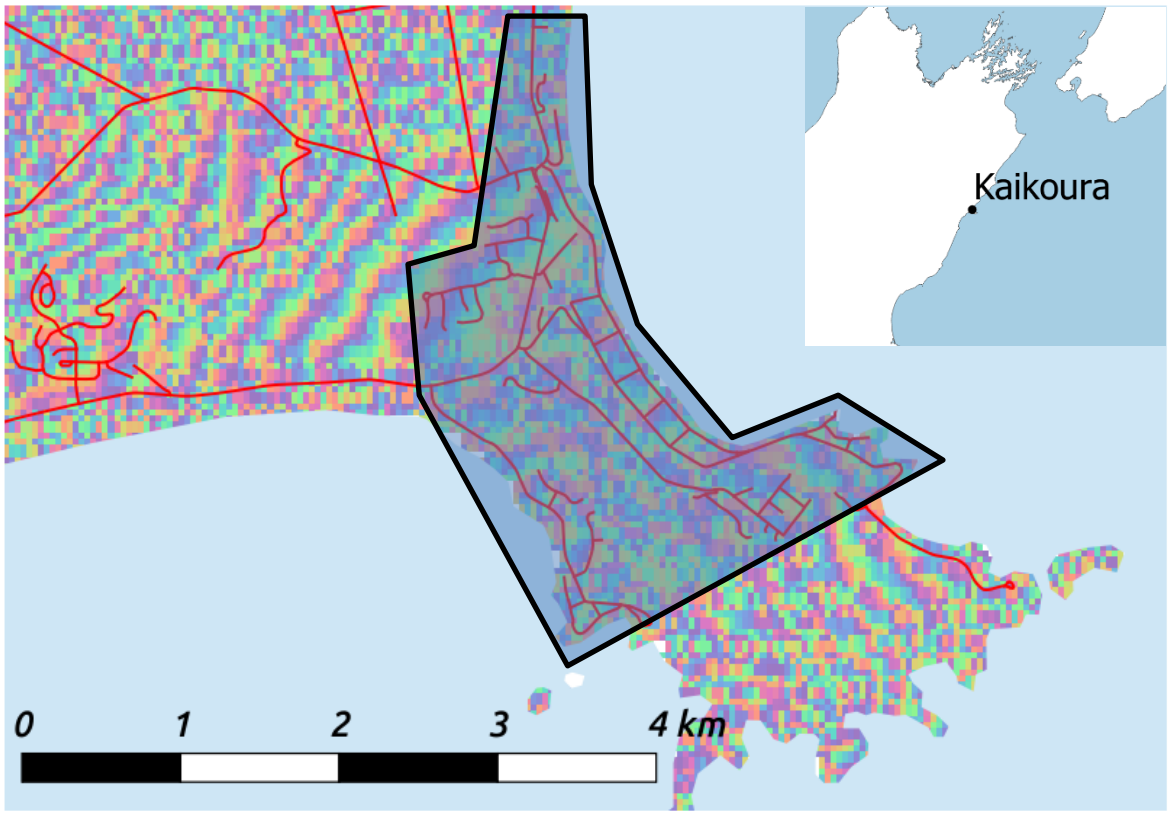

Figure 32: Kaikoura interferogram with the extent urban area indicated by the black border with road network shown as red lines.

Kaikoura has an area of eight square kilometres, thus eight post-earthquake control marks are required to recover the datum in the town.

4.4.1.4. Hanmer

Hanmer is the town closest to the epicentre of the earthquake, so might be expected to experience some of the largest movements. The interferogram (Figure 33) suggests this is not the case. The entire town is contained within a single fringe, indicating almost no vertical movement. There is a significant area of incoherence to the east of the town. While this could indicate liquefaction, overlaying the interferogram with a layer containing forested areas reveals that the incoherence is due to the vegetation.

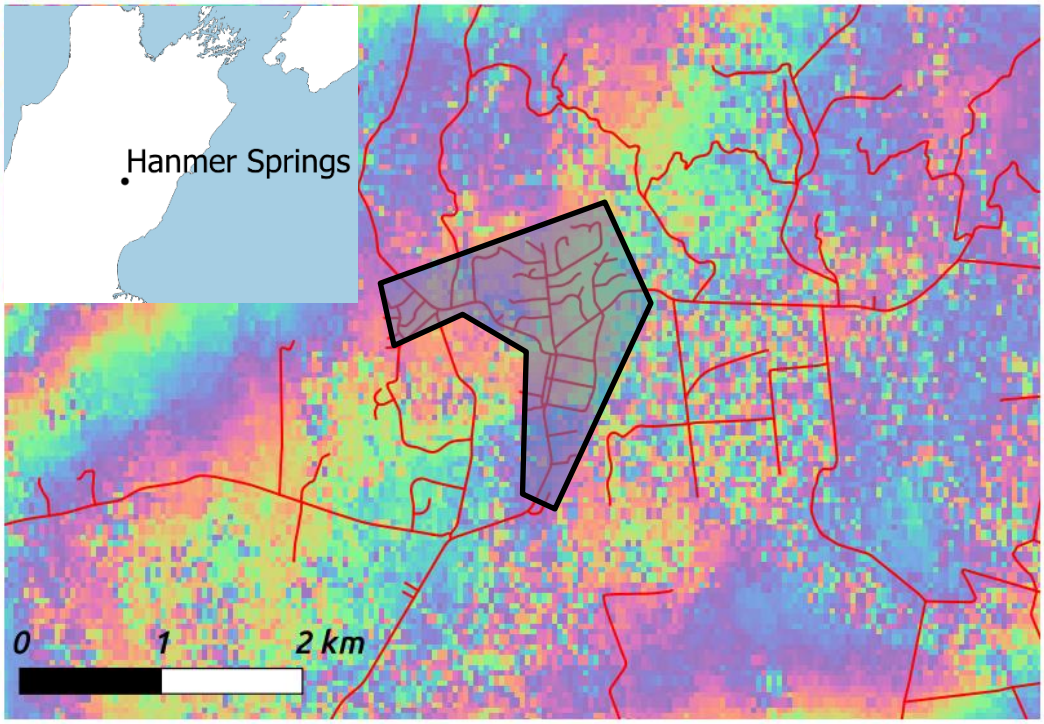

a) Hanmer.

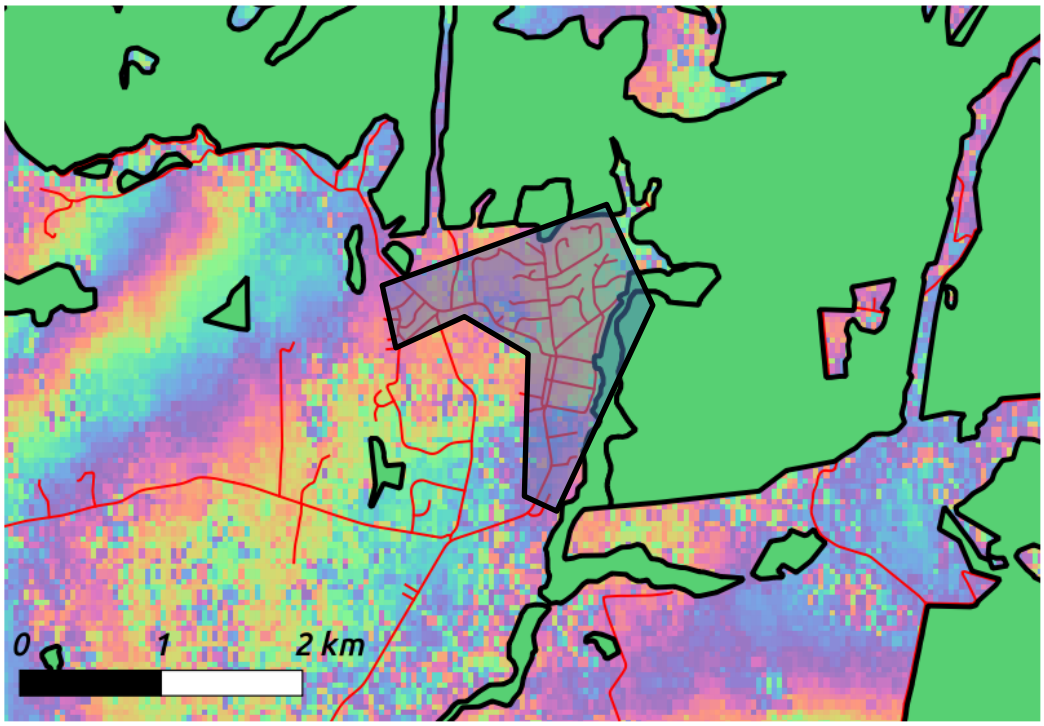

b) Hanmer overlaid with forested areas in green.

Figure 33: Hanmer interferogram with the extent urban area indicated by the black border with road network shown as red lines.

Thus, despite Hanmer being closest to the epicentre, the conclusion is that no marks need to be surveyed for vertical datum recovery purposes.

4.4.2. Data Collection Methodology

In a typical geodetic control survey, connections to datum are made by occupying existing geodetic control marks of a higher level of accuracy than the survey being undertaken. Connections may also be made to CORS, if they are nearby. In a post-earthquake scenario, there is no reliable local control to connect to. Datum connections can only be made via the CORS network.

For these earthquake recovery surveys, one efficient approach is to set up a GNSS base station on a mark, logging data. The GNSS rover(s) can then be used to collect RTK or rapid static data at a number of points in the locality over a period of several hours while the base station is logging. The logged data can then be processed against the CORS to bring the entire survey in terms of the post-earthquake datum. This assumes the CORS have already had their coordinates updated.

4.5. Re-establishing the Vertical Datum using Radar

This section describes a new technique to re-establish the vertical datum in an area after an earthquake, combining radar data with GNSS.

4.5.1. InSAR Vertical Component Extraction

The wrapped interferograms discussed in the previous section provide a powerful visualisation of an earthquake, enabling decisions to be made and qualitative analysis to be carried out. However, for quantitative analysis, the problem is that for every pixel, the phase can only vary between $-\pi$ and π radians. The integer number of cycles

(depicted as interference fringes) between the phases at any two points on the interferogram is unknown. The process of solving for these integer cycles is called unwrapping.

Phase unwrapping was carried out using the SNAPHU (Statistical-Cost, Network-Flow Algorithm for Phase Unwrapping) software developed at Stanford University (Chen & Zebker, 2002).[29] The output of the SNAPHU software is an unwrapped interferogram with total relative displacements across the image in units of radians. This is converted to a line of sight displacement value as follows:

$$d_{LOS} = -\frac{\lambda}{4\pi}\Delta\phi \qquad (6)$$

where d_{LOS} is the displacement in the direction of the line of sight of the satellite, λ is the radar wavelength (5.6cm for Sentinel) and $\Delta\phi$ is the unwrapped interferometric phase. Under the assumption that the line of sight displacement is due to vertical movement only, the vertical displacement, d_{vert} can be calculated using:

$$d_{vert} = \frac{d_{LOS}}{cos(\theta_{inc})} \qquad (7)$$

where θ_{inc} is the incidence angle, being the angle between the normal to earth surface and the line of sight to the satellite. This angle varies across the image and is contained in a grid that can be optionally produced by the Sentinel SNAP software when undertaking the terrain correction procedure.

In most earthquakes, including Kaikoura, there are significant horizontal and vertical movements. But note that the assumption above does not require an absence of

[29] Available from http://step.esa.int/main/third-party-plugins-2/snaphu/

horizontal movement, just that it not be a significant component of the 3D movement that is projected onto the line-of-sight displacement measured from the interferogram. Due to the side-looking, overhead geometry of radar, the line-of-sight is most sensitive to vertical movement. However the potential of significant horizontal movement, particularly in the east-west direction, to invalidate this assumption must be considered when using this formula, especially as the magnitude of the incidence angle increases. This is another reason why it is important to have several GNSS marks in areas where radar is used.

Figure 34 shows the relative vertical displacements calculated from the unwrapped interferogram. Compared with Figure 32, the image is very smooth, with the displacement changing in an orderly fashion across the town. But as noted in section 2.6.2, phase unwrapping is sensitive to noisy pixels, which can lead to the propagation of error through large parts of the unwrapped interferogram.

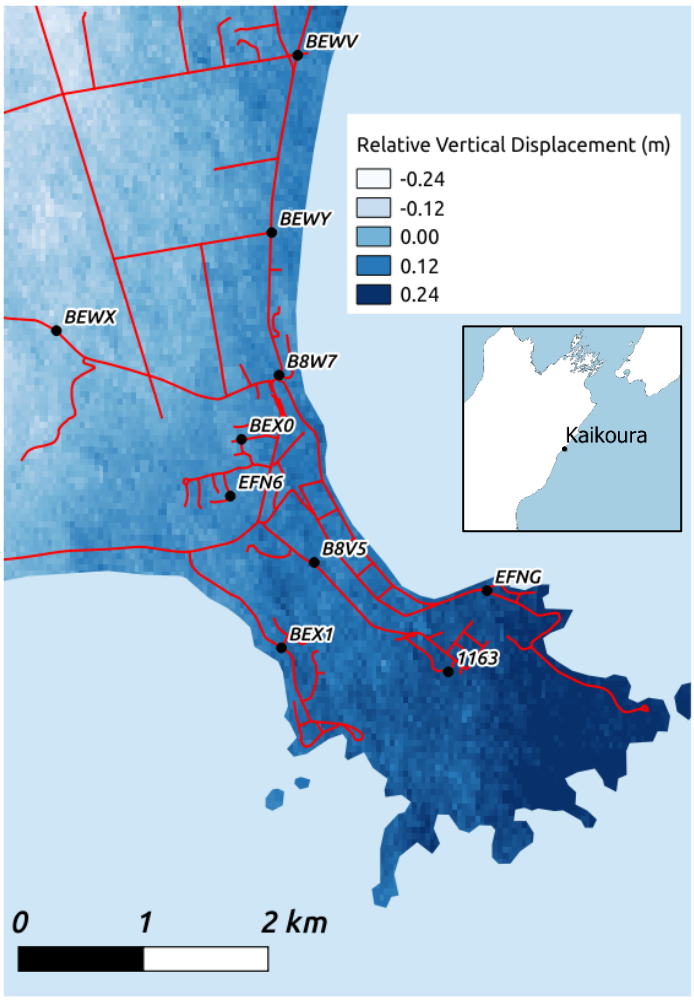

Figure 34: Unwrapped interferogram for Kaikoura, showing relative height change across the area. The ten control marks surveyed with GNSS soon after the earthquake are shown.

Table 15 shows the results of extracting height differences from the displacement values in Figure 34. The standard deviation is high at 13cm – this is not sufficiently accurate for engineering works and other precise heighting applications. Even if the obvious outlier between EFN6 and BEWV of -0.42m is removed, the standard deviation is still high at 7cm. It would appear from this that the algorithm in the SNAPHU software is failing to accurately count fringes due to excessive noise, particularly in areas of low coherence.

Geodetic Code	GNSS height change (m)	Radar height change (m)	Difference (m)
1163	-0.03	0.11	-0.14
B8V5	0.02	0.06	-0.04
B8W7	-0.01	0.04	-0.05
BEWV	-0.40	0.02	-0.42
BEWX	-0.28	-0.11	-0.17
BEWY	-0.15	0	-0.15
BEX0	0.01	-0.02	0.03
BEX1	0.01	0.06	-0.05
EFNG	0.05	0.13	-0.08

Table 15: Post-earthquake GNSS and radar height change measurements from unwrapped interferogram, relative to control mark ENF6, for the nine other control marks surveyed with GNSS soon after the earthquake.

Since the automated algorithm cannot adequately deal with the noisy interferogram in areas of low coherence, it may be possible to improve results through focussing on "fringe paths" across regions of higher coherence. Figure 35 shows coherence values for the Kaikoura area. The area shaded in blue indicates areas where there are an increased number of pixels with coherence greater than 0.75, relative to the rest of the area. As expected, these areas of higher coherence tend to be in the built-up parts of Kaikoura.

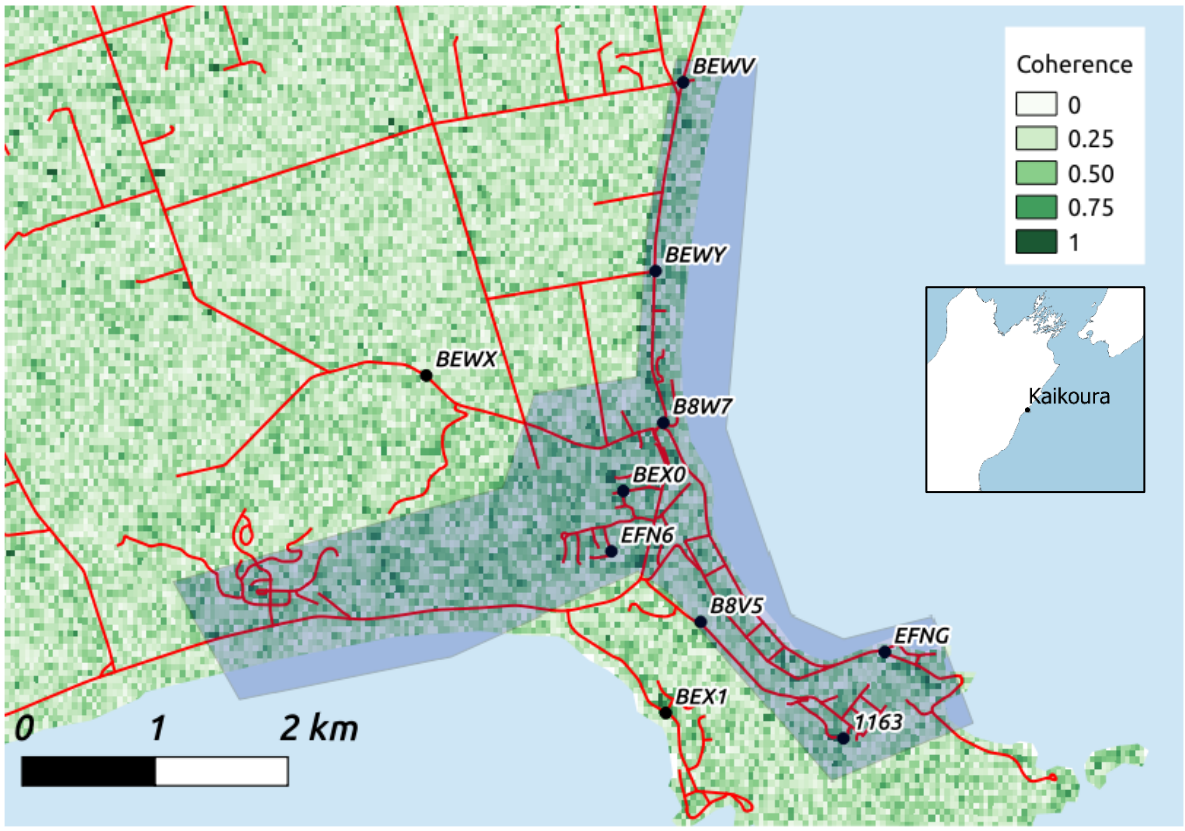

Figure 35: Coherence for Kaikoura interferogram. The area shaded blue has generally higher coherence than the rest of the image. The ten post-earthquake control marks are shown. Marks BEWX and BEX1 are outside the higher coherence zone.

Table 16 outlines the process and results of manually unwrapping the phase. EFN6 has been chosen as the reference mark or "zero change" point, to which the other marks are related. The choice of a reference mark is somewhat arbitrary, although unwrapping errors will be reduced if a mark close to the centre of the area of interest, with high levels of coherence in the surrounding pixels, is chosen. In the table, a negative value indicates that the vertical change has decreased relative to EFN6. The location of these marks is as shown in Figure 35.

Geodetic Code	GNSS (m)	Whole fringes	Part fringe (radians)	Line of Sight Displace-ment (m)	Incidence Angle	Vertical Displace-ment (m)	Diff (m)
1163	-0.03	0	0.26	0.00	30.7	0.00	0.03
B8V5	0.02	0	5.32	0.02	30.7	0.03	0.01
B8W7	-0.01	-1	-0.25	-0.03	30.6	-0.03	-0.03
BEWV	-0.40	-13	-0.35	-0.37	30.7	-0.43	-0.02
BEWY	-0.15	-6	-0.19	-0.17	30.6	-0.20	-0.05
BEX0	0.01	0	-3.42	-0.02	30.6	-0.02	-0.03
EFNG	0.05	1	5.09	0.05	30.7	0.06	0.01

Table 16: Post-earthquake GNSS and radar height change measurements, relative to geodetic mark ENF6. Two marks, BEWX and BEX1, were not included in the analysis, as coherence of the interferogram was too low in the vicinity of these marks.

The "GNSS" column contains the GNSS height change difference between reference mark EFN6 and the named geodetic mark.

The "Whole fringes" column contains the whole number of full-cycle (2π) fringes between EFN6 and the other mark. For example, BEWV has -13 whole fringes relative to EFN6. This is equivalent to 26π radians. The negative indicates that the vertical deformation at BEWV is less than at EFN6. The "Part fringe" column contains the additional fractional part of the last interference fringe between the two marks. It is calculated by averaging the phase values over the pixel containing the mark, plus the surrounding eight pixels to reduce noise, excluding any obvious outliers. Adding the fractional fringe to the whole number of fringes provides $\Delta\phi$, the unwrapped interferometric phase. This is then converted to a line-of-sight displacement in the next column using Equation (6). The next column contains the incidence angle, extracted from the Sentinel SNAP software. Equation (7) can then be used to calculate the vertical displacement.

The final column in Table 16 differences the GNSS height change and the radar height change. The standard deviation of these differences is 3cm, a significant improvement over the 7cm standard deviation from the automated unwrapping using SNAPHU. It is

therefore concluded that the manual unwrapping has significantly improved the quality of radar height differencing.

Note that the radar is measuring vertical changes due to the earthquake between two marks; it does not directly measure the actual post-earthquake height difference between the two marks. It does not practically matter whether the GNSS height difference is ellipsoidal (directly from GNSS) or normal-orthometric (transformed using a quasigeoid model); the change in the height difference to EFN6 is the same.

4.5.2. Combined GNSS and InSAR Adjustment

Having calculated coseismic height changes using radar (Table 16), the next step is to add these to the pre-earthquake height differences between geodetic marks. This provides an observed post-earthquake height difference, similar to if spirit levelling had been carried out between the two marks. This is shown in Table 17.

Geodetic code	Pre-earthquake height difference (m)	Radar coseismic height difference (m)	Post-earthquake height difference (m)
1163	45.76	0.00	45.76
B8V5	-11.73	0.03	-11.70
B8VE	-59.86	0.07	-59.79
B8VW	-53.96	-0.36	-54.32
B8W0	-54.57	-0.29	-54.86
B8W4	-54.20	-0.12	-54.32
B8W7	-57.95	-0.03	-57.98
B8WA	-55.66	0.02	-55.64
BEWV	-54.03	-0.43	-54.46
BEWY	-54.67	-0.20	-54.87
BEX0	-33.97	-0.02	-33.99
BF77	-58.48	-0.14	-58.62
EFN3	-46.00	-0.03	-46.03
EFN4	-6.38	-0.03	-6.41
EFN5	-1.40	-0.03	-1.43
EFNC	-54.98	-0.27	-55.25
EFNG	-58.62	0.06	-58.56
EFNH	-56.85	0.01	-56.84
EQD5	-55.93	0.02	-55.91

Table 17: Height differences relative to EFN6. As well as the seven marks in Table 16, it includes a further 12 marks that had pre-earthquake height differences, but no post-earthquake height differences from GNSS or levelling.

The radar height differences are now suitable for inclusion in a least squares adjustment, so that they can be combined with GNSS data using the quasigeoid model to calculate an optimum set of normal-orthometric heights for Kaikoura. There are many standard geodesy/surveying texts describing least squares analysis, for example (Mikhail & Gracie, 1981). The adjustment was carried out using the LINZ SNAP software (which is not related to the Sentinel SNAP software discussed in section 4.3.2). SNAP (Survey Network Adjustment Package) is a least squares adjustment software package developed by LINZ (LINZ, 2019). It is freely available for download from the LINZ website and the source code is available on the open-source code repository, *github*.[30] The software can consume a variety of geodetic observations, including height

[30] https://github.com/linz/snap

differences (such as those from spirit levelling), GNSS baselines, GNSS correlated point vectors, horizontal angles and distances. SNAP incorporates geoid models to bring height differences in terms of disparate reference frames into a common frame. The geoid model can also be used to transform ellipsoidal heights into the normal-orthometric frame typically required for engineering purposes. The software also incorporates deformation models and other time-dependent transformation functions, enabling observations in various frames, made at various epochs, to be reliably combined to calculate a consistent set of coordinates.

In this adjustment, the reference EFN6 was connected to three CORS (geodetic codes KAIK, NLSN and WGTN) via a set of correlated point vector observations. Correlated point vectors are referenced to the geocentre, thus there is no need to fix any stations. The standard deviation of the height of EFN6 was calculated by SNAP to be 11mm. The standard deviation of the radar-corrected post-earthquake height differences is 30mm (from analysis of Table 16). Using standard error propagation ($\sqrt{11^2 + 30^2}$), the standard deviation of the radar-derived heights is 32mm.

Table 18 shows the set of coordinates calculated in the least squares adjustment. Those marks which only had radar height differences to them have no horizontal coordinates shown. This set of coordinates is suitable for publication to aid the earthquake recovery effort.

Geodetic code	NZTM east (m)	NZTM north (m)	NZVD2016 height (m)
1163	1657333.64	5303300.01	109.00
B8V5	1656259.23	5304175.11	51.56
B8VE			3.48
B8VW			8.93
B8W0			8.39
B8W4			8.93
B8W7	1655977.54	5305672.88	5.30
B8WA			7.62
BEWV	1656127.19	5308231.50	8.82
BEWY	1655919.20	5306813.06	8.43
BEX0	1655676.35	5305160.01	29.29
BF77			4.64
EFN3			17.23
EFN4			56.85
EFN5			61.83
EFN6	1655587.05	5304705.73	63.26
EFNC			8.01
EFNG	1657644.43	5303949.35	4.71
EFNH			6.43
EQD5			7.35

Table 18: Post-earthquake recovery coordinates for Kaikoura calculated by least squares adjustment. Note that EFN6 is now included in the table as the inclusion of the GNSS observations in the adjustment has provided the required connection to datum via CORS with post-earthquake coordinates.

In 2018, an extensive GNSS control survey was carried out in the town of Kaikoura. As part of this survey, marks that had been geodetic control marks prior to the earthquake were resurveyed. This included all of the marks that had heights calculated using radar in this analysis. This provides a further opportunity to verify the accuracy and reliability

of radar height differencing as a geodetic observation technique. Three post-earthquake NZVD2016 heights for each mark are listed in Table 19.

Geodetic Code	Post-eq NZVD2016 heights (m)			Differences (m)	
	Radar (20161115)	GNSS and model (20180114)	GNSS (20181130)	20181130 minus 20180114	20181130 minus 20161115
EFNC	8.01	7.87	7.93	0.06	-0.08
EFN4	56.85	56.74	56.82	0.08	-0.03
EFN5	61.83	61.73	61.84	0.11	0.01
EQD5	7.35	7.27	7.35	0.08	0.00
B8WA	7.62	7.53	7.62	0.09	0.00
EFNH	6.43	6.37	6.49	0.12	0.06
B8VE	3.48	3.45	3.39	-0.06	-0.09
EFN3	17.23	17.1	17.25	0.15	0.02
BF77	4.64	4.54	4.66	0.12	0.02
B8W4	8.93	8.96	8.95	-0.01	0.02
B8W0	8.39	8.46	8.45	-0.01	0.06
B8VW	8.93	8.98	8.97	-0.01	0.04
Standard deviation				**0.07**	**0.05**

Table 19: Comparison of NZVD2016 heights calculated from radar with official heights published in the Geodetic Database based on GNSS and geophysical modelling.

The first column is the NZVD2016 height calculated using radar differencing in November 2016. The second is the height published by LINZ in January 2018, calculated from the National Geodetic Adjustment (NGA) which used the NZGD2000 deformation model to update these heights based on pre-earthquake GNSS observations. The third was also calculated from the NGA and published in November 2018. The main difference from the previous column is that this time all marks have post-earthquake GNSS observations to them.

Treating the November 2018 heights as the most accurate, differences are calculated with respect to each of the other two height sets. The standard deviation is then calculated for each set of differences. The standard deviation of the radar heights is 0.05m. This might seem rather high for geodetic-quality heights. However, the earthquake context is important to consider. The radar heights have better agreement

with the GNSS heights than the modelled heights published in January 2018, with their standard deviation of 7cm.

Table 19 demonstrates that two years after the earthquake, there were published heights in the geodetic database that were of lower accuracy than heights that could have been published from radar observations within days of the earthquake.

4.6. Summary

This chapter has described a novel technique for re-establishing height control in terms of the official datum after an earthquake. This technique utilises coseismic interferograms generated from radar to measure vertical changes across an urban area. It was shown that where the quality of the interferogram is poor, the accuracy of the technique can be significantly improved by manual unwrapping of the interferogram between the locations of two geodetic marks. Where these two marks have an accurate pre-earthquake height difference, the coseismic height difference from radar can be added to create a post-earthquake height difference. This is analogous to height differences derived from levelling, an observation type familiar to surveyors. As long as at least one of the geodetic marks also has post-earthquake GNSS observations to it, the radar height differences can be used to calculate post-earthquake heights at geodetic marks in a least squares adjustment.

Step	Description	Example
Identify area of high coherence	Use the InSAR coherence plot to identify the region where coherence exceeds 0.75. The rest of the analysis should only be carried out in this region.	Figure 35
Identify marks with pre-earthquake heights	Use data published by the national geodetic agency to identify marks with pre-earthquake heights. The technique only works for marks that already have heights.	
Select a reference mark	All height differences are calculated relative to this mark. Choose one near the centre of the high coherence area to minimise fringe-counting errors.	
Count the fringes	Count the number of whole fringes and the part fringe between the reference mark and every other mark with a pre-earthquake height.	Table 16
Convert to LOS displacement	Convert to a displacement in the line of sight to the satellite using Equation 6.	Table 16
Convert to vertical displacement	Convert to a vertical displacement using Equation 7.	Table 16
Calculate post-earthquake radar height difference	Add the vertical displacement to the pre-earthquake height difference to obtain a post-earthquake height difference between the reference mark and every other mark with a pre-earthquake height.	Table 17
Run least squares adjustment	Combine the post-earthquake radar height differences, with any post-earthquake levelling and GNSS data in a least squares adjustment. The GNSS baselines should be connected to CORS or other control marks that have had their coordinates updated after the earthquake.	Table 18

Table 20: Summary of process to generate post-earthquake heights from a radar interferogram.

This technique can re-establish pre-earthquake densities of geodetic height control, within a few days of an earthquake, without requiring extensive GNSS surveys. The primary limitation of the technique is that it is limited to areas where coherent interferograms can be formed. It is unlikely to give full coverage of every urban area impacted by an earthquake. But even where this is the case, the fact that some areas can be surveyed by radar frees up GNSS resources to focus on providing updated height control in areas where radar coherence is poor.

For the first time, the use of radar as a surveying observation, suitable for combining with other surveying observations in a least squares adjustment, has been demonstrated.

This provides an alternative to high-resolution modelling in the immediate aftermath of an earthquake.

5. Monitoring and Modelling Continuous Deformation: Taupo

5.1. Introduction

The preceding two chapters have focussed on the high-resolution modelling of episodic deformation caused by earthquakes. Major earthquakes have a high profile and resources are usually made available to enable geodetic system recovery. Continuous deformation presents an altogether different challenge, in terms of both data collection and modelling. GNSS campaign measurements and/or cadastral survey data does not have either the spatial or temporal resolution required to monitor and model deformation in areas of highly localised continuous deformation. Continuous GNSS stations have the high temporal resolution, but are so sparsely spaced that they are also unsuitable for high-resolution modelling. To overcome this challenge requires geodetic observations that are spatially dense, regularly repeated and cost-effective. DInSAR as a technique meets these requirements.

The town of Taupo has been selected as a test-bed for this investigation into continuous deformation for several reasons. Firstly, it is an urban area of relatively high value land and extensive engineered infrastructure, so there are strong drivers to accurate measure any ongoing deformation. Secondly, its location in the Taupo Volcanic Zone (TVZ) means the area has long been of scientific interest, including for InSAR studies. These studies provide a solid basis for the comparison of the InSAR-based model developed here. Thirdly, detailed monitoring surveys using precise levelling and GNSS have been carried out over several decades, principally at the behest of the power companies who

operate geothermal stations in the area and are required to monitor environmental impacts.

5.2. Background

The TVZ stretches for 300km through the centre of New Zealand. Back-arc rifting resulting from subduction of the Pacific Plate beneath the Australian Plate has led to extension across the area of 8-15mm/yr. Associated with this extension is subsidence of up to 20mm/yr (Hamling et al., 2015), increasing to 50mm/yr in localised areas of high geothermal activity (Samsonov & Tiampo, 2010).

5.2.1. InSAR Studies in the Taupo Volcanic Zone

Regional studies of deformation in the TVZ have utilised both GNSS and InSAR. Analysis of ERS and Envisat data spanning nine years from 1996 to 2005 demonstrated the power of InSAR to map large areas of continuous deformation (Hole et al., 2007). The unwrapped stacked interferograms clearly identified the most significant features, such as subsidence bowls at Wairakei and Spa Valley. However, the smaller Crown Road subsidence bowl, identified via contemporary levelling, is not resolved in the images. Hole et al. (2007) note there is a trade-off between coverage across the deformation field and the resolution of the radar measurements. High spatial filtering can reduce the noise sufficiently to enable large areas to be covered, but smaller areas of significant deformation can be lost.

A study by Samsonov & Tiampo (2010) utilised ALOS PALSAR interferometry over a two-year period between January 2007 and January 2009. The focus was on the Ohaaki and Tauhara geothermal fields. The Tauhara field is on the outskirts of the town of Taupo, at the northeastern end of the large lake of the same name. The radar images

were processed using the Small Baseline Subset (SBAS[31]) technique (Berardino et al., 2002). This technique uses large numbers of SAR acquisitions, grouped into small-baseline (ie small orbital separation) subsets. Images in these subsets have low levels of spatial decorrelation, so are well suited to accurate interferometry. The various subsets can then be combined, even where the baseline is relatively large, using singular value decomposition (Berardino et al., 2002). With this technique, spatial and temporal coverage of InSAR can be maximised. Samsonov & Tiampo (2010) found subsidence rates of up to 50-60mm/yr at both geothermal fields based on this InSAR analysis. This study noted that PS-InSAR was not a preferred technique, as many areas of scientific interest were in rural areas, where it was expected there would be a lack of objects with suitable characteristics to act as persistent scatterers.

A more recent study by Hamling et al. (2015) utilised ALOS PALSAR and Envisat data over the period 2003-2011, combined with GNSS CORS and campaign data. This research covered the entire TVZ and clearly identified all the major geothermal fields. Higher subsidence rates, in excess of 15mm/yr were noted in the area immediately to the east of the town of Taupo. Noting the impact of anthropogenic subsidence associated with geothermal power generation in the area, this area is masked out of further analysis. This is because the intention of this study was to investigate natural deformation associated with magmatic cooling and contraction beneath the crust.

More detailed studies of individual geothermal fields have also been carried out. It is often a requirement that the operators of geothermal power stations monitor the environmental impacts of their activities, including subsidence. These surveys typically utilise a mix of GNSS and precise levelling techniques to produce very accurate

[31] Not to be confused with the GNSS acronym SBAS (Satellite-based Augmentation System)

measurements of subsidence in specific areas of interest. More recently, permanent GNSS stations have enabled continuous monitoring at high-priority sites (Bromley et al.). The two areas of geothermal subsidence that impact parts of Taupo are the Crown Road and Spa Valley subsidence bowls, both part of the Tauhara geothermal system (see Figure 36). In 2015, maximum recorded subsidence rates were 110 mm/yr for the Spa Valley bowl and 50mm/yr for the Crown Road bowl (Bromley et al.).

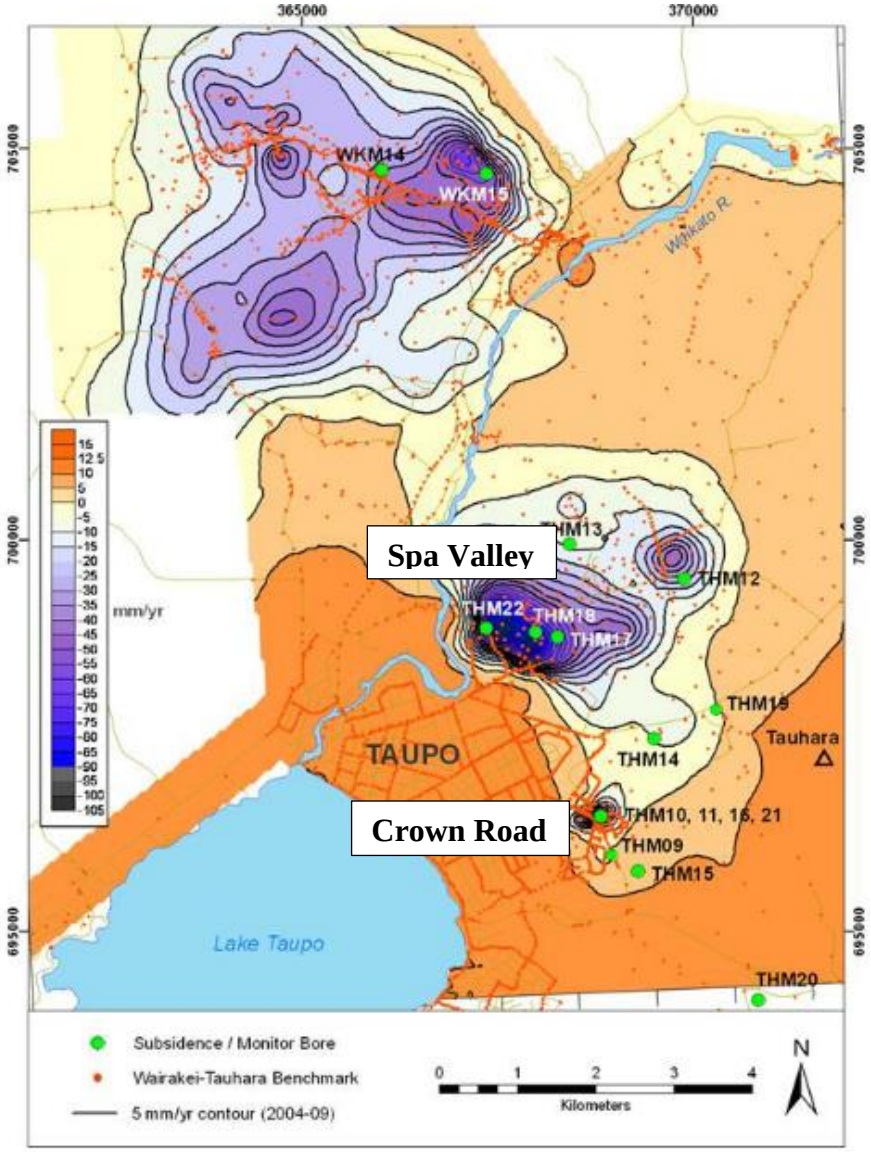

Figure 36: Geothermal subsidence in the vicinity of Taupo (Bromley et al.). THM18 is in the Spa Valley bowl, THM10 is in the Crown Road bowl.

Figure 36 shows subsidence impacting the eastern parts of Taupo. The Wairakei geothermal field is shown to the north, with the Spa Valley bowl in the centre of the plot. The small, southern-most subsidence feature is the Crown Road bowl.

5.2.2. Geodetic datum management

The primary focus of high-resolution modelling for geodetic datum management purposes is quite different to the focus of the scientific and engineering studies discussed previously. In the scientific studies, the aim is to further understand the mechanisms that are driving the observed surface deformations. For example, the deformations might be used to calculate magmatic volume changes beneath the TVZ (Bromley et al.). In the engineering studies, the focus is on monitoring the impacts of power generation activities on subsidence rates. They are highly detailed and accurate, but often do not have the coverage of the wider area desirable for datum management.

For datum management, the aim is to identify and quantify via a high-resolution model, all those features which impact on spatial data management. Identifying areas of stability is just as important as identifying areas of deformation in places such as Taupo where there are known to be a number of deformation features with relatively small spatial extents. For datum management, lower accuracies in rural areas are acceptable, as spatial data in rural areas is less accurate and/or the impact of less accurate data on decisions is generally less.

But most importantly, any technique used for geodetic datum management needs to be scalable at a national level. This makes the use of data collected in deformation monitoring surveys, such as those undertaken for the power companies, impractical in most cases. There are many instances of localised deformation, such as that associated

with slow landslides, where there may be little or no anthropogenic contribution and/or little direct hazard to the community, meaning there is no ongoing monitoring and therefore no survey data available.

This scaling at a national level is important as there is likely to be hundreds of distinct regions of localised deformation in New Zealand, ranging in size from a few hundred square metres to a few square kilometres. The intent of the LDMNs (section 2.3.3) is to identify, measure and potentially model this deformation. But as has been discussed, the expense of undertaking GNSS surveys at the densities required is prohibitive.

5.2.3. Use of PS-InSAR

Based on the forgoing discussion, PS-InSAR is a promising technique for this monitoring. While it was not considered suitable for the scientific study carried out by Samsonov & Tiampo (2010), this was due to valid concerns about the likely lack of persistent scatterers in rural areas. For the modelling undertaken for datum management purposes, the focus is on urban areas where there should be numerous objects with persistent scatterer characteristics.

As in Chapter 4, Sentinel data is used due to its ready availability and full coverage of the land area of New Zealand and its main offshore islands. This ensures that the approach developed in this chapter can be scaled up across the country. Even areas where significant localised deformation is not expected, such as Auckland, can be continuously monitored to ensure this is the case.

5.3. Synthetic Aperture Radar

5.3.1. Processing methodology

Table 21 shows the stack of 24 images identified for PS-InSAR processing covering the town of Taupo and its immediate surrounds.

Satellite	Acquisition Date	Temporal Baseline to previous image (days)	Image ID
S1B	20161123		F293
S1A	20161129	6	0322
S1B	20161205	6	31FB
S1B	20161217	12	53AE
S1A	20161223	6	F8D4
S1B	20161229	6	4F8E
S1A	20170116	18	0530
S1B	20170122	6	B5C3
S1A	20170209	18	C464
S1B	20170215	6	129E
S1B	20170227	12	4088
S1B	20170311	12	C92F
S1B	20170323	12	9AD8
S1B	20170404	12	DFA3
S1B	20170416	12	A19B
S1B	20170428	12	6FDF
S1B	20170510	12	48E8
S1B	20170522	12	F85F
S1B	20170603	12	7403
S1B	20170615	12	42EC
S1B	20170627	12	1E72
S1B	20170709	12	7D89
S1B	20170721	12	2968
S1B	20170802	12	F82C

Table 21: SLC radar image acquisitions for descending Track 81 over Taupo, New Zealand.

The images are mostly from the Sentinel-1B satellite, although four of the earlier ones are from Sentinel-1A. The two sensors have the same specifications and follow the same orbit, so images on the same track from both satellites can readily be combined. This means that in some cases, the temporal baseline (temporal separation between successive images) reduces from 12 days to 6 days, as the two satellites are offset from

each other by half of a full orbital cycle to maximise global coverage. This is particularly useful when significant and unpredictable events such as earthquakes occur. For image stacking, the shorter the temporal baseline, the more likely it is that persistent scatterers retain their brightness and coherence through the entire stack. There are two instances in Table 21 where the temporal baseline is 18 days, as the image acquisition satellite is swapped between Sentinel-1A and 1B. This is still a relatively short temporal baseline, so would not be expected to have any adverse impact on the results. There are 24 images in this stack, which is expected to be more than sufficient for atmospheric anomalies to be identified and removed from each image using the persistent scatterers. The other point to note is that by covering a period of nine months, seasonal effects such as hydrological loading will largely average out in the results.

As part of the stacking process, one image needs to be selected as the master, against which the slave images will be processed. The master image is selected based on it being the image that minimises the cumulative perpendicular baselines, which minimises topographic differences due to slightly different orbits. From the images in Table 21, choosing image 4088 acquired on 27 February 2017 minimises the perpendicular baselines, thus it became the master.

5.3.2. Interferograms

The first part of the processing is similar to that outlined in section 4.3.2. The 24 images in Table 21 were imported into the Sentinel SNAP software. Processing stacks of images is computationally intensive, so where possible, it is worth reducing the images so that only the area of interest is processed. The town of Taupo is covered by subswath 2, bursts 6 and 7. Given that each image has three subswaths, each with 10 bursts, processing just these two bursts substantially reduces processing time.

The first stage of the processing is to apply precise orbits to each of the 24 images. Unlike an earthquake scenario, where precise orbits are unlikely to be available due to the urgency of the timeframe in which the results are required, precise orbits would normally be available for some or all of the images so can be applied to assist with the co-registration of images.

Having updated the state vectors for the orbits, the next step is to co-register the stack of images. This is done by resampling the SRTM DEM onto each image using bi-linear interpolation, to remove the effects of topography. The image pixels can then be accurately correlated across the image stack. The output of the co-registration process is a single stack of images with all bands in the same product.

Next, the stack of interferograms is formed by subtracting the flat-earth phase and the topographic phase, leaving only the phase component due to deformation. Coherence bands for each pair of images in the stack are also formed at this point. Debursting over the stack is then completed. For the coseismic interferograms formed in section 4.3.3, the interference fringes were clearly visible at this stage of the processing. In this case, interference fringes are not necessarily visible in the interferograms in the stack. This is because the displacement between two successive images may be very small. For example, there is only 12 days between 27 February 2017 and the previous image acquisition on 15 February 2017. Unless the localised deformation is particularly significant, displacement over this timeframe is likely undetectable over the noise in the interferograms. However, fringes may be visible in some of the images with larger temporal baselines, if coherence is sufficient and the displacements are large enough.

At this point the spatial extent of the images in the stack is further reduced by selecting only the area immediately around Taupo. To this reduced image stack, bands for

latitude, longitude and elevation (from the SRTM 3-second DEM) are added. These additional bands are required for the PS-InSAR processing. At this stage, the stack is exported out of Sentinel SNAP for further processing using the StaMPS software.

5.3.3. PS-InSAR Processing

The StaMPS (Stanford Method for Persistent Scatterers) software is a series of Matlab scripts designed for PS-InSAR processing and analysis. It operates in conjunction with the SNAPHU software for phase unwrapping. The stacked interferograms exported from Sentinel SNAP are processed as a series of "patches" (not to be confused with the deformation model patches discussed in section 2.5.2.1). The number of patches is somewhat arbitrary, but the aim is to ensure the size of each patch is such that it can easily be processed using the resources available on the computer. In general, patches containing several million pixels are easily processed as a single entity. The *mt_prep* script distributed with StaMPS is used to create the patches.

The following description of the processing carried out in the StaMPS software is based on Hooper et al. (2013).

Phase noise estimation

Pixels containing potential persistent scatterers need to have their phase noise estimated. If the phase is noisy, then it is less likely to by suitable for PS-InSAR. Pixels were resampled onto a 50m grid, then filtered using a Combined Low-pass and Adaptive Phase (CLAP) filter (Hooper, 2008). This reduction of the phase noise makes it easier to select pixels that contain strong persistent scatterers.

Persistent scatterer selection and weeding

Pixels with persistent scatterers are initially identified based on their noise characteristics. There is then a process of removing pixels where that are present due to a significant signal contribution from a neighbouring pixel. This prevents the same scatterer being measured in two or more pixels, biasing the results. A Gaussian filter is applied to temporally smooth the phase noise distribution of neighbouring pixels. The width of this filter was set to 300 days, being representative of the time period over which long term atmospheric and other seasonal effects apply. In general, applying a filter of greater width results in a greater number of pixels being passed, but the pixels may have increased noise if the filter is too wide.

Phase correction

The phase is next corrected for incidence angle error, which relates to the presence of topography. This processing utilises the elevation data output from Sentinel SNAP, based on the 3-second SRTM DEM. If necessary, pixels can be resampled at this point onto a coarser grid. This may be necessary for large areas where the memory requirements of the processing can create issues. At the conclusion of the phase correction, the processing patches are recombined in preparation for phase unwrapping.

Phase unwrapping

Phase unwrapping is then carried out using the SNAPHU software. At this point, the unwrapped interferograms were examined for any evidence of sudden jumps in the phase, which can be indicative of noise associated with longer perpendicular baselines. In this case, there were no obvious problems, due to the relatively tight orbital control that is a feature of the Sentinel satellites, leading to short perpendicular baselines.

Plotting and export

As with all InSAR processing, PS-InSAR provides relative displacements or velocities across a scene. Therefore at least one point with known displacement/velocity needs to be fixed so that the persistent scatterers all have reliable estimates. In this case, the Taupo Airport CORS is located in the southern part of the scene. Inspection of the time series[32] reveals this station to be relatively stable in the vertical, so this location was set as the reference point for the scene.

The persistent scatterers were then exported for further analysis in the gdal raster processing toolkit and Quantum GIS software.

5.4. PS-InSAR Observations

The PS-InSAR processing described in the previous section generated just over 5,000 vertical velocity estimates in Taupo and its immediate surrounds. The observations are not evenly distributed, as can be seen in the example in Figure 37. There are almost no scatterers present in the farmland and forested land either side of the road. The road itself has a large number of scatterers due to the reflective nature of the surface. Similarly, the housing area in the western side of the image has a high density of scatterers, as the radar signal reflects off objects such as metal roofs. It can be concluded from this that, as anticipated, PS-InSAR does not work well in vegetated areas, where there is a dearth of reflective objects. However, there is very good coverage of urban areas, which are of primary interest for high-resolution modelling.

[32] Available at http://fits.geonet.org.nz/

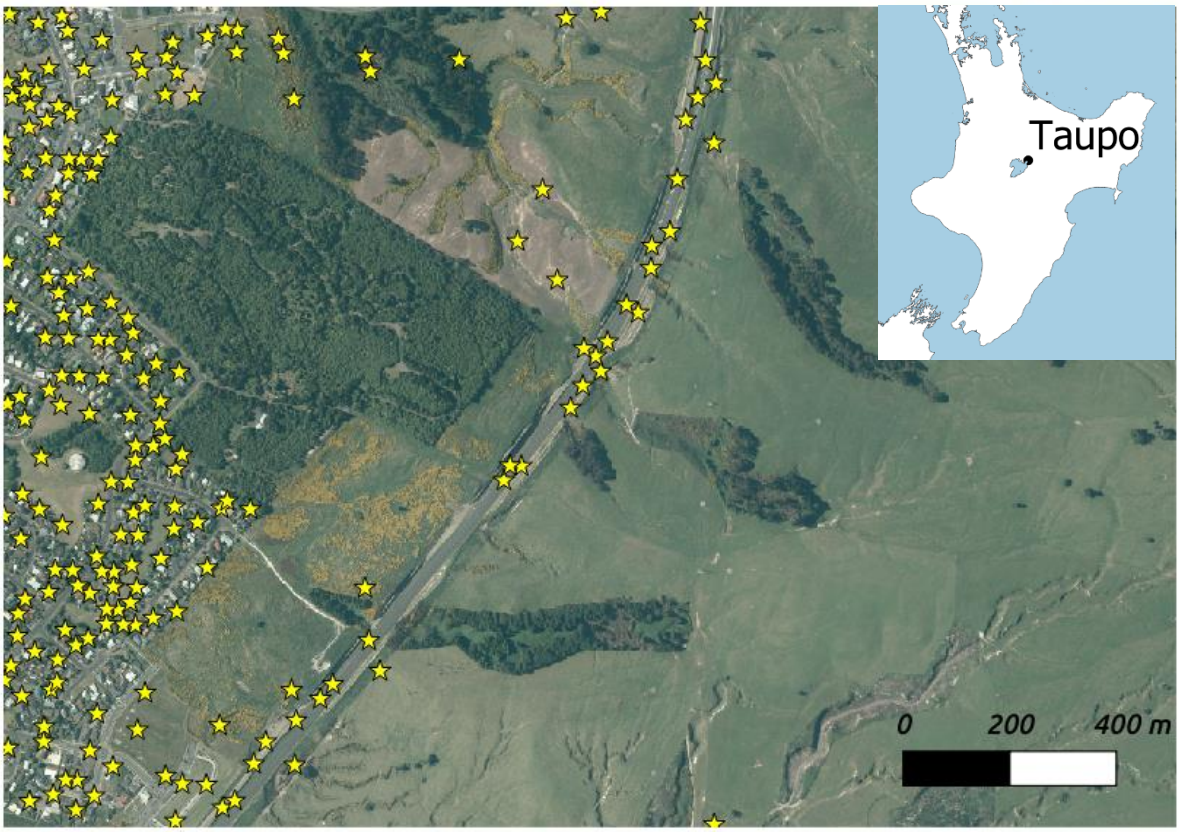

Figure 37: Persistent scatterers (yellow stars) in Taupo, over urban area to the west and road running through the centre of the image.

This conclusion is further supported by examining a smaller scale image showing the entire town and its immediate surrounds (Figure 38). Beyond the areas of urban development, there are very few persistent scatterers. This has important implications for the choice of extents of the high-resolution model. The bounds of such a model need to be tightly related to the density of persistent scatterers, otherwise there is a high risk that velocities from unreliable scatterers in rural areas bias the model. Scatterers in urban areas can also produce anomalous velocities, but the sheer weight of data strongly limits the influence of any individual observation.

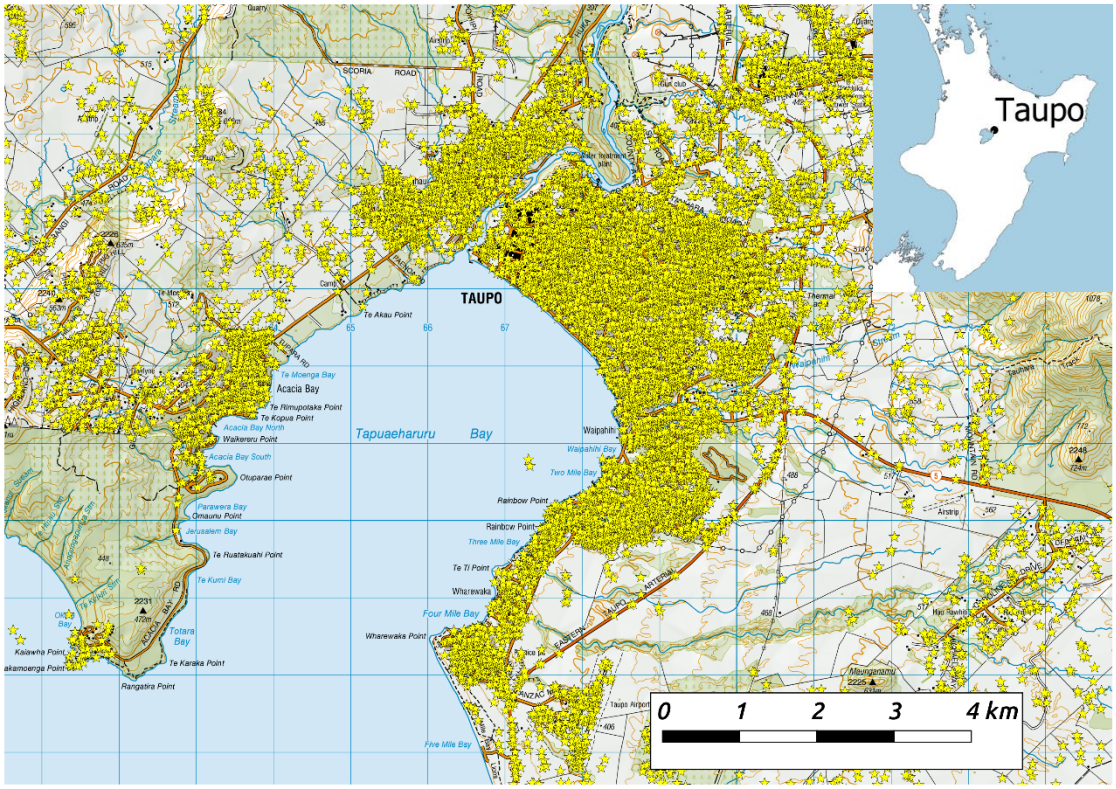

Figure 38: Persistent scatterers (yellow stars) in Taupo town and the rural area immediately surrounding it.

Figure 39: Persistent scatterers with vertical velocity estimates (mm/yr) in central Taupo where no movement is expected.

Figure 39 shows the persistent scatterers with their vertical velocity estimates for a small section of central Taupo. The first thing to note is that on average, the scatterers are separated by about 50m. Such density is unachievable using conventional GNSS surveys, even using RTK, due to the costs involved. By inspection of Figure 39, the velocity estimates are a mix of positive and negative values. About 95% of these values range between -4mm/yr and 4mm/yr. There is one particularly large anomaly of 13 mm/yr in the northwestern corner of the figure. This anomalous scatterer is on the road, so there could have been a change to the level of the road surface at some point over the time period for which the processing was carried out. Whether it represents real, highly localised, deformation or not, it is important in any modelling that this large value not inappropriately influence the model in this area.

But even if the 95% range is considered, in the far southeast corner of Figure 39, there is a velocity of -4mm/yr and about 100m due west is a value of 4mm/yr. This represents relative vertical movement of 8mm/yr over 100m. Over ten years, this would be 8cm, which is a significant change over a short distance, if these observations are reliable. Similar instances can be seen throughout the figure. Even velocity estimates at the 2-3mm level correspond to significant displacements over a decade. In reality, these sub-5mm velocity estimates are within the uncertainty of the PS-InSAR processing. A validation study by Raucoules et al. (2009) found through a comparison with levelling that PS-InSAR velocities typically have an uncertainty of 5-7mm/yr in real-world conditions. The uncertainty can reach more than 15mm/yr in areas of significant deformation, but can be as lower than 2mm/yr in stable areas (Raucoules et al., 2009). Thus while a stack of 24 images over 9 months is sufficient to accurately detect deformation, the noise in the data has a magnitude of a few mm.

From a national datum perspective, having unverified velocities of this magnitude is undesirable. Hence as part of the modelling, velocities less than 5mm/yr were set to zero. It is preferable to neglect some small potential vertical deformation, rather than produce a model which leads to the generation of significant height changes over several years where there is no other corroborating evidence. This is discussed further when the radar results are compared with GNSS in section 5.5.3.

Figure 40 shows an equivalent plot of persistent scatterers overlaid on aerial imagery, this time in an area of known deformation (section 5.2.1), the Crown Road subsidence bowl. Here there is clear evidence of subsidence, with velocities ranging from -6 mm/yr to -27 mm/yr. This is a substantial variation over a small area, which could be indicative of real variation in this high-deformation zone. But again, the uncertainty of

approximately 5mm in the PS-InSAR processing must be considered. The true velocity is likely to be more smoothly distributed across the area than the observations would suggest, based on Figure 36.

Figure 40: Persistent scatterers with vertical velocity estimates (mm/yr) in the Crown Road subsidence bowl at the eastern edge of Taupo, an area where significant deformation is expected.

5.5. Modelling

There are two main aims of the modelling from a national geodetic datum perspective. Firstly, the model should clearly identify the spatial extent of localised deformation. This ability to ring-fence the localised deformation is important for a number of purposes, not the least of which is so that surveyors and other spatial professionals know which geodetic marks they can rely on for stability. Secondly, the model should

quantify the magnitude of deformation as accurately as possible, although recognising that achieving high accuracy is challenging in areas with rapidly-varying deformation.

5.5.1. Inverse Distance Weighting

Given the success of IDW for shallow ground modelling in Chapter 3, this approach was also attempted for the modelling of subsidence in Taupo. Figure 41 shows a portion of the model generated using a power index of 2 (ie weighted by the inverse of the square of the distance) and applying a Gaussian filter of width 50m to smooth the results.

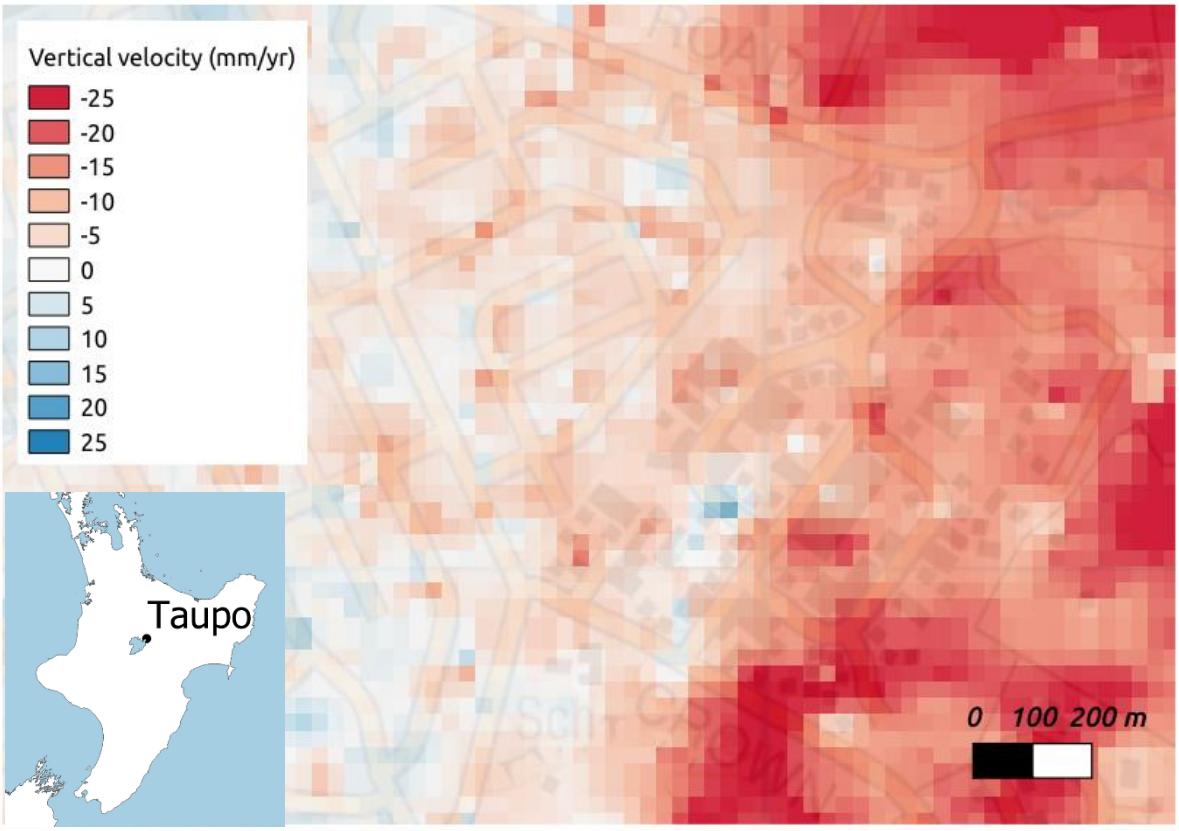

Figure 41: Model constructed from Inverse Distance Weighting algorithm.

It is clear from Figure 41 that the model is not particularly smooth, with modelled values being significantly influenced by the surrounding PS-InSAR velocity observations. As discussed in section 5.4, these can vary significantly over short

distances due to uncertainties in the observations. This leads to the “hotspot” effect seen in Figure 41.

For the Canterbury earthquakes shallow ground movement model, this high fidelity to the observations was important. This was due to the varied and discontinuous nature of earthquake-induced shallow ground movement and the cadastral requirement to respect observations made to the physical monuments, upon which the modelling was based.

In Taupo, the situation is quite different. The subsidence is caused by geothermal activity. For this type of deformation, the *a priori* expectation is that the vertical velocities decrease radially from the maximum subsidence in a smooth manner. It is therefore appropriate for the model to vary smoothly, without being so tightly constrained to the observations.

5.5.2. Moving Average Window

To address the limitations of the Inverse Distance Weighting method, a Moving Average algorithm was run over the PS-InSAR data. This averages all the observations over a specified distance to determine the value for the model at a particular point. For this model, a value of 200m was used, this being indicative of the size of the subsidence features in the area.

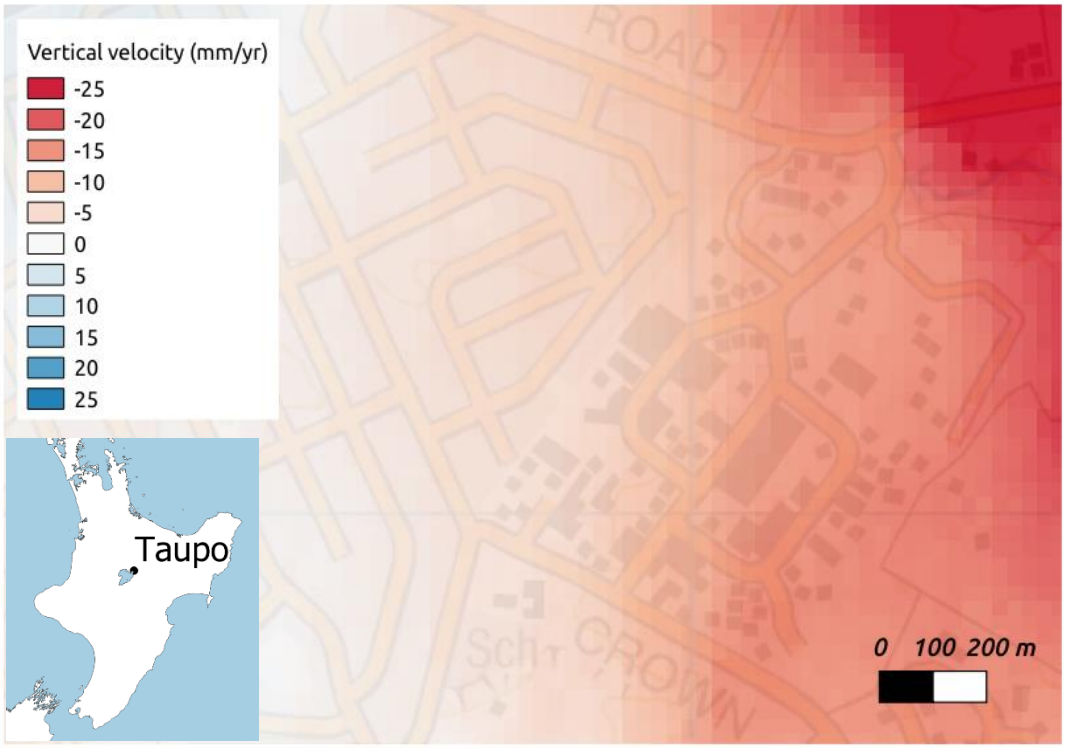

Figure 42: Model constructed from Moving Average algorithm.

Figure 42 covers an identical area to Figure 41. Comparing the two, the moving average algorithm has substantially reduced the noise in the model, at the same time reducing the prominence of some of the deformation features. Algorithm selection is a trade-off and in this case the smoother model is preferred as being more representative of the true nature of the subsidence, even if fidelity to the observations is sacrificed.

As discussed above, velocities between -5mm/yr and 5mm/yr were considered to be within the uncertainty of the radar processing. These areas were therefore set to zero. This decision is supported by the GNSS analysis in section 5.5.3.

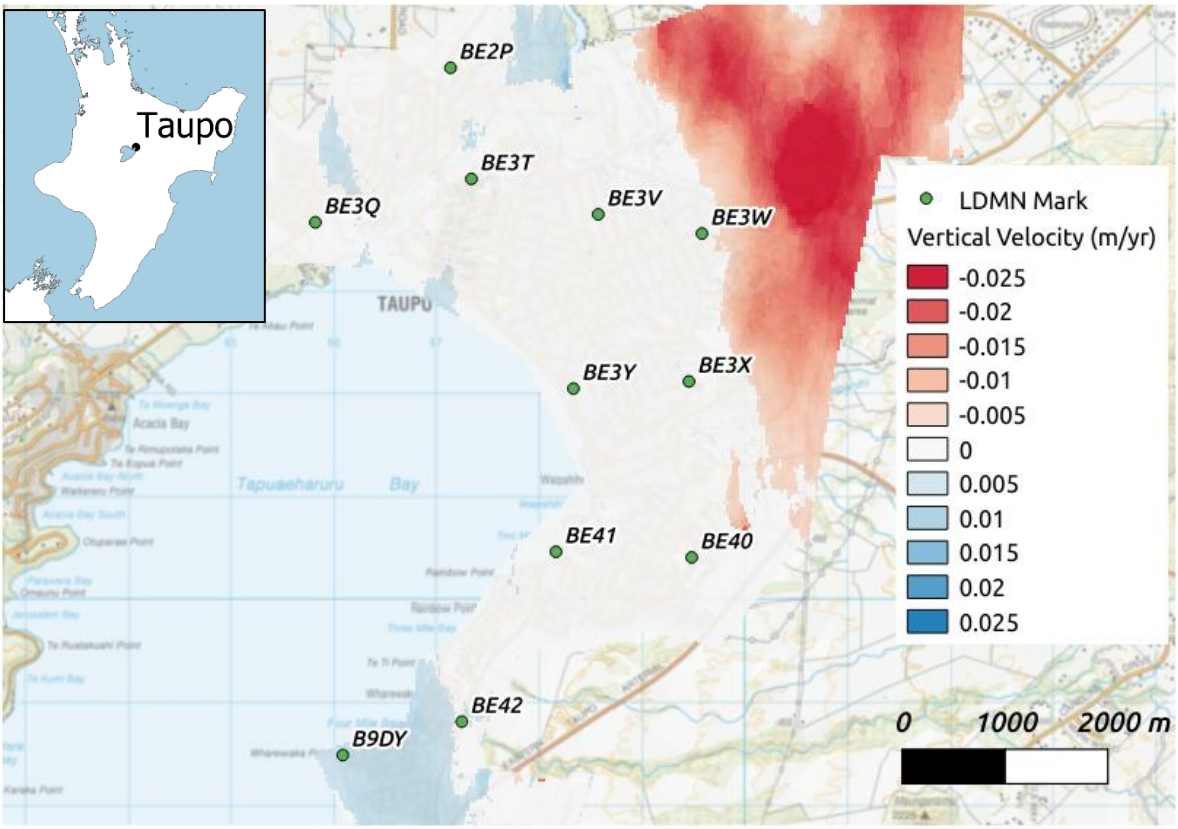

Figure 43: Taupo high-resolution vertical deformation model (25m resolution).

5.5.3. Comparison with GNSS

There have been three GNSS localised deformation monitoring campaigns carried out in Taupo since 1998.

The first, in December 1998, established the initial network of high accuracy control marks. At this time, the marks were not surveyed with the specific intention of being used to monitor deformation. Their primary purpose was to provide control for lower accuracy geodetic surveys that provide the dense geodetic control for cadastral surveying and other applications. However, the observations were made to a similar accuracy standard to that which is used for localised deformation monitoring network (LDMN) surveys, so this early GNSS data is expected to be suitable for deformation monitoring.

The second survey took place in January 2012. This was the first year that LDMN surveys were officially carried out by LINZ, other than those related to the Canterbury earthquakes. As shown in Table 22, only three marks within the modelled area were surveyed in 2012. This is because the 2012 survey utilised marks at the minimum density required by the standard.

The third survey was completed in December 2017. The number of marks was substantially increased from three to twelve, in recognition of the fact that the 2012 density was insufficient to give confidence that local deformation would be detected. Despite this increased density, Figure 43 shows that only one of the marks from this survey (B9DY) is in an area identified as having significant (more than 5mm/yr) vertical velocities.

Thus GNSS verification of the model is challenging, due to an absence of data in the areas of greatest deformation. Nevertheless, it is still worthwhile to check that the areas identified in the model as being stable are also shown to be stable through analysis of GNSS data.

To ensure that the three surveys were using a common datum, the data was combined in single least squares adjustment, where separate heights were calculated for each geodetic mark at each of the two or three epochs at which data was collected. The entire network was constrained to the nearby CORS at Taupo Airport (geodetic code TAUP). The vertical time series for TAUP calculated by GNS Science[33] shows no significant movement between 2012 and 2017 (the years of the two campaign surveys that directly connect to it). TAUP was established in 2002, so the 1998 survey could not be directly

[33] https://fits.geonet.org.nz/plot?siteID=TAUP&typeID=u&start=2011-01-01T00:00:00Z&days=3000

connected. Connection was achieved via BE3R, which was assessed to be stable by comparing movements with those at adjoining marks.

Geodetic Code	**GNSS Ellipsoidal Height 1998 (m)**	**GNSS Ellipsoidal Height 2012 (m)**	**GNSS Ellipsoidal Height 2017 (m)**	**Difference between 1998 and 2017 (m)**	**GNSS velocity estimate (m/yr)**
B9DY	388.213		388.238	0.025	0.001
BE2P	448.562	448.542	448.539	-0.022	-0.001
BE3Q	410.135	410.164	410.162	0.028	0.001
BE3T	413.369		413.366	-0.004	0.000
BE3V	431.749		431.743	-0.006	0.000
BE3W	440.994	440.930	440.916	**-0.078**	-0.004
BE3X	456.686		456.649	-0.037	-0.002
BE3Y	400.106		400.135	0.029	0.002
BE40	442.001		442.012	0.012	0.001
BE41	385.836		385.854	0.018	0.001
BE42	403.871		403.883	0.012	0.001
BEEQ	414.430		414.462	0.032	0.002

Table 22: GNSS-derived velocities. The only significant height change, at BE3W, is highlighted in yellow

Table 22 shows the heights calculated for each of these surveys, as well as the height differences over the 19 years between 1998 and 2017, as well as the estimated vertical velocity based on that height difference.

An important consideration is the accuracy of the GNSS surveys in the height component. These surveys were undertaken using fast static techniques. Baselines over short distances (a few km) typically have an RMS of about 15mm in the height component, which equates to 30mm at a 95% confidence level. Since two heights are

being differenced, the error in that difference is given by the root-sum-square of the individual uncertainties. Thus the uncertainty in the GNSS height difference is $\sqrt{30^2 + 30^2} = 42mm$. Therefore, with the exception of BE3W, none of the vertical changes is significantly different from zero. Overall, the table confirms the model in areas of stability.

There are two exceptions to this. Firstly, the mark BE3W has subsided by 78mm over 19 years, which equates to a velocity of -0.004m/yr. This is close to the cutoff of -5mm used to set the model to zero. From Figure 43, BE3W is the closest mark to the area of larger than 5mm subsidence in the model, which suggests that the value estimated from the GNSS is an accurate indicator of vertical velocity at that mark. This highlights a risk of applying the 5mm mask.

Secondly, the model indicates the B9DY is being uplifted by about 6mm/yr (Figure 43). The GNSS data shows no significant vertical change. This area of apparent uplift in the model appears too extensive to be purely due to atmospheric or other processing errors. It is possible that there is an influence from some residual seasonal effects. But it is also possible that this uplift is representative of real deformation. For example, in early 2012 a short-lived inflation event was measured at Taupo Airport (Bromley et al.), just 2km from B9DY.

5.5.4. Comparison with Engineering Surveys

The GNSS comparison in section 5.5.3 is somewhat inconclusive. This is primarily due to inaccuracies of the GNSS in the height component, particularly for the 1998 campaign, where satellite geometry was generally poorer than it is today, which disproportionately impacted the vertical component. In addition, the nature of the

deformation in the area is such that it can change significantly over time. For example, the deformation that is now referred to as the Crown Road subsidence bowl only started in about 1997. The temporal resolution of the current GNSS campaign data may simply not be sufficient for reliable comparisons with the InSAR data.

Samsonov & Tiampo (2010) estimate a 5-6cm/yr subsidence rate at Spa Valley in the Tauhara geothermal field. This compares well with the subsidence estimated from PS-InSAR observations, the largest of which is 54mm/yr. Nearby persistent scatterers (within 200m) mostly have values exceeding 40mm. The model itself has a maximum subsidence value of 35mm/yr for the Spa Valley subsidence bowl. This is indicative of the smoothing associated with the use of the moving average calculation for each pixel. By comparison, the IDW model has a maximum subsidence value of 45mm/yr. This is a good example of the trade-off that needs to be considered when constructing a model for geodetic datum purposes. Some fidelity to the observations in high-deformation areas is sacrificed to produce a smoother model overall.

Results for the Crown Road subsidence bowl are not presented in Samsonov & Tiampo (2010) However, the surveys detailed in Bromley et al. ((section 5.2.1) can be used to assess the accuracy of the PS-InSAR observations and model. As of 2015, these surveys estimate the maximum subsidence in the Crown Road bowl to be 20mm/yr. The largest PS-InSAR observation is -27mm/yr and many surrounding observations are between -20 and -25mm/yr, which represents a good level of agreement with the levelling data. Again the model has a smoothing effect, with the estimated subsidence being 15mm/yr. For the IDW method, the maximum value is -25mm/yr.

5.6. Monitoring and Managing Continuous Deformation within the Datum

Having identified and modelled areas of local deformation within the framework of the NZGD2000 deformation model, the question arises as to how this information is best used to manage and use the geodetic datum. From the perspective of the datum manager, there is a requirement to provide concise, unambiguous information about deformation as it pertains to geodetic marks in the deforming area. But this information needs to be simple enough that it can also be readily applied to other spatial datasets within the area, such as sewerage networks. The managers of these other spatial datasets are typically not geodesists, or even surveyors, hence the need to have a simple methodology that enables dynamics to be managed within that local area.

5.6.1. Publishing the Model

As discussed in section 2.5.2.2, LINZ has developed a custom deformation model format, in the absence of any international standard or convention that covers the full range of deformation that the country experiences. The major problem with this approach is that this model format is not supported by any commercially available software. The specialist software provided by LINZ (such as the SNAP least squares software) is not appropriate for general spatial data management purposes. If the localised deformation models are to be of benefit to users, they must be published in a form that can be consumed by widely used spatial software. As discussed in section 2.5.2.2, for horizontal deformation the NTv2 format meets these requirements.

For vertical deformation, NOAA (National Oceanic and Atmospheric Administration) publishes data in terms of the Datum Transformation Grid (GTX) format (NOAA, 2020). This format, which has both ASCII and binary versions, comprises a regular

array of evenly spaced height values. Being developed in the large United States market, the format is supported by major software vendors. While developed as a format to support conversions between ellipsoidal and orthometric heights using a geoid model, it can be utilised just as effectively for the application of a vertical deformation model.

Spatial software does not typically enable time-dependent transformations, whether horizontal or vertical. This means that even if a localised deformation model is published in a format that can be consumed by the software, the software will not be able to apply a velocity to the data, treating it as a displacement instead. It is expected that this situation will improve in the coming years, as major software vendors implement the latest revision ISO 19111, which supports transformations between epochs within a datum. But currently, the national datum manager must assume that most user software will not be able to process a velocity grid correctly.

The area of continuous localised deformation can be treated as a series of coordinate sets, each realised at a particular epoch. The simplest scheme would see a new “datum” created once per year, with the vertical velocities being treated as a single displacement for that year. With this scheme, the GTX file can be directly applied once per year to update all height coordinates from one epoch to the next. To ensure compatibility with other software and systems, the current realisation should be recorded as being the official datum (ie NZGD2000 or NZVD2016). As each new realisation occurs, the previous realisation has the year appended to it. For example, if an updated realisation is carried out in mid-2018, the high level process is:

- Create a custom datum called NZGD2000_2017

- Update all existing layers with heights in terms of NZGD2000 so that the datum is stated as NZGD2000 _2017
- Using the GTX file, define a vertical transformation from NZGD2000 _2017 to NZGD2000
- Apply the vertical transformation to update all heights to account for the additional one year of movement
- Update NZVD2016 heights as well

The advantage of this approach is that it provides very good traceability, with coordinates being recorded at well-defined epochs.

The temporal resolution of the above approach can be increased where the deformation is particularly significant. For example, the national datum manager could publish one-month, three-month and twelve-month GTX grids, enabling the spatial data manager to select the most appropriate interval for the data being managed.

For some applications, vertical accuracy requirements are low enough that application of the model is not required. For example, contours derived from the national 1:50000 scale mapping series are accurate to approximately 10m, so do not need updating for movements of the order of centimetres per year. In other cases, accuracy requirements are so high that specifications cannot be met using the model. For example, in the areas of high deformation on the western outskirts of Taupo, propagation of heights using the model will not be accurate enough to meet the requirements of designing a new sewerage network.

In both scenarios, the localised deformation model still has a lot of value as an additional data layer within a GIS. For example, in the case of sewer design, it clearly indicates where in the town existing benchmarks are stable and heights can be relied on.

It also indicates where survey work should be focussed, because heights are likely to have changed since they were last published.

For this reason, the localised deformation model should also be published in commonly available raster (eg GeoTiff) and vector formats (eg shapefile), so that they can be utilised within spatial software as a data layer.

5.6.2. Localised Deformation Monitoring Network (LDMN)

For the national datum manager, the PS-InSAR model of vertical deformation enables far more effective planning of the LDMN for the affected area. Consideration of the features of the model suggests two LDM networks with significantly different characteristics are required. The first is the standard LDMN, with a small number of marks spaced at low density, with repeat surveys carried out every 5-10 years. These marks would be situated in the stable part of the town, as indicated by the model. The survey methodology would most likely be rapid static GNSS. This aim of the repeat surveys is to confirm that that part of the area remains stable, validating the InSAR data. In the case of Taupo, three marks would be sufficient.

The second network is a high-density LDMN. The marks in this network would be located in the urban part of the deformation zone and would be spaced by approximately 300m. There are two main purposes for the high-density network. Firstly, it validates the vertical velocities calculated from InSAR. Secondly, it enables horizontal velocities to be calculated at a number of points within the deformation zone. In a subsidence zone, vertical velocities are much greater than horizontal, but horizontal movement may still be significant, for example there will typically be horizontal movements towards the centre of a subsidence bowl.

5.7. Summary

In this chapter, the PS-InSAR technique has been used to exploit the high reflectivity of the urban environment. This technique is particularly useful for monitoring continuous vertical deformation. The spacing of persistent scatterers at approximately 50m makes these observations well suited for high resolution deformation modelling. The persistent scatterer observations and model were validated using GNSS data and by comparison with the results of previous studies. PS-InSAR has not previously been used for modelling within a national datum and its use leads to significant efficiencies in management and use of the system. For example, the model can be used to identify areas of stability within an area such as Taupo where deformation is known to occur. This means that repeat GNSS surveys can be focussed on the areas of deformation where they will be the most valuable, rather than attempting to cover a large area at a density which is then so sparse that significant deformation features remain unidentified. But the model is far more than a tool for efficient datum management. Such models fundamentally increase the ability of the datum to fulfil its critical role of consistent management of spatial datasets. Heights can be regularly updated in a GIS system, to provide far more accuracy and currency to key spatial datasets, such as gravity-reliant infrastructure in zones of high deformation. This model is presented in a form that can be utilised using current spatial data management tools.

6. Conclusion

This research has clearly demonstrated that not only are high-resolution deformation models essential for a modern national datum, but in many scenarios they can be developed using free data.

6.1. Research Contributions

This research has made a number of contributions to advance knowledge relating to deformation modelling within a national geodetic datum. The most important are:

1) A method for refining dislocation models of deep-seated tectonic movement, based solely on dense geodetic GNSS observations, was developed (see section 3.4.6).
2) For the first time, cadastral data has been used to accurately model shallow ground deformation resulting from liquefaction. A methodology was developed that enabled cadastral surveys undertaken prior to geodetic control updates to be corrected to ensure their consistency with surveys completed after control had been updated.
3) It was shown how a cadastral-based shallow ground movement model could be used to answer important questions relating to contraction of land on a citywide scale after an earthquake.
4) A method for prioritising geodetic surveys as part of an emergency response using InSAR was developed and its use demonstrated.
5) A method for determining height difference observations from InSAR was developed, which enabled GNSS and InSAR data to be combined in a least squares adjustment for the first time.

6) For the first time, PS-InSAR observations have been used to produce a model of subsidence in an urban area, suitable for inclusion in the national datum.

6.2. Research Summary

There were a number of different aspects to this research, but the common theme was the use of novel data sources to derive geodetic observations and models of localised movements at high resolutions. Three case studies were used to identify several different techniques that could be used.

The first case study focussed on the Christchurch Earthquakes, particularly the challenges related to shallow ground movement. In this scenario InSAR-based modelling techniques are not appropriate as only horizontal modelling was required. Instead, digital cadastral data submitted as part of the earthquake recovery activities was processed to generate a dense network of displacement vectors. This was used to develop a shallow ground movement model and associated models, such as a dilatation model. These were then used to produce information about the impact of the earthquake on the land, which informed various policy recommendations made to central and local government.

In the Kaikoura earthquake case study, the focus was on how high-resolution observation/modelling of localised deformation could assist with the immediate recovery effort. The use of InSAR as both a planning tool and a technique for generating heights on survey marks was demonstrated. Of particular note was the method used to convert InSAR measurements into height differences analogous to levelling observations, making the InSAR suitable for incorporation into a least squares adjustment.

Finally, in the Taupo case study, continuous deformation was quantified using a stack of interferograms processed using the PS-InSAR technique. Several thousand persistent scatterers across the town were then used to calculate a localised deformation model for vertical deformation, suitable for incorporating into the national datum.

6.3. Recommendations

There are several recommendations arising from this research:

1) National geodetic agencies should utilise InSAR as a technique for monitoring the datums they manage, especially in urban areas where demands for an accurate datum are greater. It is rare for deformation to be purely horizontal, so almost all deformation of relevance to a national datum should be detectable with InSAR. Based on this monitoring, GNSS surveys should be appropriately directed to areas of known deformation, rather than attempting to cover an entire area with a sparse network.
2) The use of InSAR, in conjunction with rapid GNSS surveys, should be built into emergency geodetic response planning for an earthquake. In particular, attention should be given as to how InSAR results can best be communicated to audiences unfamiliar with the technology.
3) That consideration is given to the rapid deployment of temporary CORS after an earthquake, particularly in the vicinity of urban areas. As well as providing local control for the radar and rapid GNSS surveys, such stations enable post-seismic deformation to be monitored.
4) National geodetic agencies should ensure that a sufficiently dense network of vertical control marks is in place *before* an earthquake occurs so that radar can be used to calculate the height changes at these marks after an event.

6.4. Future Research

A number of further research opportunities are arise from this work. However, there are three in particular that would be of particular benefit within the national datum context:

1) Quantification of uncertainty for InSAR height change observations. This research treated these as independent height difference observations relative to an existing benchmark. A more rigorous approach would consider the correlations present in the interferogram and incorporate these into the stochastic model for the least squares adjustment. One option to explore would be the representation of InSAR height changes as a set of correlated heights.
2) Automated change detection for localised deformation. As a first step, this requires full automation of the model generation, something that was only achieved in this research for the shallow ground movement model. Successive versions of the model can then be compared with the latest published version of the model. This research would focus on appropriate triggers for publishing a new version of the model, perhaps based on tolerances related to accuracy standards for the datum.
3) Calculation of a national InSAR-based vertical deformation model. This research has focused on case studies covering localised areas and there are likely to be significant challenges if the deformation modelling is scaled up to a national level. Research would need to address the challenges such decorrelation in vegetated areas and integration with GNSS data at a national scale.
4) Turnkey radar processing should be investigated to see if it meets requirements for national datum maintenance. This could significantly reduce the current

requirement for deep technical knowledge of InSAR processing, a capability that is generally in short supply.

References

Altamimi, Z., Métivier, L., Rebischung, P., Rouby, H. & Collilieux, X. 2017. ITRF2014 plate motion model. *Geophysical Journal International,* 209**,** 1906-1912.

Altamimi, Z., Rebischung, P., Métivier, L. & Collilieux, X. 2016. ITRF2014: A new release of the International Terrestrial Reference Frame modeling nonlinear station motions. *Journal of Geophysical Research: Solid Earth,* 121**,** 6109-6131.

Amos, M. & Featherstone, W. 2009. Unification of New Zealand's local vertical datums: iterative gravimetric quasigeoid computations. *Continuation of Bulletin Géodésique and manuscripta geodaetica,* 83**,** 57-68.

Ballantyne, B. 2016. WTF—what's the fabric? The social dimension of defining boundaries using coordinates. *Geomatica,* 70**,** 223-228.

Bastin, S. H., Ogden, M., Wotherspoon, L. M., van Ballegooy, S., Green, R. A. & Stringer, M. 2018. Geomorphological influences on the distribution of liquefaction in the Wairau Plains, New Zealand, following the 2016 Kaikoura earthquake. *Bulletin of the Seismological Society of America,* 108**,** 1683-1694.

Beavan, J. 2012. GNS Consultancy Report 2012/164: Darfield Earthquake Investigations.

Beavan, J., Fielding, E., Motagh, M., Samsonov, S. & Donnelly, N. 2011. Fault location and slip distribution of the 22 February 2011 M (sub w) 6.2 Christchurch, New Zealand, earthquake from geodetic data. *Seismological Research Letters,* 82**,** 789-799.

Beavan, J. & Haines, A. 1997. Velocity map of New Zealand for provisional 1997/98 dynamic datum. Client Report 42793D.10. Lower Hutt: Institute of Geological and Nuclear Sciences.

Beavan, J. & Haines, A. 1998. Revised horizontal velocity model for the New Zealand geodetic datum. Client Report 43865B. Lower Hutt, New Zealand: Institute of Geological and Nuclear Sciences.

Beavan, J., Motagh, M., Fielding, E. J., Donnelly, N. & Collett, D. 2012. Fault slip models of the 2010–2011 Canterbury, New Zealand, earthquakes from geodetic data and observations of postseismic ground deformation. *New Zealand Journal of Geology and Geophysics,* 55**,** 207-221.

Beavan, J., Wallace, L. M., Palmer, N., Denys, P., Ellis, S., Fournier, N., Hreinsdottir, S., Pearson, C. & Denham, M. 2016. New Zealand GPS velocity field: 1995–2013. *New Zealand Journal of Geology and Geophysics,* 59**,** 5-14.

Berardino, P., Fornaro, G., Lanari, R. & Sansosti, E. 2002. A new algorithm for surface deformation monitoring based on small baseline differential SAR interferograms. *IEEE Transactions on Geoscience and Remote Sensing,* 40**,** 2375-2383.

Blick, G., Crook, C., Grant, D. & Beavan, J. Implementation of a Semi-Dynamic Datum for New Zealand. *In:* Sansò, F., ed. A Window on the Future of Geodesy, 2005// 2005 Berlin, Heidelberg. Springer Berlin Heidelberg, 38-43.

Blick, G. & Donnelly, N. 2016. From static to dynamic datums: 150 years of geodetic datums in New Zealand. *New Zealand Journal of Geology and Geophysics,* 59**,** 15-21.

Blick, G., Donnelly, N. & Jordan, A. 2009. The Practical Implications and Limitations of the Introduction of a Semi-Dynamic Datum – A New Zealand Case Study. *In:* Drewes, H. (ed.) *Geodetic Reference Frames: IAG Symposium Munich, Germany, 9-14 October 2006.* Berlin, Heidelberg: Springer Berlin Heidelberg.

Boucher, C. & Altamimi, Z. 2011. Memo: Specifications for the reference frame fixing in the analysis of a EUREF GPS campaign. Version 8 ed.

Broadbent, M. 2018. National Geodetic Adjustment and Coordinate Updates. *Surveying + Spatial,* 94**,** 17-19.

Bromley, C. J., Currie, S., Jolly, S. & Mannington, W. 2015. Subsidence: an Update on New Zealand Geothermal Deformaiton Observations and Mechanisms. World Geothermal Congress 2015, 19-25 April 2015 Melbourne, Australia.

Bürgmann, R., Rosen, P. A. & Fielding, E. J. 2000. Synthetic Aperture Radar Interferometry to Measure Earth's Surface Topography and Its Deformation. *Annu. Rev. Earth Planet. Sci.,* 28**,** 169-209.

Chatzinikos, M. & Kotsakis, C. 2017. Appraisal of the Hellenic Geodetic Reference System 1987 based on backward-transformed ITRF coordinates using a national velocity model. *Survey Review,* 49**,** 386-398.

Chen, C. W. & Zebker, H. A. 2002. Phase unwrapping for large SAR interferograms: statistical segmentation and generalized network models. *IEEE Transactions on Geoscience and Remote Sensing,* 40**,** 1709-1719.

Crook, C., Donnelly, N., Beavan, J. & Pearson, C. 2016. From geophysics to geodetic datum: updating the NZGD2000 deformation model. *New Zealand Journal of Geology and Geophysics,* 59**,** 22-32.

Denton, P. C. & Johnston, M. R. 2018. Housing Development on a Large, Active Landslide: The Tahunanui Slump Story, Nelson, New Zealand. Nelson: Soils and Foundations Ltd.

Donnelly, N., Crook, C., Stanaway, R., Roberts, C., Rizos, C. & Haasdyk, J. A Two-Frame National Geospatial Reference System Accounting for Geodynamics. *In:*

Van Dam, T., ed. REFAG 2014, 2017// 2014 Luxembourg. Springer International Publishing, 235-242.

Donnelly, N. & Hannah, J. 2006. An Assessment of the Precision of the Observational data used in New Zealand's National Cadastral System. *Survey Review,* 38**,** 502-512.

Drewes, H. Reference Systems, Reference Frames, and the Geodetic Datum. *In:* Sideris, M. G., ed. Observing our Changing Earth, 2009// 2009 Berlin, Heidelberg. Springer Berlin Heidelberg, 3-9.

Ferretti, A., Novali, F., Buergmann, R., Hilley, G. & Prati, C. 2004. InSAR permanent scatterer analysis reveals ups and downs in San Francisco Bay Area. *Eos, Transactions American Geophysical Union,* 85**,** 317-324.

Ferretti, A., Prati, C. & Rocca, F. 2001. Permanent scatterers in SAR interferometry. *IEEE Transactions on Geoscience and Remote Sensing,* 39**,** 8-20.

Gentle, P., Gledhill, K. & Blick, G. 2016. The development and evolution of the GeoNet and PositioNZ GNSS continuously operating network in New Zealand. Taylor & Francis.

Gledhill, K., Ristau, J., Reyners, M., Fry, B. & Holden, C. 2011. The Darfield (Canterbury, New Zealand) M (sub w) 7.1 earthquake of September 2010 a preliminary seismological report. *Seismological Research Letters,* 82**,** 378-386.

Grant, D. B. 1995. A Dynamic datum for a dynamic cadastre. *Australian Surveyor,* 40**,** 22-28.

Grant, D. B., Donnelly, N., Crook, C., Amos, M., Ritchie, J. & Roberts, C. 2014. Special feature – managing the dynamics of the New Zealand spatial cadastre. *Journal of Spatial Science,* 60**,** 1-16.

Hamling, I. J., Hreinsdóttir, S., Clark, K., Elliott, J., Liang, C., Fielding, E., Litchfield, N., Villamor, P., Wallace, L., Wright, T. J., D'Anastasio, E., Bannister, S., Burbidge, D., Denys, P., Gentle, P., Howarth, J., Mueller, C., Palmer, N., Pearson, C., Power, W., Barnes, P., Barrell, D. J. A., Van Dissen, R., Langridge, R., Little, T., Nicol, A., Pettinga, J., Rowland, J. & Stirling, M. 2017. Complex multifault rupture during the 2016 7.8 Kaikōura earthquake, New Zealand. *Science (New York, N.Y.),* 356.

Hamling, I. J., Hreinsdóttir, S. & Fournier, N. 2015. The ups and downs of the TVZ: Geodetic observations of deformation around the Taupo Volcanic Zone, New Zealand. *Journal of Geophysical Research: Solid Earth,* 120**,** 4667-4679.

Herman, M. W. & Furlong, K. P. 2016. Revisiting the Canterbury earthquake sequence after the 14 February 2016 Mw 5.7 event. *Geophysical Research Letters,* 43**,** 7503-7510.

Hole, J. K., Bromley, C. J., Stevens, N. F. & Wadge, G. 2007. Subsidence in the geothermal fields of the Taupo Volcanic Zone, New Zealand from 1996 to 2005 measured by InSAR. *Journal of Volcanology and Geothermal Research,* 166**,** 125-146.

Hooper, A. 2008. A multi-temporal InSAR method incorporating both persistent scatterer and small baseline approaches. *Geophysical Research Letters,* 35**,** n/a-n/a.

Hooper, A., Bekaert, D. & Spaans, K. 2013. StaMPS/MTU Manual. University of Leeds.

ICSM 2018. Geocentric Datum of Australia 2020 Technical Manual. V1.1.1 ed.: Intergovernmental Committee on Surveying and Mapping (ICSM) Permanent Committee on Geodesy (PCG)

ISO 2019. 19111:2019. Geographic information - referencing by coordinates. International Organization for Standardization.

Jiang, Z., Huang, D., Yuan, L., Hassan, A., Zhang, L. & Yang, Z. 2018. Coseismic and postseismic deformation associated with the 2016 Mw 7.8 Kaikoura earthquake, New Zealand: fault movement investigation and seismic hazard analysis. *Earth, Planets and Space,* 70**,** 1-14.

Johnston, G., Riddell, A. & Hausler, G. 2017. The International GNSS Service. *In:* Teunissen, P. J. G. & Montenbruck, O. (eds.) *Springer Handbook of Global Navigation Satellite Systems.* Cham: Springer International Publishing.

Jordan, A. 2005. *Implementing localized deformation models in a semi-dynamic datum.* MSurv, University of Otago.

Jordan, A., Denys, P. & Blick, G. 2007. Implementing Localised Deformation Models into a Semi-Dynamic Datum. *In:* Tregoning, P. & Rizos, C. (eds.) *Dynamic Planet: Monitoring and Understanding a Dynamic Planet with Geodetic and Oceanographic Tools IAG Symposium Cairns, Australia 22–26 August, 2005.* Berlin, Heidelberg: Springer Berlin Heidelberg.

Kaiser, A., Holden, C., Beavan, J., Beetham, D., Benites, R., Celentano, A., Collett, D., Cousins, J., Cubrinovski, M., Dellow, G., Denys, P., Fielding, E., Fry, B., Gerstenberger, M., Langridge, R., Massey, C., Motagh, M., Pondard, N., McVerry, G., Ristau, J., Stirling, M., Thomas, J., Uma, Sr. & Zhao, J. 2012. The M w 6.2 Christchurch earthquake of February 2011: preliminary report. *New Zealand Journal of Geology and Geophysics,* 55**,** 67-90.

Lee, Y.-H., Chen, Y.-C., Chen, C.-L., Rau, R.-J., Chen, H.-C., Lo, W. & Cheng, K.-C. 2011. Revealing coseismic displacement and displacement partitioning at the northern end of the 1999 Chi-chi earthquake, central Taiwan, using digital cadastral data. *Bulletin of the Seismological Society of America,* 101**,** 1199-1212.

Lee, Y.-H., Wu, K.-C., Rau, R.-J., Chen, H.-C., Lo, W. & Cheng, K.-C. 2010. Revealing coseismic displacements and the deformation zones of the 1999 Chi-Chi earthquake in the Tsaotung area, central Taiwan, using digital cadastral data. *Journal of Geophysical Research: Solid Earth*, 115.

Lee, Y. H., Chen, H. S., Rau, R. J., Chen, C. L. & Hung, P. S. 2006. Revealing surface deformation of the 1999 Chi-Chi earthquake using high-density cadastral control points in the Taichung area, central Taiwan. *Bulletin of the Seismological Society of America*, 96**,** 2431-2440.

LINZ 2007. Standard for New Zealand Geodetic Datum 2000 - LINZS25000. Land Information New Zealand.

LINZ 2009a. Guideline for the New Zealand survey control system - LINZG25704. Land Information New Zealand.

LINZ 2009b. Standard for the New Zealand survey control system - LINZS25003. Land Information New Zealand.

LINZ 2010. Rules for Cadastral Survey 2010. New Zealand Government.

LINZ 2013. NZGD2000 Deformation Model Format. Land Information New Zealand.

LINZ 2016. Standard for New Zealand Vertical Datum 2016 - LINZS25009. Land Information New Zealand.

LINZ 2018. LINZ Data Service: Full Landonline Dataset - Data Dictionary and Data Models. Land Information New Zealand.

LINZ. 2019. *SNAP & CONCORD Downloads* [Online]. Land Information New Zealand. Available: https://www.linz.govt.nz/data/geodetic-services/download-geodetic-software/snap-concord-downloads [Accessed 10 March 2020].

Massonnet, D., Rossi, M., Carmona, C., Adragna, F., Peltzer, G., Feigl, K. & Rabaute, T. 1993. The displacement field of the Landers earthquake mapped by radar interferometry. *Nature,* 364**,** 138.

McCubbine, J., Amos, M., Tontini, F., Smith, E., Winefied, R., Stagpoole, V. & Featherstone, W. 2018. The New Zealand gravimetric quasigeoid model 2017 that incorporates nationwide airborne gravimetry. *Journal of Geodesy,* 92**,** 923-937.

Mikhail, E. M. & Gracie, G. 1981. *Analysis and Adjustment of Survey Measurements*, Van Nostrand Reinhold Company Limited.

Miyahara, B., Kensuke, K. & Tokuro, K. 2015. Policy on National Geodetic Control Points of Japan - From Triangulation Control Points to GEONET. *FIG Working Week.* Sofia, Bulgaria.

Miyahara, B., Toyofuku, T., Furuya, T., Hiyama, Y. & Yamagiwa, A. 2016. Reconstruction of the Geodetic Reference Frame after the 2011 off the Pacific Coast of Tohoku Earthquake. *FIG Working Week.* Christchurch.

Nakano, T., Kobayashi, T., Yoshida, K. & Fujiwara, S. 2016. Field Survey of Non-tectonic Surface Dispalcements Caused by the 2016 Kumamoto Earthquake around Aso Valley. *Bulletin of the GSI.* Geospatial Information Authority of Japan (GSI).

NGS 2017. NOAA Technical Report NOS NGS 62: Blueprint for 2022, Part 1: Geometric Coordinates. National Geodetic Survey.

NOAA. 2020. *VDatum Transformation Grid Formats* [Online]. Available: https://vdatum.noaa.gov/docs/gtx_info.html [Accessed 3 March 2020].

Okada, Y. 1985. Surface deformation due to shear and tensile faults in a half-space. *Bulletin of the Seismological Society of America,* 75**,** 1135-1154.

Ordnance Survey 2018. A Guide to Coordinate Systems in Great Britain. Version 3.3 ed.

Pearse, M. 2000. Realisation of the New Zealand Geodetic Datum 2000 - OSG Technical Report 5. Land Information New Zealand.

Pearson, C., McCaffrey, R., Elliott, J. L. & Snay, R. 2010. Htdp 3.0: Software for coping with the coordinate changes associated with crustal motion. *Journal of Surveying Engineering,* 136**,** 80-90.

Pearson, C. & Snay, R. 2013. Introducing HTDP 3.1 to transform coordinates across time and spatial reference frames. *The Journal of Global Navigation Satellite Systems,* 17**,** 1-15.

Petit, G. & Luzum, B. (eds.) 2010. *IERS Conventions (2010), IERS Technical Note 36,* Frankfurt am Main, Germany: Verlag des Bundesamts für Kartographie und Geodäsie.

Raucoules, D., Bourgine, B., de Michele, M., Le Cozannet, G., Closset, L., Bremmer, C., Veldkamp, H., Tragheim, D., Bateson, L., Crosetto, M., Agudo, M. & Engdahl, M. 2009. Validation and intercomparison of persistent scatterers interferometry

PSIC4 project results. *Journal of Applied Geophysics,* 68**,** 335-347.

Reyners, M., Eberhart-Phillips, D. & Martin, S. 2013. Prolonged Canterbury earthquake sequence linked to widespread weakening of strong crust. *Nature Geoscience,* 7**,** 34.

Robertson, C., Dyer, M. & Donnelly, N. 2016. Locating property boundaries after shallow land movement - the Canterbury experience. *FIG Working Week 2016.* Christchurch.

Roman, D. 2015. Implementing geometric and geophysical datums for the United States in 2022. *FIG Working Week.* Sofia, Bulgaria.

Rosen, P. A., Hensley, S., Joughin, I. R., Li, F. K., Madsen, S. N., Rodriguez, E. & Goldstein, R. M. 2000. Synthetic aperture radar interferometry. *Proceedings of the IEEE,* 88**,** 333-382.

Samsonov, S. & Tiampo, K. 2010. Time series analysis of subsidence at Tauhara and Ohaaki geothermal fields, New Zealand, observed by ALOS PALSAR interferometry during 2007–2009. *Canadian Journal of Remote Sensing,* 36**,** S327-S334.

Simons, M. & Rosen, P. A. 2015. Interferometric Synthetic Aperture Radar Geodesy. *In:* Schubert, G. (ed.) *Treatise on Geophysics (2nd Edition).* Elsevier.

Soler, T. & Marshall, J. 2003. A note on frame transformations with applications to geodetic datums. *GPS Solutions,* 7**,** 23-32.

Soler, T. & Snay, R. 2004. Transforming positions and velocities between the International Terrestrial Reference Frame of 2000 and North American Datum of 1983. *Journal of Surveying Engineering,* 130**,** 49-55.

Stanaway, R., Roberts, C. & Blick, G. Realisation of a Geodetic Datum Using a Gridded Absolute Deformation Model (ADM). *In:* Rizos, C. & Willis, P., eds. Earth on the Edge: Science for a Sustainable Planet, 2014// 2014a Berlin, Heidelberg. Springer Berlin Heidelberg, 259-265.

Stanaway, R., Roberts, C., Rizos, C., Donnelly, N., Crook, C. & Haasdyk, J. Defining a Local Reference Frame Using a Plate Motion Model and Deformation Model. *In:* van Dam, T., ed. REFAG 2014, 2017// 2014b Cham. Springer International Publishing, 147-154.

Tanaka, Y., Saita, H., Sugawara, J., Iwata, K., Toyoda, T., Hirai, H., Kawaguchi, T., Matsuzaka, S., Hatanaka, Y., Tobita, M., Kuroishi, Y. & Imakiire, T. 2007. Efficient maintenance of the Japanese Geodetic Datum 2000 using crustal deformation models - PatchJGD & semi-dynamic datum. *Bulletin of the Geographical Survey Institute*, 54**,** 49-59.

Tonkin & Taylor 2012. Canterbury Earthquakes 2010 and 2011: Land Report as at 29 February 2012.

Tonkin & Taylor 2015a. Canterbury Earthquake Sequence: Increased Liquefaction Vulnerability Assessment Methodology: Appendix G: Accuracy and Limitations of LiDAR Data.

Tonkin & Taylor 2015b. Geotechnical information on horizontal land movement due to the Canterbury Earthquake Sequence. Christchurch.

Tregoning, P., Burgette, R., McClusky, S. C., Lejeune, S., Watson, C. S. & McQueen, H. 2013. A decade of horizontal deformation from great earthquakes. *Journal of Geophysical Research: Solid Earth*, 118**,** 2371-2381.

Walcott, R. I. 1984. The kinematics of the plate boundary zone through New Zealand: a comparison of short-and long-term deformations. *Geophysical Journal of the Royal Astronomical Society*, 79**,** 613-633.

Winefield, R., Crook, C. & Beavan, J. 2010. The Application of a Localised Deformation Model after an Earthquake. *XXIV International FIG Congress.* Sydney, Australia.

Glossary

Coseismic	Occurring at the time of an earthquake. For example, coseismic displacement.
CSD	Cadastral Survey Dataset
Deep-seated movement	Earthquake-induced movement at depths of a least several kilometres. Tectonic plate deformation in an earthquake is an example.
Deformation	A change in shape of the surface of the Earth.
Dislocation model	Model of an earthquake using nine-parameter rectangular faults within an infinite elastic half-space.
Dynamic datum	A datum which is fixed to the Earth as a whole, not just its surface. Objects on the surface move relative to this datum (for example due to tectonic motion), so coordinates of those objects continually change.
Forward patch	A type of submodel within a deformation model. It is applied to coordinates at epochs after a deformation event, to account for the displacements resulting from that event. Reference coordinates in terms of the datum are unchanged.
Incidence angle	Angle between the normal to the Earth's surface and the line of sight to the radar satellite.
Interseismic	Occurring in the period between earthquakes.
Lateral spreading	Lateral movement of sloping soils caused by liquefaction.
Liquefaction	Earthquake-induced loss of strength in saturated soil, causing it to behave as a liquid.

Look angle	Angle between the direction the radar antenna is pointing and the nadir.
Plate motion model	A three-parameter model of the rotation of a rigid tectonic plate about a pole. There is no change in shape (compare with deformation).
Post-seismic	Occurring in the period after an earthquake. For example, post-seismic displacement is that which occurs in the months and years after an earthquake.
Reverse patch	A type of submodel within a deformation model. It is applied to reference coordinates from before a deformation event, to reflect the displacements resulting from that event.
SAR	Synthetic Aperture Radar
Secular deformation	Imperceptible, continuous deformation occurring over long time periods.
Semi-dynamic datum	A datum which is fixed to a deforming part of the crust. Static coordinates are realised through use of a model to account for deformation.
Shallow ground movement	Earthquake-induced movement of material at depths of up to a few movements.
Static datum	A datum which is fixed to the rigid part of the crust.
Strain	A unitless change in length between two points, often recorded in radians or parts-per-million.